

**COMPACT PLANAR ANTENNA FOR METAL-MOUNTABLE UHF RFID TAG
DESIGN**

PHILIP TAN BOON HONG

**A project report submitted in partial fulfilment of the
requirements for the award of Bachelor of Engineering
(Honours) Electrical and Electronic Engineering**

**Lee Kong Chian Faculty of Engineering and Science
Universiti Tunku Abdul Rahman**

April 2020

COMMENTS ON FYP REPORT

Name: Philip Tan Boon Hong

Student ID: 1501690

Supervisor: Prof. Ts. Dr. Lim Eng Hock

Co-supervisor: Ir. Prof. Dr. Chung Boon Kuan

Moderator: Ir. Dr. Gobi A/L Vetharatnam

Comments by: **Supervisor/Moderator** (delete where not applicable)

Option 1

Marking and give comments on the pdf/word FYP report

Option 2

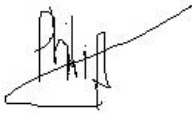
Marking and give comments on below

Comments on FYP Report

No.	Criteria	Comments
1	Abstract	
2	Introduction	
3	Literature Review	
4	Methodology	
5	Results & Discussion	
6	Conclusion and Recommendation	
7	References	
8	Any other comments	

DECLARATION

I hereby declare that this project report is based on my original work except for citations and quotations which have been duly acknowledged. I also declare that it has not been previously and concurrently submitted for any other degree or award at UTAR or other institutions.

Signature : 

Name : PHILIP TAN BOON HONG

ID No. : 1501690

Date : 22-4-2020

APPROVAL FOR SUBMISSION

I certify that this project report entitled “**COMPACT PLANAR ANTENNA FOR METAL-MOUNTABLE UHF RFID TAG DESIGN**” was prepared by **PHILIP TAN BOON HONG** has met the required standard for submission in partial fulfilment of the requirements for the award of Bachelor of Engineering (Honours) Electrical and Electronic Engineering at Universiti Tunku Abdul Rahman.

Approved by,

Signature :



Supervisor :

Prof. Ts. Dr. Lim Eng Hock

Date :

12 May 2020

Signature :



Co-Supervisor :

Prof. Dr. Chung Boon Kuan

Date :

14 May 2020

I hereby declare that this report belongs to me **PHILIP TAN BOON HONG (ID NO: 1501690)** under the terms of the copyright Act 1987 as qualified by Intellectual Property Policy of Universiti Tunku Abdul Rahman. Due acknowledgement shall always be made of the use of any material contained in, or derived from, this report.

© 2020, PHILIP TAN BOON HONG. All right reserved.

ACKNOWLEDGEMENTS

I would like to thank everyone and all the research labs and anything else that contributed to my research project, especially thanks to Universiti Tunku Abdul Rahman (UTAR) for letting me into their research labs to conduct simulations, measurements, freedom of accessing online databases such as IEEE Xplore and ResearchGate for exploring literature review which is able to assist in the development of my final year project. I would like to express my greatest pleasure and acknowledgement to my research supervisor, Prof. Ts. Dr. Lim Eng Hock and my research co-supervisor Ir. Prof. Dr. Chung Boon Kuan for their tremendous encouragement, supports, guidance, advice, patients that are not able to express my feeling and bear with my development of my research to give their best knowledge and help me throughout my entire final year project.

In addition, I would also like to express my enormous and greatest gratitude to my beloved parents throughout the entire period of the project with their greatest support in any occasions especially when I am facing difficulty. Their supports really boost up my motivation to complete this project successfully. Moreover, I would like to thank my seniors, Dr. Lee Yong Hong and Dr. Bong Fwee Leong whom already had the very good experience of doing this kind of related projects relentlessly help me throughout the project. Without my seniors help, I am not able to complete this project within the span period of final year project.

ABSTRACT

An electrical small planar folded patch composes of a rectangle Split-Ring Resonator (SRR) which is excited and fed by a meandered T-match, is proposed for designing an electrically small passive UHF RFID tag antenna for mounting on various dielectric constant dielectric surfaces. It has a dimension of $28 \text{ mm} \times 28 \text{ mm} \times 3.293 \text{ mm}$ ($0.0854\lambda \times 0.0854\lambda \times 0.01004\lambda$). The tag antenna is able to generate stable omnidirectional read patterns when placed on dielectric material. The notches have been merged with an inductive stub for the purpose of tuning the tag's resonance frequency. Good power transmission coefficient of $\sim 90\%$ is attainable. Measurements are conducted with reference to a transmitting power of 4W EIRP, and it has been shown that the proposed tag antenna is able to generate omnidirectional radiation patterns with a stable realized gain of -6.28 dB to -5.90 dB when it is placed on dielectrics with permittivity in the range of 1 – 5.8 in all directions in the azimuth plane. The tag's resonant frequency is also very stable and it is not affected by the dielectric with different permittivity backing surface much as the resonant frequency varies only in the range between 910 MHz to 917 MHz when the permittivity changes.

TABLE OF CONTENTS

COMMENTS ON FYP REPORT	ii
DECLARATION	iii
APPROVAL FOR SUBMISSION	iv
ACKNOWLEDGEMENTS	vi
ABSTRACT	vii
TABLE OF CONTENTS	viii
LIST OF TABLES	x
LIST OF FIGURES	xi
LIST OF SYMBOLS / ABBREVIATIONS	xvi
LIST OF APPENDICES	xix
CHAPTER	
1 INTRODUCTION	
1.1 The Background and History of Radio Frequency Identification (RFID)	1
1.2 Comparison between Passive and Active RFID	7
1.3 Problem Statement on the Challenges in UHF Band Level RFID Design	9
1.4 Aim and Objectives	11
1.5 Limitation and Covered Scope of the Project	12
1.6 Contribution of the Study	13
1.7 Outline of the Report	14
2 LITERATURE REVIEW	
2.1 The UHF Passive RFID Tag design following the Conventional Method	16
2.2 Challenges of Impedance Matching Techniques between the UHF tag Antenna and the Microchip	18
2.3 Quasi-Isotropic Radiation Pattern	18
2.3.1 The First Method to Achieve Quasi-Isotropic Radiation	19

	Pattern	
2.3.2	The Second Method to Achieve Quasi-Isotropic Radiation Pattern	23
2.3.3	The Last Method to Achieve Quasi-Isotropic Radiation Pattern	25
2.3.4	Theory to Generate Quasi-Isotropic Radiation Pattern	27
2.3.5	Folded-Patch Antenna	28
2.4	UHF RFID Tag dimension Scales down Approach	29
2.4.1	High Dielectric Constant Substrate	29
2.4.2	Shorting-Inductive Stubs and Via	31
2.4.3	Meandering the Slotting on Radiating-Patch	32
2.5	Summary of the Literature Review	33
3	METHODOLOGY AND WORKPLAN	
3.1	The Design Procedure of UHF Passive RFID Tag	34
3.2	Tag Antenna-Characterization	36
3.3	Actual UHF RFID Tag Measurement using Anechoic Chamber	40
3.4	Read Pattern-Measurements	42
3.5	Summary of the Methodology and Work plan	43
4	RESULTS AND DISCUSSION OF THE PROPOSED PASSIVE UHF RFID TAG	
4.1	Introduction	45
4.2	Proposed Passive UHF RFID Tag Antenna Configuration and Radiation Field Working Principle	48
4.3	Parametric Analysis and Radiated Field Pattern Results and Discussion	52
4.4	Real Practical Scenario Simulation Results and Comparison with other Researched Quasi-Isotropic Radiation Pattern UHF RFID Tag	63
4.5	Summary of Results and Discussion	70
5	CONCLUSIONS AND RECOMMENDATION	
5.1	Conclusions of the Proposed Passive UHF RFID Tag design	72
5.2	Disadvantages and Advices for Future Work	73
	REFERENCES	75
	APPENDIX	79

LIST OF TABLES

<i>Table 1.1:</i> Differences between the barcode systems and the RFID systems.	5
<i>Table 4.1:</i> The key parameters to affect the changes of tuning sensitivity.	58
<i>Table 4.2:</i> The comparison of the performance of the UHF RFID with quasi-isotropic radiation pattern.	70

LIST OF FIGURES

<i>Figure 1.1:</i> The communication between the radar and the airplane with the usage of backscattered signal.	1
<i>Figure 1.2:</i> The typical components of an RFID system which can be seen nowadays.	4
<i>Figure 1.3:</i> The worldwide RFID UHF spectrum.	6
<i>Figure 1.4:</i> Near-field inductive coupling for LF and HF and far-field backscatter modulation for UHF RFID system.	8
<i>Figure 2.1:</i> (a) Two crossed curved dipoles antenna structure, (b) Only dipole 1 is functioning, (c) Only dipole 2 is functioning, (d) both dipole 1 and dipole 2 are operating with equal magnitude of current feeding, (e) both dipole 1 and dipole 2 are operating with 90° phase-shift of current feeding (Pan et al., 2012).	20
<i>Figure 2.2:</i> (a) Four L-shaped monopoles antenna structure in y-z plane, (b) 3-D radiation pattern of the particular antenna structure when the sequential-phase feeding method activated all 4 monopoles with phase-shift of 90° of each other (Deng et al., 2014).	22
<i>Figure 2.3:</i> Combination of two magnetic slots with an electrical monopole orthogonally structure (Long S., 1975).	23
<i>Figure 2.4:</i> (a) Proposed dielectric resonator antenna structure, (b) Field patterns generated which fulfil quasi-isotropic radiation pattern. (Pang et al., 2014)	24

<i>Figure 2.5:</i> (a) Proposed split-ring resonator with driven striplines antenna structure, (b) Far field radiation pattern at x-z plane, y-z plane, and x-y plane (Wang et al., 2019).	26
<i>Figure 2.6:</i> Red in colour is the magnetic dipole align in the y-axis and blue in colour is the electric dipole align in the x-axis (Pan et al., 2014).	28
<i>Figure 2.7:</i> (a) Unwrapped fabricated inlay, (b) Complete folded tag's antenna wrapped around a soft-foam (Moh et al., 2018).	28
<i>Figure 2.8:</i> Proposed tag with high relative permittivity malleable ceramic polymer composite substrate (BaTiO_3) (Babar et al., 2012).	30
<i>Figure 2.9:</i> Proposed planar dipole tag antenna structure (Chen and Lin, 2008).	31
<i>Figure 2.10:</i> The comparison among different tag antenna structures by changing or adding additional slots (Bong et al., 2017).	32
<i>Figure 2.11:</i> Realized gain against frequency profile for different tag antenna structures (Bong et al., 2017).	33
<i>Figure 3.1:</i> Procedure of designing passive UHF tag.	36
<i>Figure 3.2:</i> The typical measurement system for UHF RFID.	37
<i>Figure 3.3:</i> The measurement setup to obtain the read distance pattern across all the three different planes.	43

<i>Figure 4.1:</i> (a) The overall configuration of the optimized proposed tag antenna with parameters $L_1 = 28, L_2 = 28, w = 1.9, L_3 = 11, L_7 = 1.7, L_4 = 1.4, L_6 = 0.9, j = 0.3, L_5 = 1.6, L_{12} = 1.8, L_a = 8.8, L_8 = 6.9, L_9 = 0.3, i = 0.2, a = 0.5, L_{11} = 3.6, L_{10} = 7, L_{13} = 2.6, L_{14} = 0.6, e_2 = 0.53, g = 1.9, L_c = 0.6, f = 3, e = 0.4, b = 0.6, c = 0.5, e_1 = 0.4, L_b = 9.7, d_1 = 0.5, d_2 = 2.8, d_3 = 2, d_4 = 3.293$ and $d = 1$ (all in mm). (b) Naked inlay of the fabricated proposed tag before wrapped.	49
<i>Figure 4.2:</i> The top-down and side view of the completed fabricated tag.	50
<i>Figure 4.3:</i> The working principle of electric dipole in perpendicular with magnetic dipole (Wang et al., 2019).	51
<i>Figure 4.4:</i> The equivalent surface current contributed by the magnetic and electric dipole.	51
<i>Figure 4.5:</i> The proposed RFID tag surface current simulated using CST MWS.	51
<i>Figure 4.6:</i> The changes of input impedance when the T-match loop thickness a is varied	53
<i>Figure 4.7:</i> The changes of power transmission coefficient when the T-match loop thickness a is varied.	53
<i>Figure 4.8:</i> The changes of input impedance when the length of the pair of the notches d_3 is varied.	54
<i>Figure 4.9:</i> The changes of power transmission coefficient when the length of the pair of the notches d_3 is varied.	55
<i>Figure 4.10:</i> The changes of input impedance when the length of the extended strip-line L_8 is varied.	56

<i>Figure 4.11:</i> The changes of power transmission coefficient when the length of the extended strip-line L_8 is varied.	56
<i>Figure 4.12:</i> The changes of input impedance when the narrow gap length L_c is varied.	57
<i>Figure 4.13:</i> The changes of power transmission coefficient when the narrow gap length L_c is varied.	58
<i>Figure 4.14:</i> Measurement setup in the anechoic chamber.	59
<i>Figure 4.15:</i> Simulated realized gain when the tag is attached in the middle of the 24×12 (all in cm) dielectric constant of 5.8 dielectric back object.	60
<i>Figure 4.16:</i> The surface current distribution on the tag's antenna when it resonates at 910 MHz by using CST MWS simulation.	61
<i>Figure 4.17:</i> Simulated realized gain at the (a) H-plane ($\theta = 90^\circ$ cut) and (b & c) E-planes ($\varphi = 0^\circ$ & $\varphi = 180^\circ$ cut and $\varphi = 90^\circ$ & $\varphi = 270^\circ$ cut).	63
<i>Figure 4.18:</i> Simulated realized gain with respect to the frequency to the case of (a) W changes while L kept constant and (b) L changes while W kept constant.	65
<i>Figure 4.19:</i> (a) The dielectric back objects used are manufactured by NXP and (b) the realized gain response as simulated by CST MWS.	67
<i>Figure 4.20:</i> The simulated realized gain response mounted on metal.	67
<i>Figure 4.21:</i> The simulated 3-dimensional realized gain response mounted on metal.	68
<i>Figure A.1:</i> The first design of the passive UHF RFID tag.	79

Figure A.2: The finalised design of the passive UHF RFID tag. 80

Figure A.3: The measured read distance shown for the first tag design as shown 80
In *Figure A.1* above shows the read distance measured has shifted
to above 1 GHz

LIST OF SYMBOLS / ABBREVIATIONS

d	Distance between the reader antenna and the tag antenna, m
d_{max}	Maximum read distance, m
E^e	The electric field due to electric dipole
E^m	The electric field due to magnetic dipole
$Ee\varphi$	Electric Field contributed by the electric dipole in the φ component, V/m
$Ee\theta$	Electric Field contributed by the electric dipole in the θ component, V/m
$Em\varphi$	Electric Field contributed by the magnetic dipole in the φ component, V/m
$Em\theta$	Electric Field contributed by the magnetic dipole in the θ component, V/m
E_{φ}^T	Total Electric Field at the φ component, V/m
E_{θ}^T	Total Electric Field at the θ component, V/m
FSL	Free Space Loss factor
$G_r(\theta, \Phi)$	Realized gain of the tag antenna
$G_{tag}(\theta, \Phi)$	Gain of the tag antenna
G_{tx}	Gain of the reader antenna
H^e	The magnetic field due to electric dipole
H^m	The magnetic field due to magnetic dipole
I	Current across the small loop antenna, A
I_e	Current flow in the electric dipole, A
I_m	Current flow in the magnetic dipole, A
L_{cable}	Cable loss factor
l_e	Length of the electric dipole, m
L_{fwd}	Signal path loss
l_m	Length of the magnetic dipole, m
L_{length}	Length inductance, H
L_{loop}	Loop inductance, H
L_1	Inner length of the split-ring resonator, m
L_2	Outer length of the split-ring resonator, m
$P_{chip}(\theta, \Phi)$	The power received at the surface of the microchip, W

$P_{c,on}$	Microchip sensitivity, W
P_{EIRP}	Effective Isotropic Radiated Power, W
$P_{tag}(\theta, \Phi)$	Tag sensitivity, W
P_{th}	Threshold power transmitted by the reader to activate the microchip, W
P_{tx}	Reader transmitted power, W
R_a	Resistance of the tag antenna, Ω
R_c	Resistance of the microchip, Ω
S	Area of the small loop antenna, m^2
$\tan \delta$	Dissipation factor
X_a	Reactance of the tag antenna, Ω
X_c	Reactance of the microchip, Ω
Z_a	Impedance of the tag antenna, Ω
Z_c	Impedance of the microchip, Ω
η	Wave impedance, Ω
η_{pl}	Polarization loss factor
τ	Power transmission coefficient
μ	Permeability, H/m
ϵ_r	Dielectric constant or relative permittivity
ω	Angular frequency, rad/s
λ	Wavelength, m
δ	Phase angle between the electric and magnetic dipole, degrees ($^\circ$)
φ, Φ	Azimuth angle in the spherical coordinate system, degrees ($^\circ$)
θ	Elevation angle in the spherical coordinate system, degrees ($^\circ$)
Auto-ID	Automatic Identification
CST MWS	CST Microwave Studio software
EAN	European Article Number
EIRP	Effective Isotropic Radiated Power
EPC	Electronic Product Code
ETSI	European Telecommunication Standards Institute
FCC	Federal Communication Commission
Glass	Pilkington Optifloat Glass

HF	High Frequency
IEC	International Electrotechnical Commission
IFF	Identify Friend or Foe
ISO	International Standards Organization
KITE	Phenolic Paper
LF	Low Frequency
PC	Polycarbonate
PET	Polyethylene Terephthalate
PMMA	Polymethylmetacrylate
PTFE	Teflon
PU/PUR	Polyurethane
RFID	Radio Frequency Identification
SRR	split-ring resonator
UHF	Ultra-High Frequency

LIST OF APPENDICES

Appendix A: The investigation of the error in the first proposed tag design to the finalised design.	79
--	----

CHAPTER 1

INTRODUCTION

1.1 The Background and History of Radio Frequency Identification (RFID)

The history of RFID technology can be traced back when during the World War II (Mark R., 2005). During that time, the radar system was discovered by a Scottish physicist Sir Robert Alexander Watson-Watt, where the radar system can be used to detect any approaching planes from miles away from the radar system. However, the radar system cannot identify which of the plane approaching was enemies or allies. As a consequence, the German found out a way that the returned waves would change when the planes were undulating as they were returned to the base. At this instant, the radar crews were vigilant by this cheap method as it could use to identify the return German planes were enemies or allies. As a result, this has been the first ever discovery of the passive RFID system.



Figure 1.1: The communication between the radar and the airplane with the usage of backscattered signal.

After that, British established the first ever active Identify Friend or Foe (IFF) system in a secret facility project, which was headed by the Scottish physicist Sir Robert Alexander Watson-Watt (Mark R., 2005). After being researched and developed, engineers build in such device, also known as transmitter on each of the British planes. It was the beginning of that time such system was used to identify the approaching aircraft were foes or allies. The passive RFID system works as where the reader transmits a signal to the tag also known as a transponder, which activates the transponder and either echoes back a signal, whereas, for active RFID system, it broadcasts a signal to the system. The improvement of RF communications systems continued through the 1950s and 1960s. Many scientists and researchers around the world did research on how the uses of electromagnetic waves in the radio frequency spectrum able to search for something very far away. The first U.S. patent for an active RFID tag with writable memory was being discovered by Mario W. Cardullo (Mark R., 2005) on January 23, 1973. Meanwhile, during that period in the same year, a copyright on an invention for a passive tag utilize it to open a door without using a key was also being tried by the California businessperson, Sir Charles Walton. As for a discovery, a tag antenna planted in the nearby of the tag was being utilized to communicate a signal to the interrogator to unlock the door which was installed adjacent to the door. The door would be unlocked when the correct identity being stored in the tag was identified by the reader. In the 1970s, the U.S. government was also working on RFID systems and requested Los Alamos national laboratory establish a system for tracking nuclear materials. During that system establishment, the scientists in the laboratory had proposed of putting the RFID tag on the truck and putting the reader at the gate of the security gate. In this way, the recognition data of the corresponding tag is able to verify as if the electromagnetic waves propagate the signal from the reader to the tag and backscattered back to the reader. The working concept of RFID system was beginning to utilize in the cashless toll transaction systems and was advertised in the 1980s. This kind of cashless toll transaction systems broadly used around the world, particularly in Malaysia, currently in recent years where the government started to implement an RFID system into the cashless toll transaction systems.

In the early stage development, the companies developed a low frequency system with operating frequency of 125 kHz with a smaller size of transponder. But, after that, the low operating frequency tends to limit the read range and data transfer rates. As a result, the companies moved up the operating frequency to radio frequency in the frequency spectrum of 13.56 MHz,

which can be seen nowadays for better read range and data transfer rates for access control, payment systems and contactless smart cards. After that, the Ultra High Frequency (UHF) RFID system was being developed and patented by IBM engineers in the early 1990s, which offered a long read range up to 20 feet and very fast data transfer. Nonetheless, IBM suffered from financial issues during the mid-1990s, which forced IBM to sell its patents to Intermec. Intermec attracted a good image of RFID system which have been installed in several different applications such as warehouse tracking to farming, but unfortunately, such system failed to attract the market due to the system failed to show its valuable which can be worth to that price and lack of international standard to comply that such system will be safe for the user to use. As a result, from the early 1980s to the late 1990s showed a very slow progress of the further enhancement of RFID system due to high cost setup, lack of international standard results in non-worthy investment to further develop such technology in the worldwide.

However, “the UHF RFID further improvement breakthrough started in 1999 again, when the Uniform Code Council, European Article Number (EAN), Procter & Gamble and Gillette subsidized the Massachusetts Institutes of Technology (Mark R., 2005) to set up an Automatic Identification (Auto-ID) Center”. This research was carried out by two professors, David Brock and Sanjay Sarma on the possibility of sticking inexpensive transponder on all items to document them through the market user. As a result, the Automatic Identification Center commenced to establish two air junction classes (Classes in 0 and Classes in 1), the universal identifier Electronic Product Code (EPC) digits blueprint, and the global structure system which all merged together to form an architecture which had described the actual and reasonable demands of the RFID system which consists of the reader and the tag from the year of 1999 to 2003. Hence, such “technology was licensed to the Uniform Code Council in 2003, and the Uniform Code Council created EPCglobal”. Nowadays, some of the biggest well-known retailers in the world such as Albertsons, Metro, Target, Tesco, Wal-Mart and the U.S. Department of Defense have already widely implemented the RFID system technology to record their goods in their supply chain factory. Apart from that, healthcare and pharmaceuticals have also been largely demanded to use RFID technology because it allows the hospital staff to decrease the time usage of counting, allowing pharmaceuticals to be counted more regularly, ensuring the accuracy of the data and that correct types and amounts of drugs are on hand. RFID tags installed inside or on the bottle can be read

with portable handheld readers during the inventory process, or invariably documented through the fixed readers and shelf antennas (Suzanne S., 2017). As of nowadays, the EPCglobal embraced EPC Gen 2 Class 1 which consists of UHF band or HF band; write once, read many (WORM) adopted from the standard of “Gen 2 ISO18000-6C after obtaining consent from the International Standards Organization (ISO)” of which applied to the RFID system operating in the range of 860 MHz to 960 MHz in the UHF band. Most of the RFID measurement procedure development is based on this standard as of today. In today’s market, there were several manufacturers developed the RFID chips in the current market. Those microchips consist of Monza R6, Monza R5, Monza 5 and Monza 4 from Impinji, Alien Higgs-2, Alien Higgs-3 and Alien Higgs-4 from Alien technology as well as many other manufacturers such as Zebra Technologies, Avery Dennison, Checkpoint Systems, Tyco international, Smartrac, and many more. These chips have their own read sensitivities and write sensitivities also known as the minimum power to activate the tag to read and write, variable impedance value which consists of real and reactive parts throughout the spectrum, memory storages to store data and data transfer rate. From *Figure 1.2* below shows a complete system of RFID which consists of components of tag (transponder), the reader (interrogator), which is connected to the network operating system or computer for decoding the information which has been retrieved and stored from the tag and display in the computer. Electromagnetic waves transmitted by the reader antenna propagates wirelessly to the tag antenna which activates the tag’s information backscattered wirelessly back to the reader antenna and decodes the information stored in the tag in the reader, which can be seen in the computer which the computer could recognize the data being stored which the particular tag is activated.

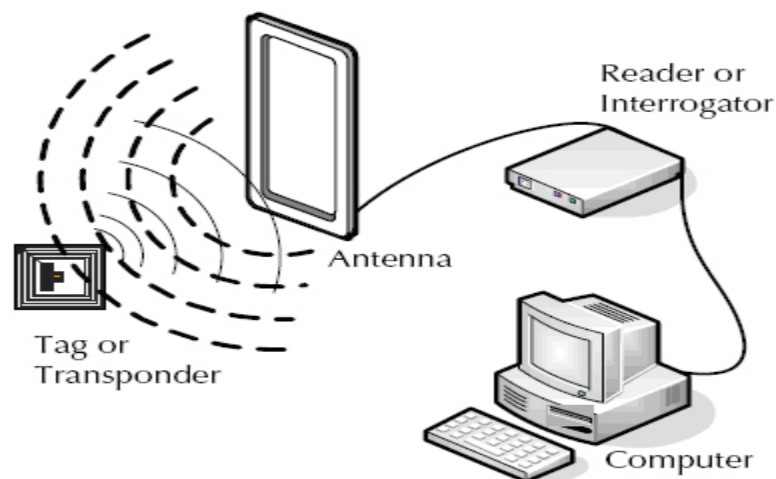


Figure 1.2: The typical components of an RFID system which can be seen nowadays.

Table 1.1: Differences between the barcode systems and the RFID systems.

Property	RFID Tag	Barcode
Reading capability	Does not require transponder to be in line of sight	Barcode readers require a direct line of sight to the printed barcode
Information identification	Multiple tag identification – Read numbers of information simultaneously	Single tag identification
Rate of reading	Tags read faster	More time consuming due to the fact that line of sight is required
Reading range	RFID tags can be read at much greater distances up to 3000 feet	The range to read a barcode is much less, typically no more than fifteen feet
Usability	Reusable	Not reusable
Information configuration	RFID tags, however, can be read/write devices; the RFID reader can communicate with the tag, and alter as much of the information as the tag design will allow	Barcodes have no read/write capability; that is, you cannot add to the information written on a printed barcode
Cost	RFID tags are typically more expensive	Barcode tags are cheaper

As in *Table 1.1*, the table above shows the differences between barcode and RFID by referring to it (Khosravi et al., 2016). Based on this table, these were all the advantages of RFID technologies over the barcode technologies. As an obvious comparison, the main functions of RFID technologies are targeted for applications like identification being done automatically, said to be focused on substituting the aspect of the original identification, which make use of the optical approach adopted from the visible light spectrum which targeted for the technology of barcode. As described in the *Table 1.1* (Khosravi et al., 2016), the transponder such as barcode required to be in the electromagnetic waves propagate in a direct path from the source which is the scanner to the receiver which is the barcode for the system to read. However, this is not necessary at all for the RFID transponder as the reader emits electromagnetic waves in a covered area which give rise to the advantages of activating multiple tag within the covered area while this is not the case of barcode transponder. Since the barcode transponder can only be activated one by one, in large scale applications may not be suitable for it to be implemented due to time consuming. Multiple

RFID tags can be activated less than a second when it receives the signal. The read range of RFID technologies is much greater as it adopted the radio frequency propagating of electromagnetic waves in free space, whereas the barcode technologies using optical identification where the LED or laser light tends to attenuate very greatly at long range which limits its read range at very short distance. On top of that, the barcode cannot be reused once the code stored in the barcode is damaged because the structure of the code defines the identity of the particular. However, for the RFID, the tag can be reused as long as the chip is not damaged, although it may weaken the properties of the tag if the antenna is damaged because the of impedance mismatch. Next, the barcode has no read/write capability, which it had been defined the information or the barcode once it is printed, but, for RFID tags, it can modify the information being stored inside and alter the tag characteristics by changing the tag's chip and its antenna. For cost wise, RFID tags are more expensive the barcode because of the fabrication materials being used and the fabrication process being done, whereas for barcode it is just a code printed on a piece of paper.

From the point of view of advantages of RFID tag over the barcode technologies, enforcing the RFID system will certainly change the working lifestyle in the seller and consumer side, particularly in applications like in the warehouse where the reader can put in a fix position, whereas for the tag installed in the items can be scanned fully automated in long distance unlike the barcode which require human intervention in a near range tagging. This allowed the rapid speed up the process, improve efficiency and prevention of human error.

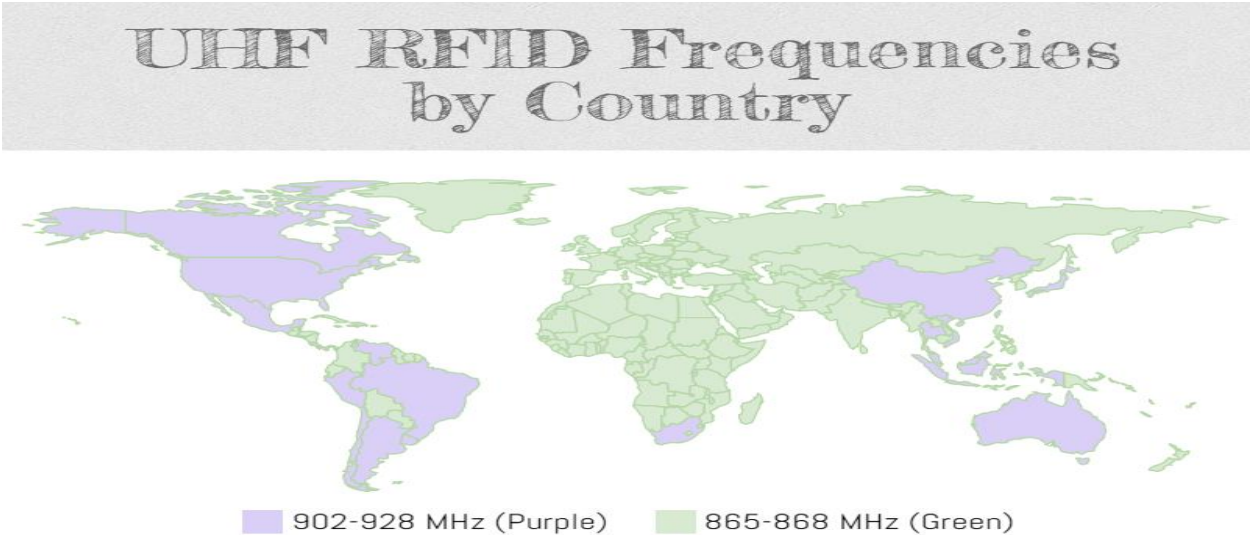


Figure 1.3: The worldwide RFID UHF spectrum.

From *Figure 1.3* (Suzanne S., 2014), the regulated operating frequencies among all the countries in the world are different. Not a specific single band had been implemented across the world. These frequency ranges were being adopted by a group of organizations – the International Organization for Standardization (ISO), the International Electrotechnical Commission (IEC), ASTM international, and EPCglobal. These frequency bands are now known as the ISM bands. The European Union, Middle East, and Africa adopt the bandwidth ranges from 865-868 MHz with maximum allowable transmits reader Effective Isotropic Radiated Power (EIRP) up to 2W. While in the Western Hemisphere, and South East Asia are operating in the frequency ranges from 902-928 MHz with maximum acceptable EIRP up to 4W. Meanwhile, in Australia, they have restricted their operating frequency ranges from 920-926 MHz. Whereas in China, both spectrums range 840-845 MHz and 920-925 MHz were allowed to be implemented. As a result, Engineers, which to design the RFID tag has to be taken care of the impedance matching characteristic as the operating spectrum varies from different countries.

1.2 Comparison between Passive and Active RFID

In the passive RFID system, an RFID reader transmits AC signal to the reader antenna via an RF cable and the reader antenna received this signal and propagates this signal in the form of electromagnetic waves through free space and received by the tag antenna. The electromagnetic energy will activate the tag's chip and its stored information inside the chip is backscattered its electromagnetic waves back to the reader antenna and received by the reader and the information is decoded in the reader and display in the computer. There are 3 different operating spectrums of passive RFID system, consist of in Low Frequency (LF) ranges from 120-150 kHz, High Frequency (HF) operating in 13.56 MHz and Ultra High Frequency (UHF) ranges from 865-868 MHz for European Union and 902-928 MHz for North America. There are two different methods for operating passive RFID system. The first method is targeted for LF and HF RFID, which makes the use of near-field magnetic coupling between the tag and the reader, which can be seen commonly in Malaysia for Touch 'n Go system. The second method is targeted for UHF RFID, which makes the use of far-field backscatter modulation between the tag and reader antennas both which are implemented recently in Malaysia toll payment system MyRFID. *Figure 1.4* (Kynix

Semiconductor, 2018) below shows the differences between the near-field inductive coupling and the far-field backscatter modulation.

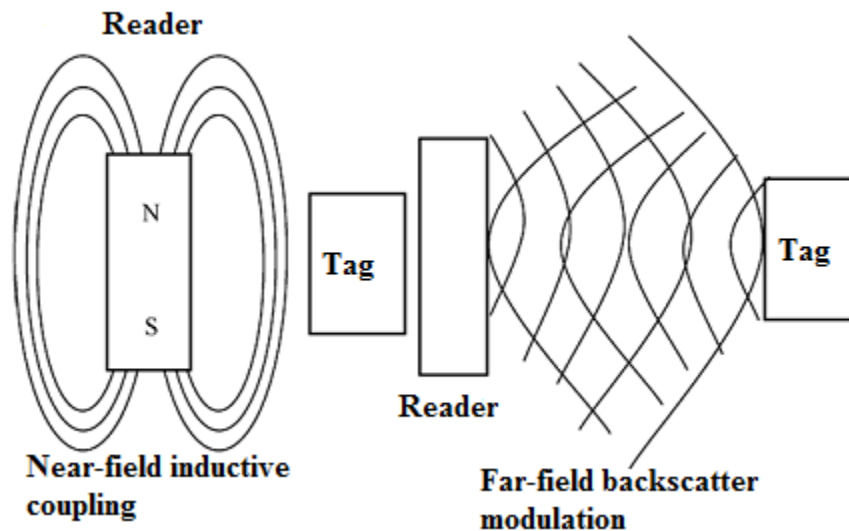


Figure 1.4: Near-field inductive coupling for LF and HF and far-field backscatter modulation for UHF RFID system.

In the active RFID system, the tag requires an internal battery act as a source for the tag to power up to communicate with the reader. Because of that, the active RFID system has a read range much greater than the passive RFID system typically more than 100 m in the current market. In general, transponder and beacon type active RFID tags are normally available in the market. For the beacon type active RFID tag, it is mainly targeted for real-time locating system like embedding a chip in a patient, which allows a real-time tracking the patient all the time to prevent any emergency happen to the patient. The prearranged interval time-continuous signal is emitted by the beacon type, where the signal is targeted over some area which the reader was located in the instance of monitored area. However, for the transponder type active RFID tag, predetermined interval signals will not be emitted. It emits solely the backscattered signal when the signal transmits from reader activated the tag. As a result, active RFID system tends to have a much shorter lifespan than passive RFID system because the battery life cycle is limited, normally the life span is about 5 years. Some exclusive tags are made to handle tough circumstances, such as low temperature, extreme humidity and craggy applications like remote sensing to detect any landmines hidden below extreme cold environment of the ice surface like in south-pole Antarctica.

Commonly, the active RFID system is not commonly used and hot research topic as more cost is incurred due to extra power up battery and complicated electronic circuits as compared to the passive RFID system.

In the semi-passive RFID system, it is almost the same operation as a passive RFID system because the mechanism for both of the system is almost the same, while the only difference with the semi-passive RFID system is that it is equipped with a battery source to power up the circuitry of the tag. For the passive RFID system, the tag required the power from the reader to activate its functionality, whereas for semi-passive RFID system, higher energy of EM is reflected and absorbed by the reader as it does not require energy from the reader to excite the tag. As a result, the typical read range of semi-passive RFID system has a higher read range than the passive RFID system, but with much higher cost because of the extra battery to function the tag and the lifespan of the battery may be limited.

1.3 Problem Statement on the Challenges in UHF Band Level RFID Design

In the current industry market, RFID technology has shown to be a very potent technology for any applications that require tracking of goods and wireless system. The passive RFID functioned on the UHF spectrum shown to have a greater attraction to the market as compared to LF and HF spectrum, due to all the advantages of UHF over LF and HF, which has been stated in section 1.2. However, designing an RFID tag particularly in the UHF band involves unavoidable offset of the tag antenna performance, such as G_r , impedance bandwidth, detection distance and overall dimension of the tag (Rao et al., 2005). The detection distance is greatly affected by the G_r of the tag as the read distance is a function of the G_r and the G_r is affected by the compactness of the tag as well. The antenna's tag tends to have a better read distance because of the stronger backscatter fields reflected and absorbed by the reader antenna. But, large size tag antenna fails to gravitate in many applications because it is not efficient to be attached to some surfaces which require a smaller size tag antenna. So, miniaturizing the size of a UHF passive tag tends to preserve the attraction of the market while maintaining the same read distance as the larger size tag can be considered as a very challenging design for RFID engineers because there will certainly offset in between reducing the overall dimension of the tag and optimizing the tag antenna performance.

In the early design of UHF RFID, dipole structure was the most famous design as compared to other structure because of its omnidirectional radiation pattern and it was the first breakthrough of antenna design. However, dipole tag antenna performance was greatly affected when the metallic surfaces are in the vicinity of the dipole tag antenna (Dobkin and Weigand, 2005). To overcome such performance degradation, many researchers have been undergoing a lot of research to propose in designing a new structure which is suitable for RFID tag in vicinity of metal. In the previous research, some academics recommended a thicker dielectric material such as a substrate to mitigate the effect of metallic structures near to the tag (Kanan and Azizi, 2009). Later that, the inverted-F tag antenna structures (Chen and Tsao, 2010) also known as PIFA structures and folded-patch structures (Cho et al., 2008) have been proposed to insert a ground plane underneath the dielectric substrate to segregate the radiating patch from the back-metallic surface. But, the deficiency of these antenna structures is very huge in dimension, profile wise is large, inflexible, and very costly to produce due to the fabrication process is much complicated.

As therefore the beginning stages of UHF RFID tag design, the first thing to be considered is where the tag to be attached on the surface. When the back-metal material with dielectric constant which is different from what is has been designed for the tag, the resonant frequency will be shifted to other frequency other than the desired frequency and will ultimately leading to impedance mismatch and degradation of the tag performance (Xi and Ye, 2011). This is because different materials have different conductivity, dielectric constant, and magnetic constant which constitutes to different absorption loss and reflection loss to signals in radio frequency as it propagates to these materials (Ott, 2009), which can affect the realized gain of the tag antenna ultimately lead to the read range of the tag decrease drastically. As a result, designing RFID tag antenna has to be taken care, according to the application as the overall performance of the tag reduced because of loading effect, if the object is vicinity of it. In the current market, especially in the retail industry, the demand for RFID tagging technology has been increased tremendously due to time efficiency and cost saving. Since the goods and items came into different sizes and shapes. Therefore, compactness tag is very much desirable so that it can be conveniently attached to the surfaces of the goods and items. As a consequence, maintaining the tag performance while the size of the tag can shrink into the desirable requirement of the market is very essential and huge

challenges for RFID tag design because the offset in between reducing the overall dimension of the tag and optimizing the tag antenna performance.

1.4 Aim and Objectives

The aim of this final year project is to design a miniaturized passive UHF RFID tag which can produce adequate read range performance mounted on a substrate surface will give rise to quasi-isotropic radiation pattern. On the other hand, this project investigates a new breakthrough of giving the radiation pattern of quasi-isotropic in a substrate-mountable, which most of the current UHF RFID tag design metal-mountable are in the bore-sight radiation pattern. The antenna structure consists of a pair of driven strip-lines and a split-ring resonator (SRR) with two extended strips on the same side of the substrate. The microchip is placed in the meandered T-match loop for impedance matching purpose and notches are etched around the stub for fine frequency tuning, which are made by depositing a thin layer of copper with thickness a of 9 μm mounted on a flexible PET (polyethylene terephthalate) substrate with a thickness of 50 μm . The Duroid[®] 6010 laminates substrate (RT/duroid[®] 6010, 2017) with a thickness of 3 mm is mounted on another flexible PET substrate with a thickness of 50 μm followed by a ground plane. The Duroid[®] 6010 laminates substrate can be easily found in the market and chosen as substrate for the tag antenna to isolate the radiating conductive material from the material surface and the fabrication method is much easier because of the ease of drilling and milling processes. The flexible PET substrate can be easily found in the market as well. The reason of implementing the flexible PET substrate is to increase the tag's durability and to avoid it from being easily damaged when handling with measurement. Apparently, the first objective is to search for different types of antenna structures which can be mounted on substrate surface and give rise to quasi-isotropic radiation pattern, and improve the performance of the selected antenna structure. Once the desired antenna structure is selected, the second objective of the final year project is to employ scale down tag's size methods that have been researched by another scholar for UHF tags, which include folding, high-impedance stubs shortening, meandering the slotting on the T-match loop and increasing the dielectric constant of the substrate to further scale down the size of the tag without embedding extra lumped elements to save cost. Once the objectives are achieved, the RFID tag is ready for fabrication and measurement is carried out in an anechoic chamber for read-distance pattern measurement in each

of the 3 planes. After that, the design parameters will be analysed by carrying out the parametric analysis to check the effect of frequency tuning. Lastly, the generated radiation pattern of the RFID tag is discussed and comparison of RFID tags designed by other authors which were able to generate quasi-isotropic radiation pattern is compared to see the differences.

1.5 Limitation and Covered Scope of the Project

The overall scope of the study of this RFID design is making use of the time-varying electromagnetic concept where all the theory and practical results were always fulfilled with the Maxwell's equations. The time-varying electromagnetic is able to propagate in a very long distance in free space, especially in the range of the UHF spectrum. The RFID tag design is quite an interesting research topic to tackle because it is making use of the evolvement of the conventional half wave dipole antenna which has been a studied long time ago in antenna theory. In antenna theory, the half wave dipole antenna is the most extraordinary antenna ever been discovered as it is able to generate the omni-directional radiation pattern which is very prominent in many applications in RFID tag design. However, most of the RFID tag design is not able to generate omni-directional patterns because of the dipole type structure RFID tag is hugely jeopardised by the materials which is mounted on it which resulted in different types of antenna structures being studied together that the new structures are able to provide omni-directional pattern regardless of the tag mounted on which surfaces is the most challenging part in RFID tag design. Moreover, the impedance matching is one of the most important factors in the study. Therefore, the chip impedance to be conjugated match with the RFID tag antenna structure is very important as to minimise the electromagnetic field energy being reflected back instead of transmitted to the chip. As a result, impedance matching study design is very important so that the maximum signal magnitude is able to be transferred between the chip and tag's antenna at the desired UHF spectrum without reflection. The radiation pattern of the designed RFID tag can be solved by using Maxwell's equation. However, it is too complicated to solve it manually, simply because the mathematical manipulation is too complex. Therefore, most of the time it is solved using the CST MWS to achieve the desired radiation pattern. As a result, the study of electromagnetism concept is very important in order to explore new research in RFID tag design.

As for project's limitation wise, the finalised design RFID tag is not able to generate omnidirectional pattern when the metal is being mounted by the tag. When the finalised design RFID tag is mounted on the metal platform, it becomes a bore-sight radiation pattern tag and the resonant frequency shifted out of the desired resonant frequency. Therefore, this is one of the weaknesses of proposed RFID tag. The proposed strip line is also very narrow in size as therefore the first design is a narrow T-match loop as shown in *Figure A.1* in appendix without meandering in the size of 0.2mm thick is to be fabricated using the conventional chemical etching as the tolerance is simply too high which jeopardised my first proposed RFID tag design before change it to meandered T-match loop as shown in figure as the fabricated narrow T-match loop structured as shown in *Figure A.2* in appendix is resonated at 1050 MHz which is far away from the UHF spectrum. This is also one of the limitations in my study as the university does not provide a good PCB etching technology, which limits our tag design structure is not favourable in narrow strip line RFID tag structure design.

1.6 Contribution of the Study

This proposed RFID tags contributed to more research on SRR structure as SRR structure exhibits the behaviour of magnetic dipole and electric dipole perpendicular with each other (Pan et al., 2014). Because of the properties of SRR, it is able to generate quasi-isotropic radiation pattern when it is mounted on any platform except metal platform. Therefore, the quasi-isotropic radiation pattern is very useful for RFID tag design as the tag can be faced in any position with respect the reader antenna to detect it except at the angle of $\theta = 0$. Hence this is very useful for applications, particularly tracking system where the objects which the tag is installed in moving in any directions all the time as compared to bore-sight RFID tag is not possible to do as if the object moves with respect to the reader is not in bore-sight direction as missing of tracking is very much possible and the target will be lost. The read distance in the xy-plane is in the ranges of 8.0 m to 8.4 m by using the equation (3.18) below. As a result, long range read distance and quasi-isotropic radiation pattern is the most optimized result ever achieved in RFID tag design. Therefore, any long range tracking applications up to 8.0 m is very much desired by designing the RFID tag as proposed in this final year project as a commercial RFID tag to help the industry which required long range tracking system. However, this only defect of this finalised designed tag is when the metal surface

is being placed by the tag, performance will be deteriorated as this needed to be aware when it is implemented in the commercial area level.

1.7 Outline of the Report

Overall five chapters will be consisted in this report. The first chapter begins with the history of how RFID is being developed trace back to World War II and slowly being enhanced to current RFID technology, which is functioning in the UHF band, and also the comparison and advantages of the RFID technology over the barcode technology. After that, a brief comparison of different operating spectrums across all the countries over the world. Next, the comparison between active RFID tag and passive RFID tag was being introduced. On top of that, the problems and challenges currently face by engineers to design UHF RFID tag for current industry market was being mentioned and ways to mitigate the problem to achieve the optimum performance that can best suit for industrial applications. Lastly, in the last part of this chapter, the objectives and aim to achieve miniaturization and quasi-isotropic radiation pattern tag antenna has also been defined.

In chapter 2 focuses on the literature review in which the methods for antenna structures that are commonly designed for quasi-isotropic radiation pattern UHF RFID tag which assist the author's current design to achieve such performance when it is mounted on a substrate is discussed briefly to achieve the objective. The design of folded patch is investigated, which is to help the author's design in quasi-isotropic radiation pattern with folded patch structure. The importance of impedance matching is discussed as well. After that, the techniques to reduce the size of the UHF RFID tag proposed by other researches is reviewed which is able to assist the miniaturization process of the author's tag. Furthermore, the advantages and disadvantages of implementing such technique for miniaturization process are also elaborated and discussed, followed by the typical requirement done by the previous researchers to implement passive UHF RFID tag design is also discussed.

In chapter 3 sums up the methodology on the systematic way of proper design of UHF RFID tag. A flowchart has been illustrated on the proper way of designing of UHF RFID tag to act as a step-by-step guideline for UHF RFID tag design. Lastly, the actual UHF RFID tag

prototype measurements in an anechoic chamber is briefed and the tag antenna parameters for the read distance is derived in a systematic manner.

In chapter 4, the introduction of passive UHF RFID tag and its early design until the current design is briefed and the design of the proposed tag which is an electrical small planar folded patch composes of a rectangle Split-Ring Resonator (SRR) which is excited and fed by a meandered T-match for substrate-mountable applications is discussed. The high dielectric constant and shorting stub is used to scale down the tag's size and pair of notches is used to tune the fine resonant frequency and meandered T-match loop is implemented for impedance matching are discussed. The working principle of quasi-isotropic radiation pattern is discussed as well. Parametric analysis of the key parameters is done to identify the tuning sensitivity and the realized gain radiation pattern is simulated by using CST MWS across the E-planes and H-plane. Then, practical real life scenarios to determine the tag's performance were also being done. The last part of this chapter compares the proposed tag with other literature's tag in terms of performance and tag configuration.

Lastly, in chapter 5, a conclusion to sum up the thesis as well as the disadvantages of the proposed tag currently faced are discussed and future amendment due to technology advancement to improve the current design of the proposed tag is suggested and listed.

CHAPTER 2

LITERATURE REVIEW

2.1 The UHF Passive RFID Tag design following the Conventional Method

Designing a UHF passive RFID tag always comes with a lot of responsibilities for RF engineers, especially with the various parameters which were very sensitive to achieve and the trade-off between the parameters in order to achieve a good performance for the particular UHF passive RFID tag for the desired application. Hence, RF engineers are able to achieve a good practice to design the tag in such a way that the tag size is compact and can have a good performance for the following design requirement guideline. The design requirements can be summarized as listed below:

- **Standards for the usable bandwidth and the power transmitted by the reader**

Different countries have their different targeted usable bandwidth and maximum magnitude of transmitting signals to the passive UHF RFID tag. For example, the standard body “Federal Communication commission (FCC)” use by the United States, which the standard stated for applications like UHF RFID has the usable bandwidth between 902 MHz to 928 MHz, and up to 4 W EIRP maximum magnitude of transmitting signal from the reader. In Europe, the standard regulatory body “European Telecommunication Standards Institute (ETSI)” has governed the usable bandwidth from 865 MHz to 868 MHz, and up to 3.28 W EIRP maximum magnitude of transmitting signal from the reader. Whereas in China, no particular regulatory body has been adopted by China yet as China’s RFID standards are coming soon (China’s RFID standards, 2018). China adopted the operating bandwidth from 920.25 MHz – 924.75 MHz with maximum ERIP of 2W. As a result, the tag design has to fulfil the regulated operating bandwidth and reader transmitted power in the country that is intended for.

- **The size and dimension for the desired tag:**

As a rule of thumb, the larger the size of the tag antenna structure, the better it receives electromagnetic waves from reader antenna, and the stronger the gain of the backscattered radiation from the tag antenna. In other words, the longer the read distance of the tag when its size is larger. However, there is always a trade-off between the tag's performance and the dimension of the tag as their relationship is inversely proportional. Therefore, it is important to know the optimum condition at which the application is suitable to use for.

- **The tag reading performance:**

The tag reading performance is the most important parameter as it determined the maximum read distance between the tag and reader antennas both, which is required by the customer. It also specifies the read distance pattern in the 3D radiation pattern, which targeted at which the angular-distance in the spherical coordinate system has the higher radiation gain. The angular-distance at a specific location in the spherical coordinate system which has higher radiation gain gives rise to a longer read distance with respect to the reader antenna.

- **Materials at which the tag is mounted on:**

The tag attached to the materials will greatly influence the performance of the tag. This is because the materials' dielectric constant, ϵ_r will give rise to the effective electric field path flowing is altered, which the tag structure effective dielectric constant will be changed as well. This will vary the tag's resonant frequency, which leads to an enormous deterioration of the tag antenna performance as matching is not achieved at the UHF spectrum as well as the matching is very bad. Hence, the tag's performance is greatly dependent on the back objects made out of what materials which the tag is to attach or adjacent to the tag.

- **Materials use to design the tag and its influence on the costing factor:**

The performance of the tag antenna is greatly influenced by the materials used to fabricate the structure. A Tag antenna structure which made up of aluminium conductor is very common practice in the market because the production cost is very cheap, although the performance parameters of the tag are a little poorer. Whereas, in the early design, RF engineers used silver conductor as the antenna structure. It has exquisite RF performance and it gives rise to the tag

antenna to achieve very long reading distance, but the cost of silver conductor is very expensive and not economically friendly in large volume manufacturing. Furthermore, high dielectric constant low loss tangent substrate has also been implemented to effectively shrink down the dimension of the tag. However, the dielectric losses and the cost have to be taken into account. As a result, materials selection also gives rise to some trade-off of tag antenna structure design.

2.2 Challenges of Impedance Matching Techniques between the UHF tag Antenna and the Microchip

In the market of different manufacturers, the RFID microchip available for the UHF RFID technology is an energy storage device which presents a large capacitance imaginary part of the impedance approximately in the range between -100Ω to -400Ω depending of the chips being used (Marrocco, 2008). In contrast, for its resistance part, the effective resistance present in the RFID microchip is very low in magnitude usually in the range of 5Ω to 20Ω depending on the type of microchip designed by the manufacturers. In the author's proposed tag design, impedance characteristic at 915 MHz of $14.56 - j161.25 \Omega$ Monza 5's microchip (IPJ-W1600, 2016) manufactured by Impinj is used. From the microchip impedance characteristic itself is more capacitive. Hence, impedance matching can be achieved by making the antenna structure of the tag to be more inductive to compensate the capacitive part of the microchip and near to equal resistive for both of them. The microchip is manufactured at low cost in the market, therefore, lumped elements embedded in the external circuit to achieve a conjugate match is not advisable. As a result, designing the tag antenna structure to achieve a conjugate match to the microchip is not an easy job for RF engineers. In fact, this is one of the most challenging tasks to do so in the overall procedure of RFID tag design. Several UHF RFID tag antenna structures have been widely adopted by RF engineers to achieve quasi-isotropic radiation pattern will be discussed in the following subsections.

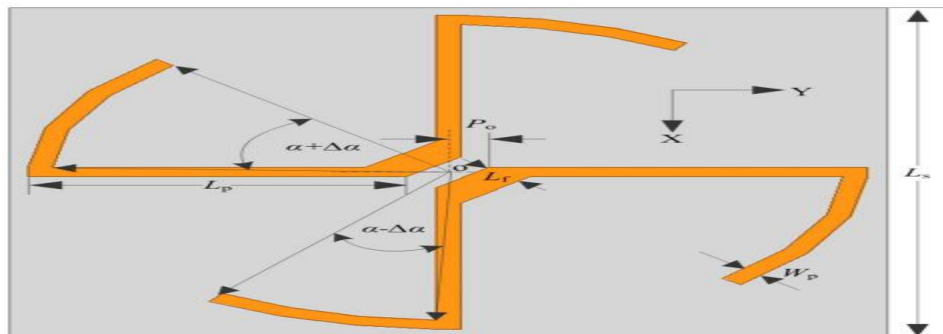
2.3 Quasi-Isotropic Radiation Pattern

In general, ideal quasi-isotropic radiation pattern, which the antenna radiates consistent polarizations in every direction in the spherical coordinate system is proven to be practically

impossible (Mathis, 1951). In the current stages, there are several antenna structures which are able to achieve near-isotropic radiation pattern. There are three main methods which researchers have found to be practically possible to achieve. The first method is the structure which consists of numerous monopoles or dipoles separating within some distance embedded in the radiating patch. The second method makes use of the combination between electric and magnetic dipoles with the perpendicular radiation patterns. Lastly, the third method employs of only conducting loops that has electric and magnetic dipoles linked function with it. The following sub-sections will discuss these three methods in detail to achieve quasi-isotropic radiation pattern.

2.3.1 The First Method to Achieve Quasi-Isotropic Radiation Pattern

The first method adopted numerous monopoles or dipoles conductive patches that are separated within some distance. In the structure shown in *Figure 2.1 (a) below* (Pan et al., 2012), the author uses the structure consisting of two crossed curved dipoles conductors deposited on one side of an FR4 1mm thick substrate. By varying the length of the two crossed curved dipoles, the quasi-isotropic radiation pattern is able to achieve in the frequency range of 2.4 GHz to 2.48 GHz in which the structure is able to employ in the UHF range as well by changing the dimensions of the crossed curved dipoles. The realized gain of such structure varies between -1.88 dB to 1.82 dB in the coverage of 97% of the full space. At maximum realized gain of 1.812 dB employed in the RFID design by using the same Monza 5 chip, the read distance is about 20m. However, the structure of the antenna is quite large in order to maintain the same performance at UHF spectrum, although the structure currently in the spectrum of 2.4GHz is $32 \text{ mm} \times 32 \text{ mm} \times 1 \text{ mm}$ ($0.256\lambda \times 0.256\lambda \times 0.008\lambda$) is considered quite compact. *Figure 2.1 (b), (c), (d) and (e)* (Pan et al., 2012), shows the radiation pattern in the x-y plane.



(a)

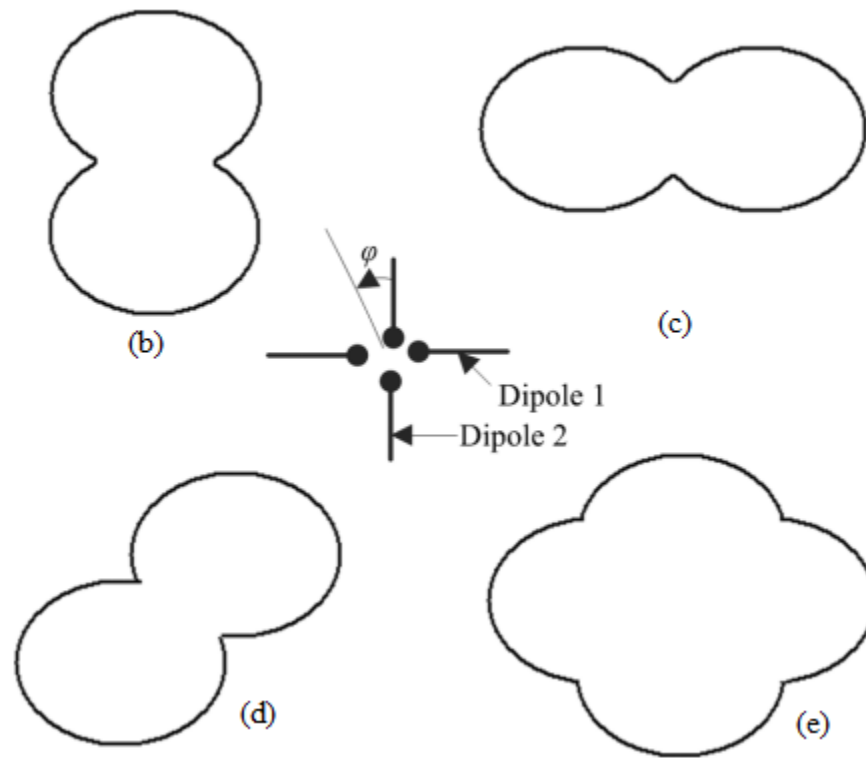
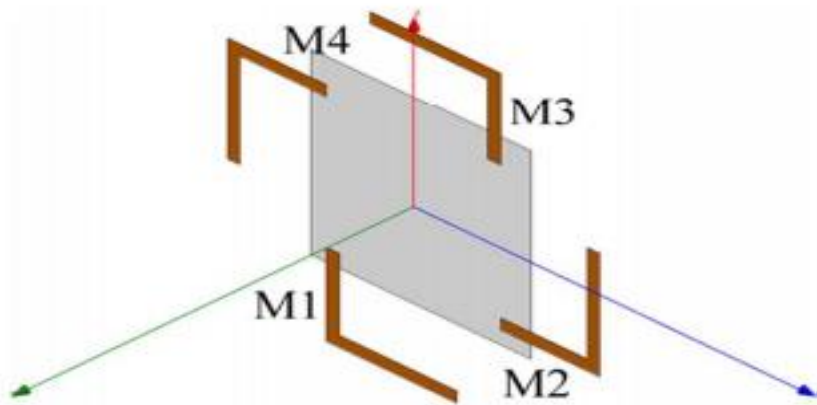
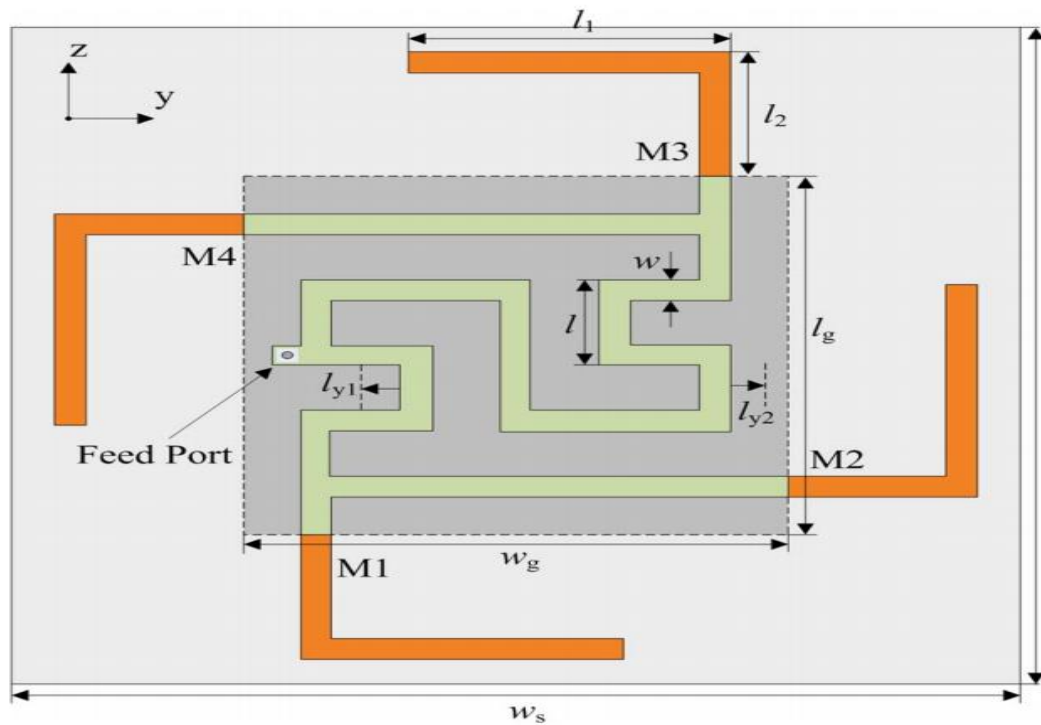


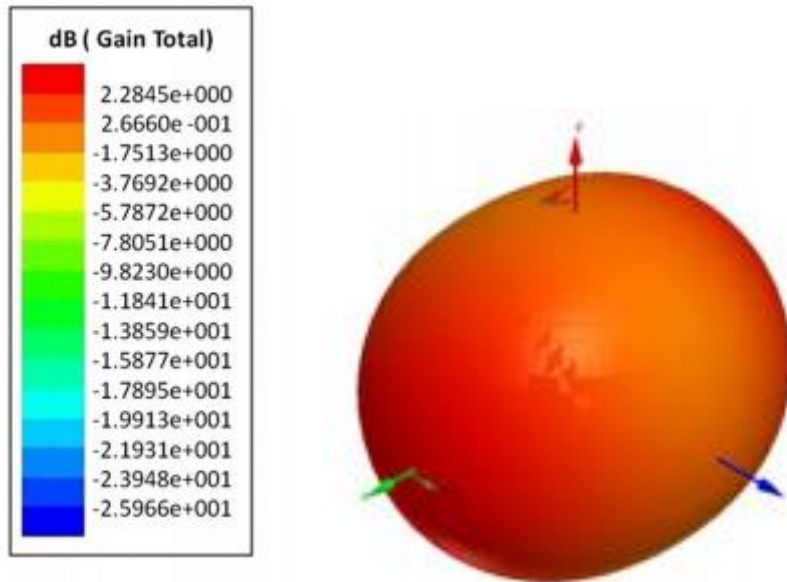
Figure 2.1: (a) Two crossed curved dipoles antenna structure, (b) Only dipole 1 is functioning, (c) Only dipole 2 is functioning, (d) both dipole 1 and dipole 2 are operating with equal magnitude of current feeding, (e) both dipole 1 and dipole 2 are operating with 90° phase-shift of current feeding (Pan et al., 2012).

Next, another kind of planar antenna structure was identified and studied which will be able to provide quasi-isotropic radiation pattern. In this structure, the antenna structure proposed by the author consists of four occurring in an order go around in circle L-shaped monopoles printed on one side of an FR4 0.8mm thick substrate were shown in *Figure 2.2(a)* below (Deng et al., 2014). Based on the rotated field method, the coverage of wide bandwidth from 2.3 GHz to 2.61 GHz was achieved with a maximum realized gain of 2.2845 dB. If this structure is implanted with UHF RFID, the read distance of about 22m is able to achieve if the same performance is able to perform at UHF spectrum matches the microchip. The dimension of proposed antenna is 45 mm x 45 mm

x 0.8 mm ($0.36\lambda \times 0.36\lambda \times 0.0064\lambda$). However, the implementation in RFID UHF was very large in dimension as well. Sequential-phase feeding method was employed varies from 0° , 90° , 180° , and 270° for such antenna structure. Hence, this structure is not quite suitable in RFID as the microchip will not vary its power in the way of phase shifting because the reader antenna will only emit certain EIRP in fixed frequency and phase shift to excite the tag antenna. So the tag antenna will only energize in 0° phase shift which leads to the quasi-isotropic radiation pattern is not achievable.



(a)



(b)

Figure 2.2: (a) Four L-shaped monopoles antenna structure in y-z plane, (b) 3-D radiation pattern of the particular antenna structure when the sequential-phase feeding method activated all 4 monopoles with phase-shift of 90° of each other (Deng et al., 2014).

These first proposed antenna structure which can achieve quasi-isotropic radiation pattern has the advantages of compact profile, low cost, light weight, simple antenna structure and easy to fabricate. However, the second proposed antenna structure having the disadvantages of complex structure and feeding network. As a result, the first proposed antenna structure has a chance to be part of the RFID tag antenna implementation for quasi-isotropic radiation pattern. However, for both structures, complex feeding network of phase difference 90° must be employed in order to function fully in quasi-isotropic radiation pattern.

2.3.2 The Second Method to Achieve Quasi-Isotropic Radiation Pattern

The second method utilizes the combination between the electric dipoles and magnetic dipoles with the perpendicular radiation patterns. A monopole is placed orthogonally with respect to the ground plane adjacent to two magnetic slots placed in parallel to the ground plane. Such structures are able to achieve the quasi-radiation pattern as well, but the structure is not planar with the cost of fabrication and it is not practically convenient for certain applications. The proposed antenna structure by the author was shown in *Figure 2.3* below (Long S., 1975).

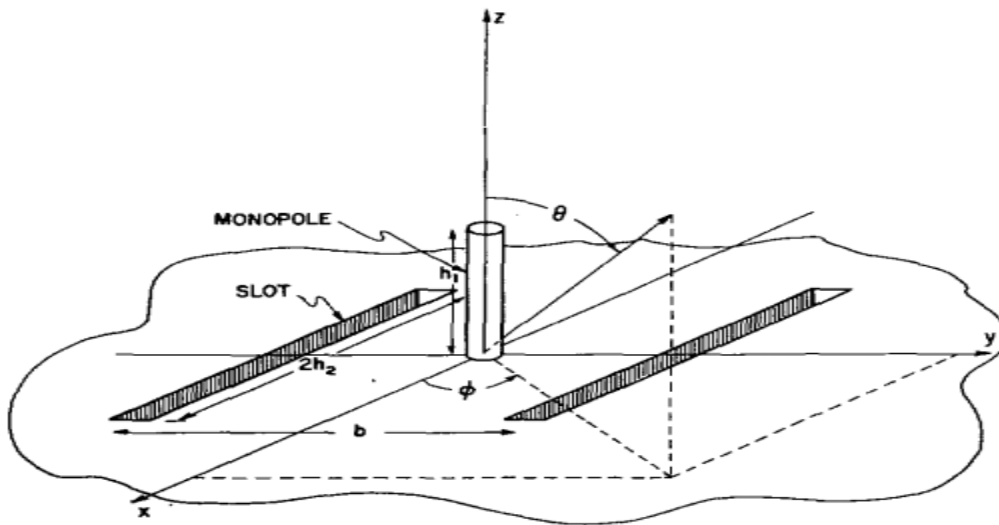


Figure 2.3: Combination of two magnetic slots with an electrical monopole orthogonally structure (Long S., 1975).

After that, another antenna structure was investigated, which is able to provide quasi-isotropic radiation pattern is a dielectric resonator antenna with the small ground plane deposited at the back of the substrate. The small ground plane acts as an electric dipole while the dielectric resonator antenna acts as a magnetic dipole. The equivalent effect of this structure behaves as the electric dipole perpendicularly with the magnetic dipole. The maximum realized gain of the antenna structure is 3.79 dB, read range detected about 26m in RFID implementation provided the

same performance was able to perform at UHF spectrum. The antenna structure has a compact size of 27 mm x 27 mm x 14.5 mm ($0.22\lambda \times 0.22\lambda \times 0.12\lambda$) in 2.4GHz and that would be 72 mm x 72 mm x 39 mm in the UHF spectrum. The implementation which is very large in size and not suitable for certain applications. *Figure 2.4* (Pan et al., 2014) below shows the proposed configuration of the antenna structure and the radiation patterns.

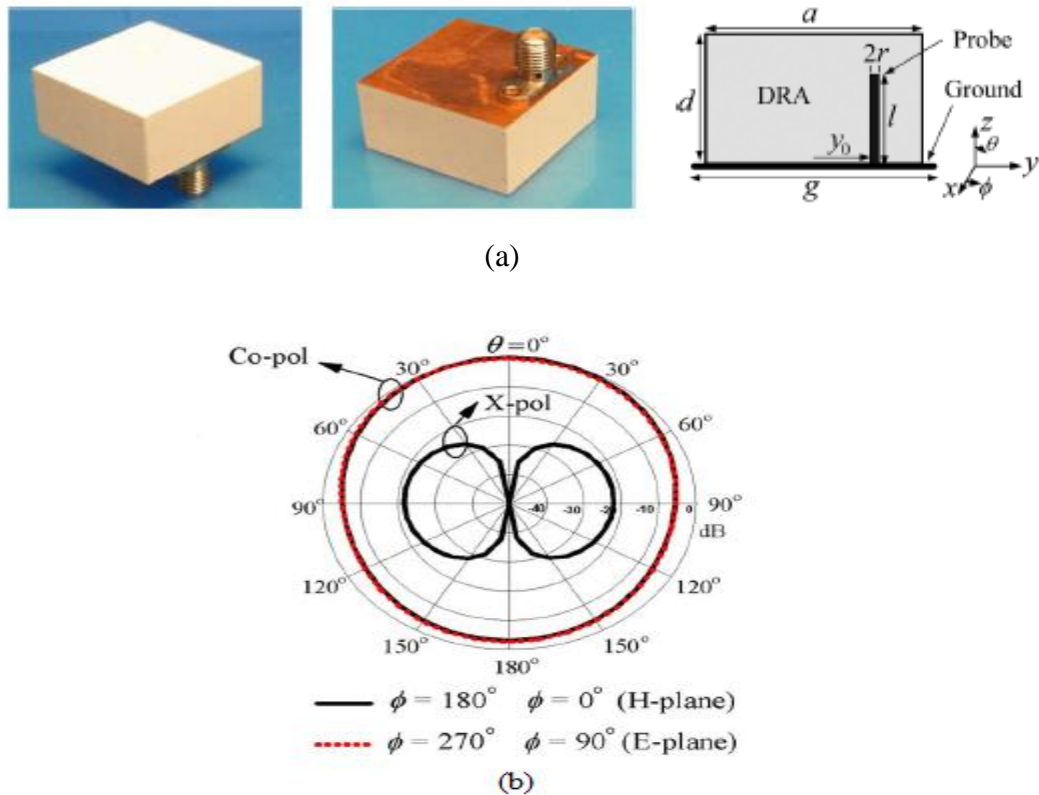
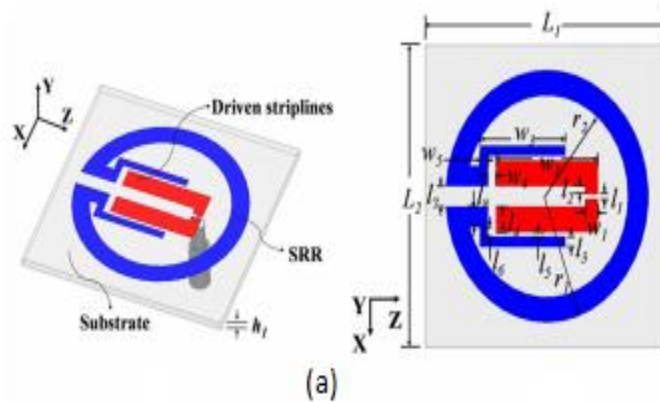


Figure 2.4: (a) Proposed dielectric resonator antenna structure, (b) Field patterns generated which fulfil quasi-isotropic radiation pattern. (Pan et al., 2014)

Over the past few decades, the dielectric resonator antenna structure has been studied enormously by the researchers as such antenna structure attracts a lot of features in certain application as the advantages of the antenna structure is able to provide small size, less in weight, low dielectric, conductive losses and without complex feeding network, ease of excitation and relatively huge impedance bandwidth which attracts the implementation in RFID design to be in consideration. However, this method is not electrically small enough to achieve practical usage.

2.3.3 The Last Method to Achieve Quasi-Isotropic Radiation Pattern

Finally, the last method makes use of solely conducting loops with the function of having its own equivalent electric and magnetic dipoles. Split-ring resonators itself can be function as electric dipole and magnetic dipole perpendicular to each other (Wang et al., 2019). Hence, quasi-isotropic radiation is able to achieve by just solely the split-ring resonators itself. In reference to *Figure 2.5 (a)* (Wang et al., 2019), the antenna structure consisted of a pair of driven striplines and a split-ring resonator with two extended strips on the same side of the substrate to achieve magnetic coupling effect. The dimensions are electrically small as $60 \text{ mm} \times 60 \text{ mm} \times 0.16 \text{ mm}$ ($0.154\lambda \times 0.154\lambda \times 0.0004\lambda$). Hence, this antenna structure is practically compact and possible for UHF RFID application as the dimension was considered electrically small. The maximum realized gain of the proposed antenna structure is -0.6 dB , which in turns if it is able to perform the same realized gain in the UHF spectrum, such antenna structure is able to detect up to 20m in range. The radiation pattern was shown in Figure 2.5 (b), (c), (d). As a result, this kind of configuration was able to provide quasi-isotropic radiation pattern as well.



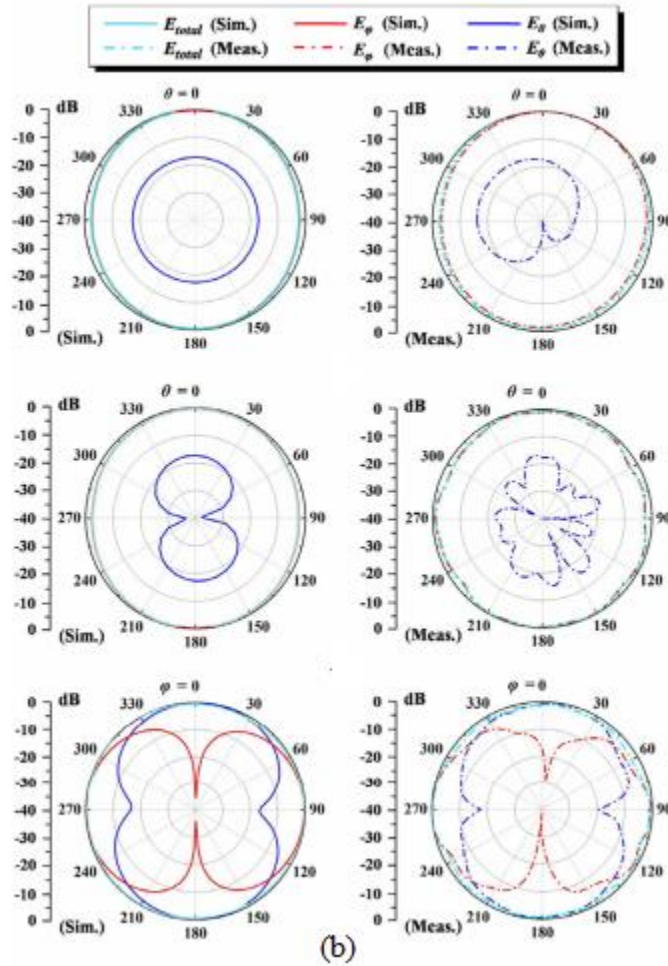


Figure 2.5: (a) Proposed split-ring resonator with driven striplines antenna structure, (b) Far field radiation pattern at x-z plane, y-z plane, and x-y plane (Wang et al., 2019).

As a conclusion of the three methods, structure to achieve quasi-isotropic in method 3 is the most suitable as it does not require complex feeding network, complex fabrication process, and it is electrically small. Therefore, for the current research stages, method 3 antenna structure for UHF RFID application is the most suitable because of the ability to accomplish omnidirectional radiation pattern without the disadvantages mentioned above.

2.3.4 Theory to Generate Quasi-Isotropic Radiation Pattern

In order to achieve quasi-isotropic radiation pattern, magnetic dipole and electric dipole have to place orthogonally also known as complementary antenna as shown in *Figure 2.6* (Pan et al., 2014) below. From antenna theory, it is confirmed that the x-z plane (E-plane), y-z plane (E-plane), and x-y plane (H-plane) of an electric dipole are in the shape of a figure-8 and a figure-O, respectively. For magnetic dipole, the shape of a figure-8 and of a figure-O interchange with the electric dipole as E-plane contains the figure-O and H-plane contains the figure-8 (Luk and Wu, 2012). Hence, the null-field direction at each of the dipoles are superimposed, making it to have a quasi-isotropic radiation pattern. By analysing the sum of vectors individually contributed by each of the dipoles (Long S., 1975), the electric fields (E-fields) of the magnetic dipole align in the x-axis ($E_{m\theta}$, $E_{m\phi}$) and the E-fields of the electric dipole align in the y-axis ($E_{e\theta}$, $E_{e\phi}$) are given as follows:

$$E_{m\theta} = jI_m l_m F_m \sin \phi \quad (2.1)$$

$$E_{m\phi} = jI_m l_m F_m \cos \theta \cos \phi \quad (2.2)$$

$$E_{e\theta} = -jI_e l_e F_e \cos \theta \sin \phi \quad (2.3)$$

$$E_{e\phi} = -jI_e l_e F_e \cos \phi \quad (2.4)$$

It is worth mentioning that the fields of magnetic dipole deduce from the results of a small electric loop for a magnetic moment of $I_m l_m = j\omega\mu IS$ (Balanis, 2005). When the phase difference, δ . F_e and F_m are just some constants. The respective field components of the two dipoles can be defined as follows:

$$\begin{aligned} E_{\theta}^T &= E_{e\theta} + E_{m\theta} \\ &= -jI_e l_e F_e \sin \phi \cos \theta + e^{j\delta} jI_m l_m F_m \sin \phi \end{aligned} \quad (2.5)$$

$$\begin{aligned} E_{\phi}^T &= E_{m\phi} + E_{e\phi} \\ &= -jI_e l_e F_e \cos \phi + e^{j\delta} jI_m l_m F_m \cos \theta \cos \phi. \end{aligned} \quad (2.6)$$

Let $\eta l_e I_e = l_m I_m$, the total field E_T is then given by

$$E_T = \sqrt{|E_{\theta}^T|^2 + |E_{\phi}^T|^2} = IlF \sqrt{1 + \cos^2 \theta - 2 \cos \theta \cos \delta}. \quad (2.7)$$

From equation 2.7, the magnitude of the total field, E_T generated is dependent on δ and θ and independent on φ . This is proven that at the x-y plane, the field generated is omnidirectional because regardless of the value of φ , E_T has been always constant. Hence, quasi-isotropic radiation pattern is achieved.

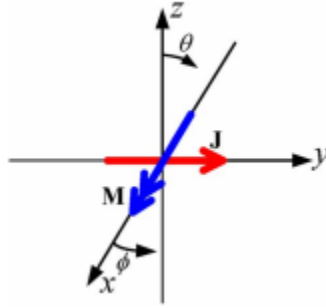


Figure 2.6: Red in colour is the magnetic dipole align in the y-axis and blue in colour is the electric dipole align in the x-axis (Pan et al., 2014).

2.3.5 Folded-Patch Antenna

Next, another new kind of printed antenna is done by printing the conductor to the bendable substrate normally made of Polyimide or PET also known as the folded patch antenna. Instead of printed on the conventional way in the physical stiff substrate. It is very easy to make and design as the fabrication process is very simple and low cost. By referring to *Figure 2.7* (Moh et al., 2018) below, the aluminium metal part which consists of stubs, radiating patch and ground flat plane is done by etching away the unwanted aluminium metal part and printed on the bendable substrate. The folded patch tag fabricated prototype as shown in the flexible inlay in *Figure 2.7 (a)* can be wrapped easily around a soft-foam with relative permittivity near to free space.



(a)



(b)

Figure 2.7: (a) Unwrapped fabricated inlay, (b) Complete folded tag's antenna wrapped around a soft-foam (Moh et al., 2018).

By referencing to *Figure 2.7* again, a tag attached to the metal RFID applications done by the authors with size of $40 \times 25 \times 3$ (all in mm). But, the furthest detection distance of 5 m is also achievable when attached to the substrate. Therefore, this type of tag designing is very good as the shorting stubs to short the both ground plane and patch path can make in a good location as they were aligned exactly with each other. Hence, tolerance of the tag fabrication can be reduced. Apart from that, this type of tag design together with the bendable soft-foam substrate as it is able to mount on any non-linear material.

2.4 UHF RFID Tag dimension Scales down Approach

In the current design stages, many of the researchers have found a way to solve the problem of any materials adjacent to the tag deteriorates the tag antenna's performance. However, such tag is dimensionally in electrically large and it is not able to attach to some objects in a practical manner. Hence, the profile to scale down the dimension of the tag is necessary to study in order for practicability for certain applications. However, the small tag will not resonate in the UHF spectrum because it will resonate above UHF spectrum. Apart from that, designing an RFID tag particularly in the UHF band involves unavoidable offset of the tag antenna performance, such as G_r , impedance bandwidth, detection distance and size of the tag (Rao et al., 2005). As a result, it is most desirable to optimize the few parameters to shrink the overall size of the tag electrically small in a way that it suits the application provided that the performance of the tag, such as the most important parameter which is the read distance is able to suit the application as well. In the next few sub-sections, discussion, analysis and comparison of different methods of scaling down the tag's size, which had been researched by other researchers to tune the tag antenna that resonates in the UHF spectrum is justified.

2.4.1 High Dielectric Constant Substrate

Increasing the dielectric constant of the substrate is one of the most conventional ways of miniaturizing the size of the tag. It utilizes the effect of slowing down the electromagnetic wave propagates as it passes through the high dielectric constant medium which in turns lower down the

resonant frequency. High magnetic constant materials have been used in the early development. But, researcher found out that high magnetic constant materials have much higher magnetic losses as compare with high dielectric constant material. Therefore, high magnetic constant materials are rarely used in UHF RFID tag design. One of the most commonly available high relative permittivity substrate being used in the commercial level RFID design with electrical characteristics can be found in (RT/duroid, 2017). However, high dielectric losses will be incurred in the tag's performance and high material cost when the tag is equipped with a high relative permittivity substrate. Based on *Figure 2.8* below (Babar et al., 2012), the author's tag design had chosen a malleable ceramic polymer composite substrate (BaTiO_3). The substrate having the electrical characteristics of dielectric constant = 12, a loss tangent of 0.01 and with thickness of 1.5 mm. A volume = $\pi \times r^2 \times h = \pi \times 16 \times 16 \times 1.5$ (all in mm) substrate which is being mounted by the author's tag structure, which consisted of a modified dipole structure in T-match planar is designed by the author. The proposed antenna structure has a read distance of near 2.3 m at resonant frequency when is mounted on a 100×100 (all in mm) back metal object. Apart from that, when the tag is attached to cylinder metallic material with a diameter of 12.5 mm, read distance of near 2.7m is achieved. As a result, the proposed tag structure is very compact with make use of high dielectric constant substrate technique. However, implementation of high dielectric constant is quite expensive as it may not practically cheap in large scale production. On top of that, high dielectric constant materials tend to increase the dielectric losses which in turn reduce the gain of the tag antenna by practical reasoning of the author's tag design is only able to achieve up to 2.7 m which may not be suitable for certain applications.

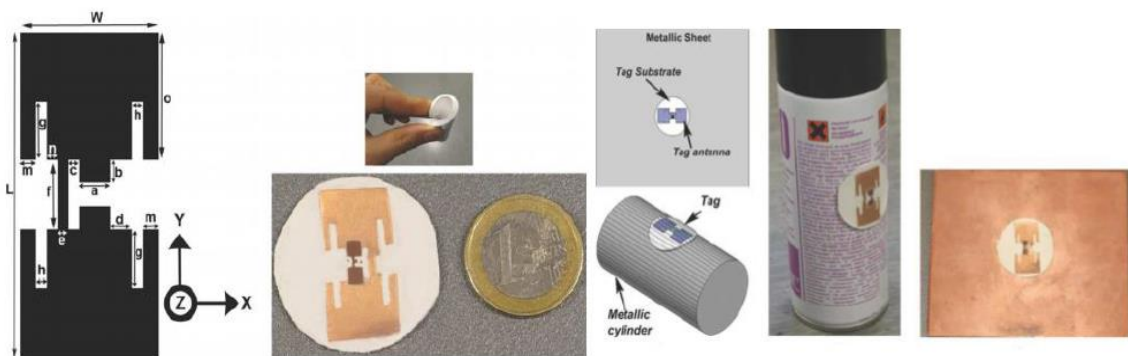


Figure 2.8: Proposed tag with high relative permittivity malleable ceramic polymer composite substrate (BaTiO_3) (Babar et al., 2012).

2.4.2 Shorting-Inductive Stubs and Via

One of the other methods to shrink tag compactness is discussed. It is done by shorting the conductive radiators patch to the ground plane by using several methods such as either short circuit inductive stubs, vias or walls. This will create a short circuit path to allow the surface current to flow between the radiating patch and the ground plane by using the above mentioned methods. The walls tend to have a more inductive reactance which can use to have better impedance matching to cancel out the capacitive reactance of the microchip as well as to optimize the tag resonates at UHF spectrum. From the reference of *Figure 2.9* (Chen and Lin, 2008), the largest lag of the author's proposed tag is 65 mm as which the typical resonant frequency will be greater than 1GHz. After that, when the author inserted the vias which shorted the radiating patch and the ground, the characteristics of the tag's antenna became more inductive and able to resonate in the UHF spectrum.

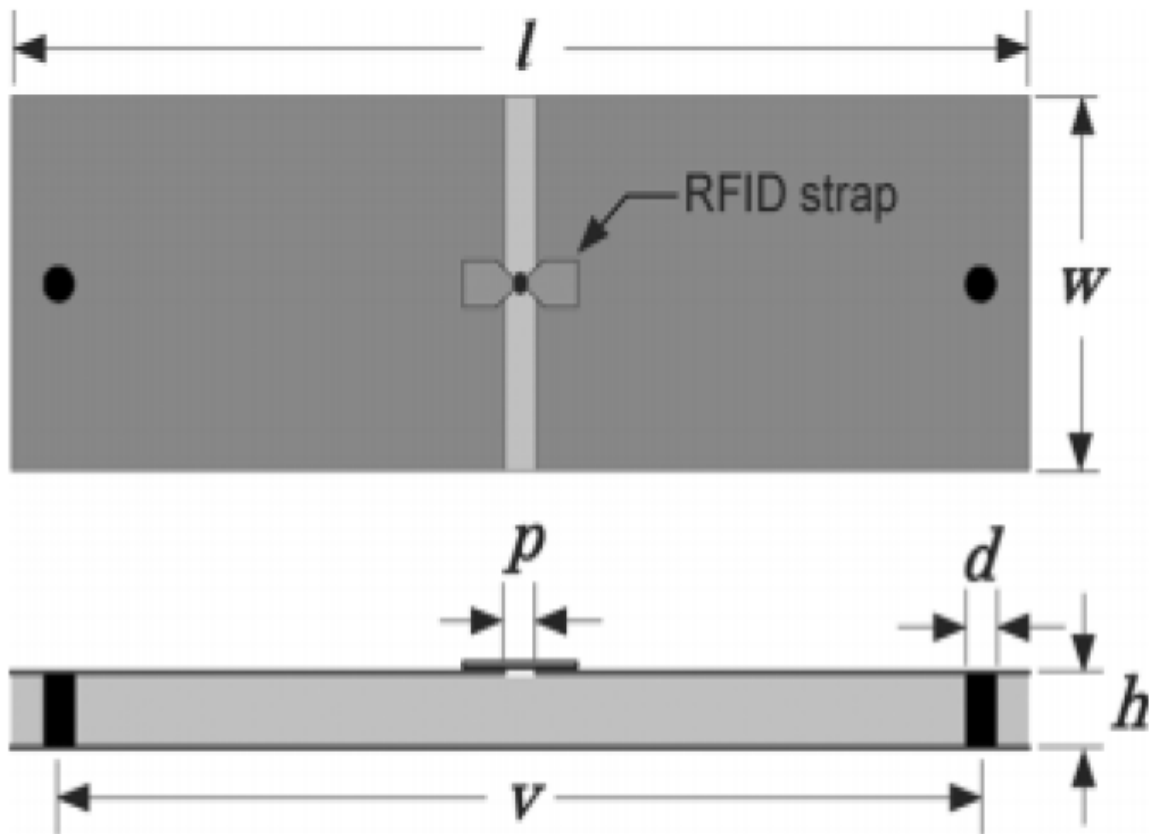


Figure 2.9: Proposed planar dipole tag antenna structure (Chen and Lin, 2008).

2.4.3 Meandering the Slotting on Radiating Patch

In this method, the authors make use of changing the different slotting method and analysed how it has affected the tag antenna performance, such as gain and matching impedance at that particular frequency by fixing the dimension of the tag antenna structure. The structure of the tag antenna is folded method with modified dipole into the dipolar patch with the dimension of $23 \times 16 \times 1.6$ (all in mm & $0.07\lambda \times 0.049\lambda \times 0.0049\lambda$). From *Figure 2.10* below (Bong et al., 2017), the most simple way of the structure is a radiating patch cut in half symmetrically with a recessed slot for the microchip feeding. In this structure, a G_r of near -2.1 dB resonates at 1.8 GHz is observed. At this particular resonant frequency, it is not in the UHF spectrum, although the G_r is able to give manageably satisfied read range. Hence, to mitigate the problem, the straight slot is replaced by different slotting patterns for extending the current flow path. With reference to *Figure 2.10* and *Figure 2.11* below (Bong et al., 2017) again, by changing the slotting pattern, the resonant frequency can be seen clearly reduces. However, the realized gain is also affected to a much lower value which reduced the effective read range of the tag. As a result, the author proposed to maintain the straight slot line with the current patch is still flowing in the middle slot line, but meandered the slot and splitting the patch into two halves instead of changing or additional slot on the dipolar patches. Refer to *Figure 2.11* (Bong et al., 2017) again, by meandering the middle slot has greatly reduced the tag resonant frequency as well as the realized gain is able to maintain at an acceptable read range.

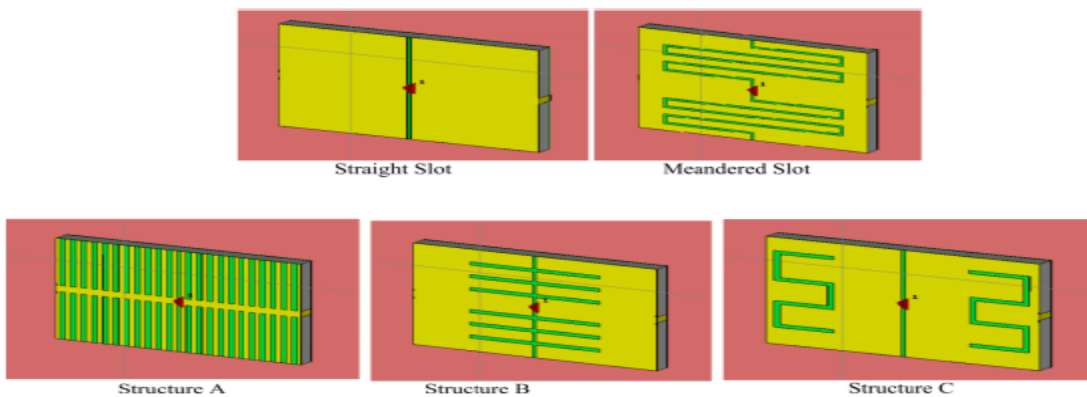


Figure 2.10: The comparison among different tag antenna structures by changing or adding additional slots (Bong et al., 2017).

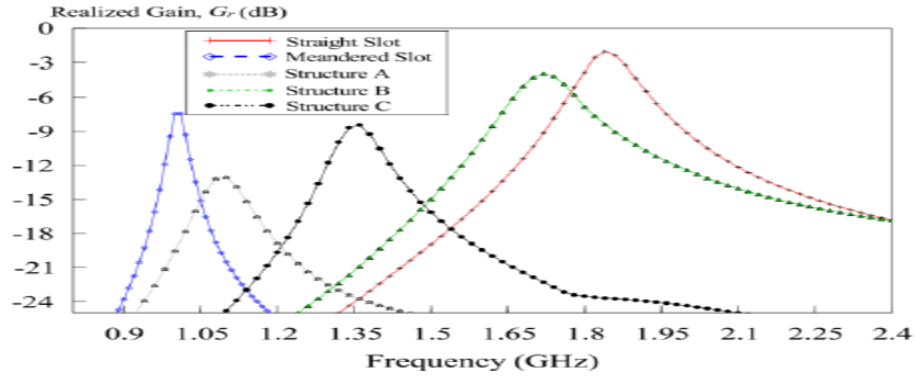


Figure 2.11: Realized gain against frequency profile for different tag antenna structures (Bong et al., 2017).

2.5 Summary of the Literature Review

As a summary of the literature review, section 2.1 talks about the design requirement of the passive UHF RFID tag design as what is proper procedure to achieve the most optimized results of the passive UHF RFID tag so that it can fit in properly for that particular application to maximize the full potential of the tag. In section 2.2, this section discussed about what are the challenges faced to obtain conjugated match impedance so that the desired frequency, full signal communication will be achieved in the RFID system with minimum reflection. After that, section 2.3 is discussed and break down into subsection 2.3.1 up to 2.3.5 and this section is discussed about what is the definition of quasi-isotropic radiation pattern and the three different methods of antenna structures that are able to generate quasi-isotropic radiation pattern and its theory to generate such pattern and finally in subsection 2.3.5 talk about what is folded patch antenna and what are the advantages of folded patch antenna in passive UHF RFID tag design. Lastly, in section 2.4 breaks down into subsection 2.4.1 to 2.4.3 talks about what are the techniques currently available to scale down the overall tag dimension while maintaining the tag resonant frequency in the UHF spectrum. The subsection 2.4.1 mentioned about using the high dielectric constant substrate, 2.4.2 talks about the shorting-inductive stubs and via and last but not least, in subsection 2.4.3 mentioning about meandering the slotting on the radiating patch.

CHAPTER 3

METHODOLOGY AND WORK PLAN

3.1 The Design Procedure of UHF Passive RFID Tag

In standard passive RFID tag design, the process or workflow of the design is shown in *Figure 3.1* flowchart below provides the basic guideline of all the different frequency spectrums of passive RFID tag design. For passive UHF RFID tag design, the costs, shapes, sizes, structure of the tag antenna may be different from other spectrum passive RFID tag, but the general procedure for the design is the same. Once the application for the particular UHF RFID tag is decided, the engineers whom design the tag is able to follow the guideline provided in *Figure 3.1* systematically because the tag performance is highly affected by its surrounding environment. For example, the environment with high humidity like freezer room or it is place vicinity to a metal will affect the performance of the tag drastically. As a result, if the UHF RFID tag is design adjacent to a metal or mounted on a metal, particularly for this kind of applications will ease the effort of the engineers.

First of all, the materials chosen to be fabricated for the tag antenna is very important as it will not only affect the performance of the tag, but also the cost of the passive UHF RFID tag. After that, the selection of the microchip is one of the most important factors to be considered as well for tag antenna design. This is because the impedance of the microchip is different from different manufacturers usually it is more capacitive because it is able to discharge its energy backscatter back to the reader. Hence, impedance matching can achieve by designing the tag antenna structure to be more inductance of the imaginary part of the tag antenna impedance to cancel out the imaginary part of the microchip so that maximum power transfer can be achieved. Apart from that, the microchip has also had its own read or write sensitivities which is important for tag design to determine the minimum power to activate the microchip. Next, selection of proper tag antenna structure is very important so that it can optimize the tag antenna performance suited for the particular application which can work well in that particular environment. For metal-mountable UHF RFID tag design, the best design antenna structure would be PIFA antennas,

microstrip patch antennas, and slot antennas. If it is for substrate-mountable applications, the best antenna structure would be dipole antenna.

After that, the tag antenna structure is decided and the results are simulated fully in CST MWS. The foundation of CST MWS is using the finite integration method discretizing each Maxwell Equation (governing equation in Electromagnetics) which is a simulation software that can model the real-life environments accurately. Since RFID technologies are working in far distance detection, it is done by far-field simulation in such a way that a distance of $\frac{1}{4}$ wavelength away from the modelled setup is set by default in the boundary condition. It is also assumed that zero reflection absorbing boundary is ensured. Design sequences such as impedance matching, performance optimization, and parametric study until the requirement for the particular application are fulfilled. In RF applications like RFID design, the performance of the tag is very hard to estimate by using analytical solutions. Hence, the advance numerical method like CST MWS makes use of the finite integration method to estimate the performance of the tag while it is simulated. The simulations are done by frequency spectrum sweeping from 800 MHz to 1000 MHz using frequency-domain solver and tetrahedral mesh are chosen to be the simulation. A 24×12 (all in cm) dielectric platform with relative permittivity of 5.8 is chosen as the platform for the proposed tag to be mounted in the middle. A default 50Ω discrete port is treated to be the microchip before the simulation. After the simulation, the discrete port is then modelled as a microchip, which the impedance consisting of the real part and the imaginary part in the post-processing tab at which the impedance of the microchip is $14.56 - j161.25 \Omega$ at 915 MHz using Monza 5 (IPJ-W1600, 2016) manufactured by Impinj to determine the reflection coefficient matching result. Important parameters to determine the tag's performance, such as radiation patterns, G_r , antenna impedance, reflection coefficient, surface current distribution and etc. can be simulated using CST MWS to optimize the tag. When the optimization requirements are achieved for the particular proposed tag using the CST MWS software, it is ready to be tested in the Anechoic Chamber after the prototype is fabricated.

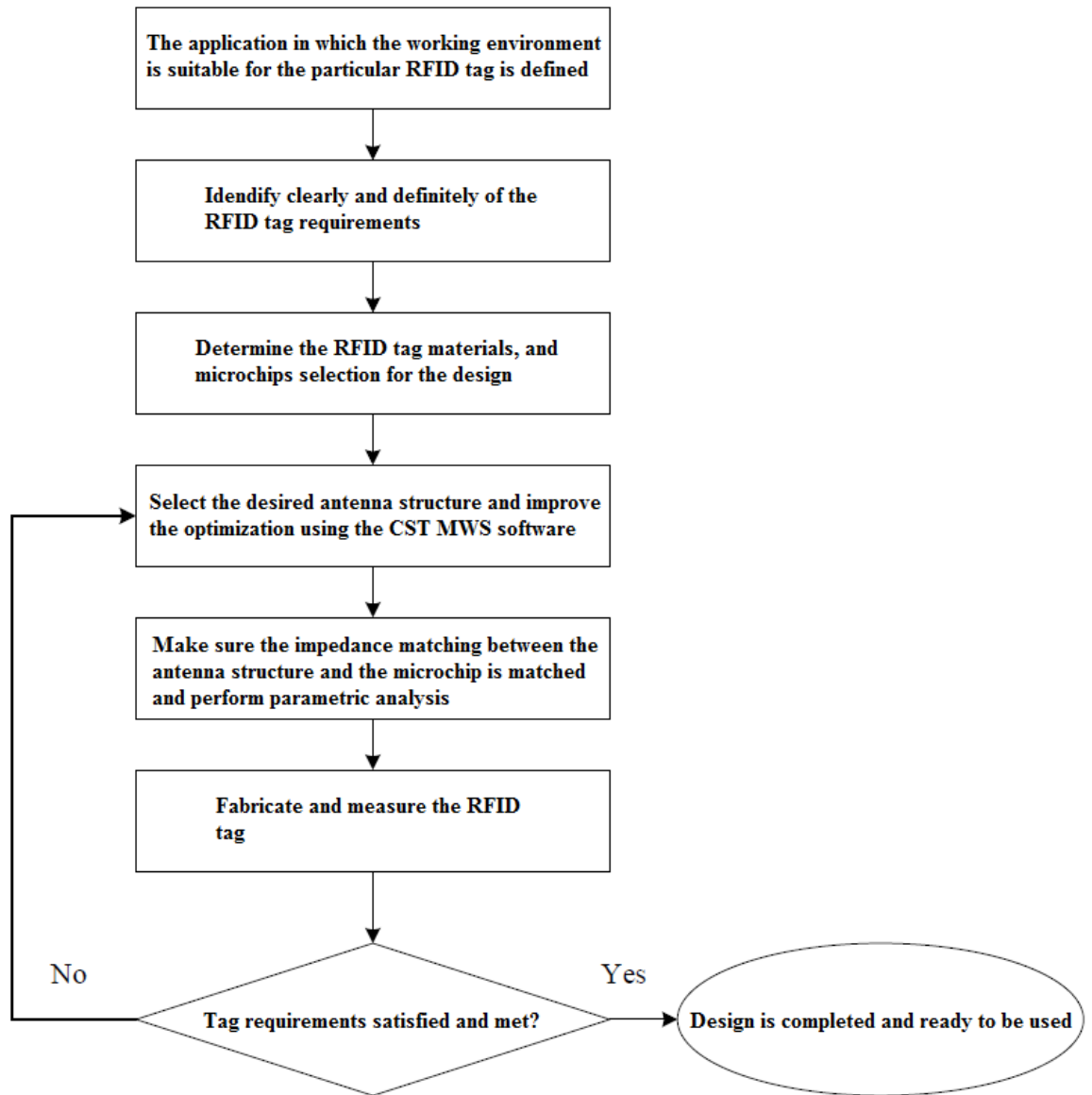


Figure 3.1: Procedure of designing passive UHF tag.

3.2 Tag Antenna-Characterization

As a reference to *Figure 3.2* (Moh et al., 2018), this is the typical method of tag antenna performance characterization. Far-field condition must be satisfied in such a way that the separation distance (d) as shown in *Figure 3.2* below must at least one wavelength away. The transmitted signal magnitude power, P_{tx} is gradually increased up until a threshold at which the

tag antenna emits backscattered electromagnetic waves received by the reader. At this amount of threshold power, the tag will be excited. The detection distance calculation estimation is very accurate for this type of measurement method (Bjorninen et al., 2013; Virtanen et al., 2013). Most of the UHF RFID performance benchmarks are done by this measurement method at the commercial level.

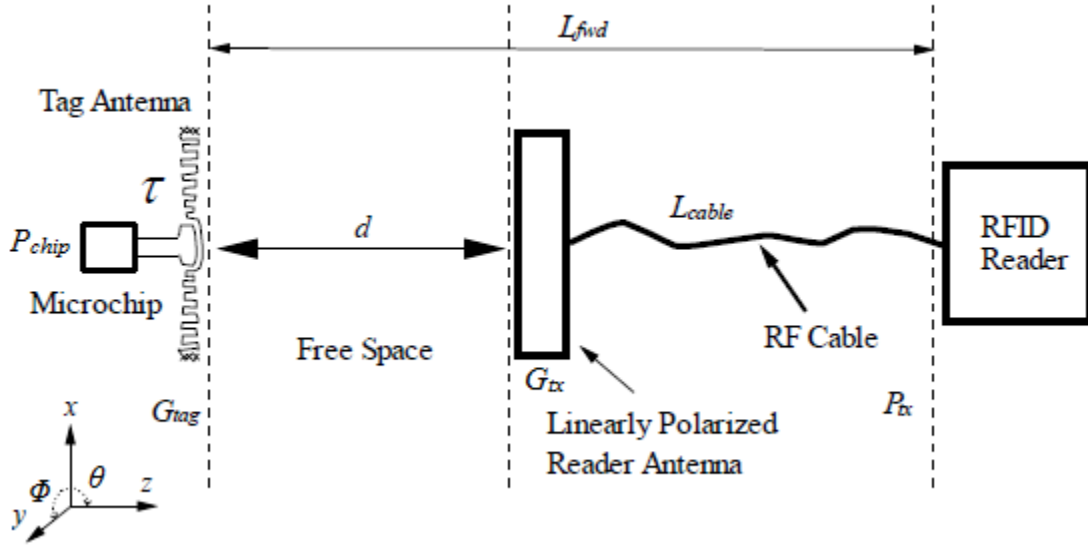


Figure 3.2: The typical measurement system for UHF RFID.

On top of that, both the reader and tag antennas have to place in parallel direction face-to-face straight in the x - y plane at the measurement procedure. The position of the reader antenna is fixed, while the tag rotates in the x - y plane as reference to *Figure 3.2* again. The power received as of the signal reaches in the surface of the tag microchip, $P_{chip}(\theta, \Phi)$ (Colella et al., 2016) in the Friis's Transmission Equation can be defined as,

$$P_{chip}(\theta, \Phi) = P_{tx} * G_{tx} * G_{tag}(\theta, \Phi) * \tau * \left(\frac{\lambda}{4\pi d}\right)^2 * \eta_{pl} * L_{cable}, \quad (3.1)$$

The transmitted signal magnitude power from the reader antenna is defined in the symbol of P_{tx} , while the reader antenna's gain is defined in the symbol of G_{tx} . As for the tag is rotating at Φ with reference to *Figure 3.2* as well as θ when it is rotating at other two planes. Hence, the tag antenna's gain defined in the symbol of G_{tag} is a function of Φ and θ in the spherical coordinate system. λ is the wavelength which can be calculated by the ratio of the speed of light, C and operating spectrum,

f of the system, while d is the separation distance horizontally between the tag antenna and the reader antenna. η_{pl} represents the polarization loss factor between the tag and the reader, while the signal attenuation between the RFID reader and the reader antenna is represented by L_{cable} . Power transmission coefficient, τ measures how well is the conjugate match between the microchip and antenna, which indicates how much power is being transferred to the microchip from the tag antenna. It is defined as (Rao et al., 2005),

$$\tau = \frac{4R_c R_a}{|Z_c + Z_a|^2}, \quad 0 \leq \tau \leq 1, \quad (3.2)$$

Denotation of Z_c and Z_a is defined as $Z_c = [Re(Z_c) = R_c] + j [Im(Z_c) = X_c]$ and $Z_a = [Re(Z_a) = R_a] + j [Im(Z_a) = X_a]$ are the impedance of the microchip and the impedance of the tag antenna. R_c and R_a are the real part (resistive part) of the microchip and tag antenna, while X_c and X_a are the imaginary part (reactive part) of the microchip and tag antenna.

In the real case scenario, the tag is activated only when the power received by the tag transmitted by the reader had reached its threshold level. At this threshold level, P_{th} can be used to rewrite P_{tx} in equation (3.1) to define this power is the minimum power transmitted from the reader in order to excite the tag. Hence, in equation (3.1), the term $P_{chip}(\theta, \Phi)$ can now be rewritten as the microchip sensitivity, $P_{c,on}$. It is defined as the least power required in order to turn on the microchip. This parameter has already been defined by the manufacturer before the production of the microchip which is a fixed value. In this circumstance, the equation (3.1) is substituted as,

$$P_{c,on} = P_{th} * G_{tx} * G_{tag}(\theta, \Phi) * \tau * \left(\frac{\lambda}{4\pi d}\right)^2 * \eta_{pl} * L_{cable}, \quad (3.3)$$

In the experiences of RFID engineers, the microchip sensitivity may not be sufficient to determine the true existing performance of the overall performance of the tag characterization. This is because some aspects which include antenna structure, reflection coefficient to determine the matching, and antenna gain are not included. In fact, it is much more applicable to evaluate the tag's performance by using the term tag sensitivity, $P_{tag}(\theta, \Phi)$. This is because the microchip and the tag antenna together have taken into account for the power. In equation (3.3), the constant parameters are factored and normalized as follows,

$$P_{c,on} = P_{tag}(\theta, \Phi) * G_{tag}(\theta, \Phi) * \tau, \quad (3.4)$$

Rearranging the equation (3.4),

$$\begin{aligned} P_{tag}(\theta, \Phi) &= [P_{c,on}] / [G_{tag}(\theta, \Phi) * \tau], \\ &= P_{th} * G_{tx} * \left(\frac{\lambda}{4\pi d}\right)^2 * \eta_{pl} * L_{cable}, \end{aligned} \quad (3.5)$$

The term $G_{tag}(\theta, \Phi) * \tau$ is tag antenna's realized gain which includes the impedance matching factor,

$$G_r(\theta, \Phi) = G_{tag}(\theta, \Phi) * \tau, \quad (3.6)$$

Not to forget that the tag sensitivity, $P_{tag}(\theta, \Phi)$ is not only a function of angle-dependant, it is also a parameter which is frequency dependant. In different regulated frequency, the tag antenna is not resonating and will affect the overall tag performance when measurement is being carried out because of the significant loss in the realized gain of the tag. Hence, equation (3.5) can be further modified as follows,

$$\begin{aligned} P_{tag}(\theta, \Phi, f) &= [P_{c,on}] / [G_{tag}(\theta, \Phi, f) * \tau(f)], \\ &= P_{th}(f) * G_{tx} * \left(\frac{\lambda}{4\pi d}\right)^2 * \eta_{pl} * L_{cable}, \end{aligned} \quad (3.7)$$

Equation (3.6) can also then be formulated as,

$$G_r(\theta, \Phi, f) = G_{tag}(\theta, \Phi, f) * \tau(f), \quad (3.8)$$

In order to find the read distance, d , which is the most important parameter in passive UHF RFID design. By rearranging equation (3.5), the read distance, d is defined as the path where the electromagnetic waves propagate from both the tag and reader antennas shown as,

$$d = \frac{\lambda}{4\pi} * \sqrt{\frac{L_{cable} * \eta_{pl} * P_{th} * G_{tx}}{P_{tag}(\theta, \Phi)}}, \quad (3.9)$$

Likewise, the read/detection distance d is a function of angular and frequency can be defined as shown in equation (3.10) below as,

$$d(f) = \frac{\lambda}{4\pi} * \sqrt{\frac{L_{cable} * \eta_{pl} * P_{th} * G_{tx}}{P_{tag}(\theta, \phi, f)}}, \quad (3.10)$$

The reader transmitted power, P_{tx} has already been specified in every country. Hence, the Effective Isotropic Radiated Power (EIRP) is already fixed differently in every country and therefore, the P_{tx} cannot exceed the required EIRP in the particular region under the regulated rules and regulations.

3.3 Actual UHF RFID Tag Measurement using Anechoic Chamber

After all the previous procedures mentioned have been done, the measurement system of the typical RFID system is used to measure and test the performance of the fabricated tag. The measurement system uses to measure RFID tag, Voyantic Tagformance (Tagformance, 2012) has been well-known to all around the world which is being used to measure RFID tag performance. This measurement system is free from external interferences such as wall reflection, environmental factor and electromagnetic wave interference from the outer environment. In order to make sure that the measurement is measuring the tag's performance meticulously at the far-field zone, make sure that the electromagnetic waves are not stored in either the of the antennas also known as near-field zone and the waves are propagating at a distance d must satisfy at least in minimum one wavelength from each other or higher in the UHF spectrum. In this circumstance, the acceptable separation distance between 50 cm to 60 cm is functional. A calibration tag is placed horizontally in the x-y plane as in the same *Figure 3.2* to the reader antenna is used to calibrate the propagation path in the frequency range of 800 MHz to 1000 MHz, with a resolution of 1 MHz. By referencing to *Figure 3.2* above, the signal where it reaches to the surface of the tag antenna which constitutes from the reader output port, also known as signal path loss can be symbolised as L_{fwd} and defined as,

$$L_{fwd} [dB] = G_{tx} [dBi] - |L_{cable}| [dB] - FSL [dB], \quad (3.11)$$

Where loss factor in free space can be abbreviated as FSL, which the electromagnetic waves propagate in the free space between both the tag and reader antennas.

The tag-under-test is placed at the middle of a rotatable Styrofoam with low permittivity ($\epsilon_r \sim 1$) to avoid any parasitic interaction throughout the measurement. The tag-under-test is placed in the x-y plane of the spherical coordinate system which is directly in line-of-sight with the reader antenna with a separation distance of d . Polarization loss factor, $\eta_{pl} = 1$ can be achieved by placing the tag-under-test and the reader antenna in parallel. The tag-under-test will emit a backscattered power when the reader radiates and alters its power continuously until it reaches the threshold level. This power is the minimum transmitted power which the tag is activated which is defined as P_{th} . With P_{th} is being defined, the sensitivity of the tag, P_{tag} can be computed as,

$$\begin{aligned} P_{tag} [dBm] &= P_{th} [dBm] - G_{tx} [dBi] + |L_{cable}| [dB] + FSL [dB], \\ &= P_{th} [dBm] - |L_{fwd}| [dB], \end{aligned} \quad (3.12)$$

It is known as L_{fwd} is the signal attenuation due to signal path loss. As a result, a minus sign is always displayed because in dB scale attenuation is minus sign. Hence, from equation (3.12) can be reformulated as follows,

$$P_{tag} [dBm] = P_{th} [dBm] + L_{fwd} [dB], \quad (3.13)$$

At the minimum power to turn on the tag measurement. The microchip sensitivity, $P_{c,on}$ which is the power received by the microchip in this circumstance. This parameter can be found in the datasheet stated by the microchip manufacturer is defined as,

$$P_{c,on} [dBm] = P_{tag} [dBm] + G_r [dBi], \quad (3.14)$$

Rearrange the equation (3.14) as G_r as one of the tag's antenna important parameters in terms of other parameters and formulated as,

$$G_r [dBi] = P_{c,on} [dBm] - P_{tag} [dBm], \quad (3.15)$$

Converting equation (3.15) into the linear scale, the G_r of the antenna in the tag can then be formulated as,

$$G_r = P_{c,on} / P_{tag} , \quad (3.16)$$

Substitute equation (3.13) into (3.16) after all have been converted into linear scale and G_r of the antenna by the tag can be finalised and computed as,

$$G_r = P_{c,on} / (P_{th} * L_{fwd}) , \quad (3.17)$$

As in (Rao et al., 2005), the Friis's transmission equation can be used and derived the read distance, d formula as shown in equation (3.18) below. By fixing the allowable EIRP, where $P_{EIRP} = P_{tx} * G_{tx}$, which is already defined by the regulation of that particular country, the longest read distance, d_{max} can be done calculated by putting P_{EIRP} and equation (3.16) into equation (3.18) calculated as,

$$\begin{aligned} d_{max} &= \left(\frac{\lambda}{4\pi} \right) * \sqrt{\frac{P_{tx} * G_{tx} * G_r}{P_{c,on}}} , \\ &= \left(\frac{\lambda}{4\pi} \right) * \sqrt{\frac{P_{EIRP}}{P_{tag}}} , \end{aligned} \quad (3.18)$$

3.4 Read Pattern Measurements

The read pattern measurements are important for passive UHF RFID tag design as it shows how the radiation pattern in response to the reader antenna when its tag is activated. In most of the metal-mountable RFID tag design is having the maximum magnitude of radiation at the bore-sight angle ($\theta = 0^\circ$). In this proposed tag, the radiation pattern is a quasi-isotropic radiation pattern in response to the reader antenna which is particularly very useful in tracking applications. The read distance patterns are measured in 3 different planes consist of x-y plane, x-z, plane and y-z plane, at a frequency which resonated at the usable UHF spectrum. The 3D radiated detection distance pattern by the tag-under-test can be predicted by the 3 different cut planes radiation characteristics as mentioned above. Throughout the measurement system, the reader antenna is static at a distance

from the tag antenna, while the tag antenna is rotating with respect to its own origin towards all the three different planes. From the *Figure 3.3* (Moh et al., 2018) below, the read distance pattern generated from the x-z plane is obtained via the tag rotates 360° to the y-axis. Similarly, y-z plane generated read distance pattern can be obtained from the tag rotating 360° to the x-axis. From the reference of *Figure 3.3* (Moh et al., 2018) again, the read distance radiation pattern is obviously generated from both the x-z plane and the y-z plane comply with those for the spherical coordinate system. However, when the UHF RFID tag rotates about the z-axis to obtain the read distance pattern in the x-y plane, it shows the EM wave polarization in the bore-sight direction characteristics for the particular UHF RFID tag-under-test and the display of the xy-plane read distance pattern will be generated.

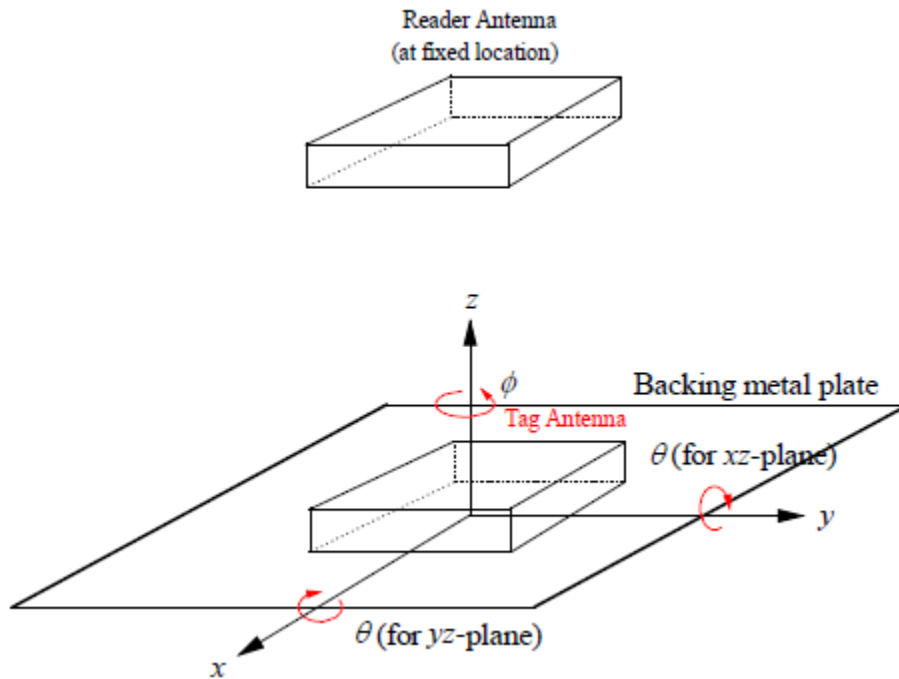


Figure 3.3: The measurement setup to obtain the read distance pattern across all the three different planes.

3.5 Summary of the Methodology and Work Plan

In section 3.1, the *Figure 3.1* above shows the summarised design procedure of any passive RFID tag design in the UHF spectrum. After that, in section 3.2 talks about the tag antenna-

characterization where how the measurement system is being conducted and the respective read distance formula is being derived step by step. As in section 3.3, the actual UHF RFID tag measurement using an anechoic chamber to measure the performance of the tag such as the read distance radiation pattern across all the three planes and how far the tag can be detected between the distance of the reader and the tag. The measurement setup using Voyantic is already illustrated in *Figure 3.2* above is used for the measurement and the formula and equations what is happening in the measurement system, especially the read distance formula is being derived step by step clearly. Lastly, in section 3.4, the read pattern measurement is illustrated as how the measurement is being carried out across all the three planes so that the estimation of the 3D radiation field pattern can be carried out to identify the overall radiation pattern of the designed tag.

CHAPTER 4

RESULTS AND DISCUSSION OF THE PROPOSED PASSIVE UHF RFID TAG

4.1 Introduction

Throughout the technology changes over the year, RFID system has become one of the most prominent technologies ever existed and discovered by human beings as it helps to solve so many problems and ease up our workforce in the industrial and commercial level for applications such as internet of things, toll collection system, human/animal tracking system, system identification, security assessment, etc.. Recently, due to the advancement and improvement of the field in electronics such as semiconductor where the microchip embedded inside the tag itself is a semiconductor device, the microchip has a significant boost of increase in data transfer rate and due to large scale manufacturing, the overall production cost is very low and efficient to be produced. In components of a passive UHF RFID tag consists of a microchip, the tag antenna structure. The tag antenna structure is very important as it controls the overall performance of the tag as well as the overall size of the tag. In commercial levels, it is much desirable to design the RFID tag into much smaller size as possible, but it will deteriorate the performance of the tag such as realized gain, impedance matching, impedance bandwidth, detection distance and tag's size as these trade-offs are unavoidable (Rao et al., 2005). Therefore, many techniques have been explored by the researchers to scale down the overall size of the tag antennas as well as it is still able to provide good radiation characteristics to fit the application.

The few techniques have been done by previous researches can be listed down as meandered structure lines (Marrocco, 2003; Bong et al., 2017), using substrate with high relative permittivity (Babar et al., 2012), folded patch (Moh et al., 2018), vias and high inductive shorting stub (Chen and Lin, 2008) are being commonly adopted and used to scale down the tag structure. When scaling down the technique is decided, the tag antenna to choose to generate what kind of radiation patterns is also needed to be considered. The first antenna structure being widely adopted in the tag RFID design in UHF Spectrum is dipole type antenna because it is the most versatile and conventional structure and quasi-isotropic radiation pattern is generated according in (Balanis,

2005). However, one of the major disadvantages of the dipole type antenna structure is the radiation characteristics is being deviated when it is put in any area vicinity with metals. This is because the electric fields of the radiated image currents and the current projected on the antenna itself is 180° out of phase and same magnitude which resulted in the phenomenon known as destructive interference which had been studied in physics for a long time ago which resulting in deviating the radiation characteristics of the typical dipole antenna (Dobkin and Weigand, 2005). Therefore, alternative structures are being studied which lead to the slight modification of dipole antenna also known as inverted-F antenna structure (Chen and Tsao, 2010) also known as PIFA structures. This structure added an extra ground metal plane to separate the radiating part of the antenna from foreign vicinity objects as it found out that this method is useful and manage to tackle the conventional dipole issues. However, this structure requires a different kind of feeding method where shorting metallic walls/vias which is a vertical feeding scheme can be difficult during the fabrication process as it involves high technology machine to fabricate and ultimately lead to costly fabrication process. After all the disadvantages of the previous antenna structure being discovered is not beneficial to UHF RFID tag design, a new structure which is a modification of dipole structure, also known as folded dipolar patch antenna (Yang et al., 2011). This dipolar patch antenna is done by widening the radiating arms of the dipole antenna and the technique of inserting a ground plane is adopted from the inverted-F structure but without the vertical scheme. This dipolar patch antenna has shown to be the most versatile antenna for the current passive UHF RFID design because the scaling down process can be done by inserting a stub anywhere to create a short circuit path from the radiating patch to the ground plane. However, there is nothing perfect in this world as there will be still some downside of this miniaturized dipolar patch antenna as the resonant frequency is normally shifted to higher frequency which is not within the UHF spectrum range. Therefore, some tuning mechanism has to be implemented such as the line being slotted and recessed in a meandered way (Bong et al., 2017) is helpful for adjusting the desired resonating frequency back to the desired UHF spectrum range by making the surface current paths longer as seen by the antenna to lengthen its electrical length. Although it is useful for adjusting the tag's frequency to be resonating at the UHF spectrum, it has a trade-off of deteriorating the antenna structure quality factor which affects the radiation efficiency to be worse (Bong et al., 2017).

As of today, most of the RFID tag currently available in the market is bore-sight radiation pattern with linear-polarized. In real life scenario, the orientation of the tag with respect to the reader can be in random directions. Therefore, circular-polarized RFID tag has been researched (Tran et al., 2015) and found out that it can be done in that kind of scenario. However, circular-polarized RFID tag normally is very complex in antenna structure which lead to complicated fabrication process and high cost. Moreover, circular-polarized RFID tag is only able to portray its ability in certain beamwidth as not cover in all of the azimuth or elevation planes, in some of the beamwidth is just a normal linearly-polarized tag. Therefore, due to this trade-off, a quasi-isotropic radiation pattern antenna structure for passive UHF RFID tag is required to explore. There were several quasi-isotropic radiation pattern UHF tags being discovered by other literature such cube in shape (Kholodnyak et al., 2006) and sphere in shape (Ryu et al., 2010). Both of these are 3-dimensional tag antenna structures as required high fabrication cost and large in size. Therefore, to achieve compactness in size and low fabrication cost, a 2-dimensional antenna structures is much preferable. The 2-dimensional structures quasi-isotropic radiation pattern can be generated by bending the dipole arm in such a way that two perpendicular current flows (Cho et al., 2005). Apart from that, the techniques which its antenna structure is placed in a form of electric dipole and magnetic dipole in perpendicularly (Lin et al., 2011; Wang et al., 2019) were also shown to produce quasi-isotropic radiation pattern. Therefore 2-dimensional structures quasi-isotropic radiation pattern antenna structure will be studied and implemented in this final year project.

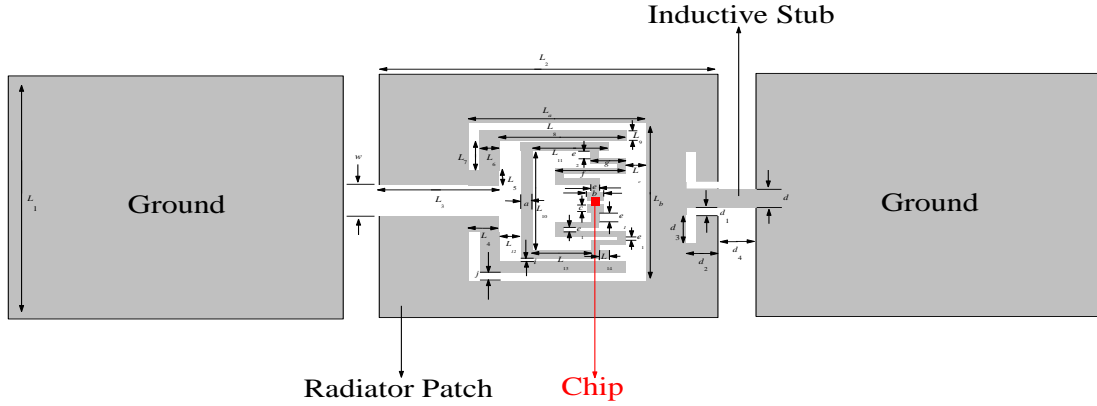
In this final year project, an electrical small planar folded patch composes of a rectangle Split-Ring Resonator (SRR) which is excited and fed by a meandered T-match, is suggested for designing a compact passive UHF RFID tag antenna for mounting on various dielectric constant dielectric surfaces. It has a stub shortening both the ground and the patch for scaling down the tag size and a pair of notches for fine frequency tuning. The meandered T-match loop is employed for impedance matching as very good matching is achieved up to 90% transmission coefficient. The combination of meandered T-match loop and the pair of notches has shown to have very good tuning the resonant frequency and impedance matching between the tag antenna structure and the microchip. A high dielectric constant substrate using the Duroid[®] 6010 laminates (RT/duroid[®] 6010, 2017) was used to scale down the overall size of the tag antenna as well. Hence, the proposed

tag has a combination of shorting stub and high dielectric constant methods to scale down the tag size. This structure is shown to provide promising quasi-isotropic radiation pattern when mounted on a dielectric material. In the azimuth plane, the variation of realized gain at the desired resonant frequency varies from -6.28 dB to -5.90 dB shown to be stable and prove quasi-isotropic radiation pattern. The finalised design tag is able to achieve compactness with the size of $28 \times 28 \times 3.293$ (all in mm & $0.0854\lambda \times 0.0854\lambda \times 0.01004\lambda$). The configuration of the proposed tag and its radiation field working principle will be discussed in section 4.2. The radiation field pattern and parametric analysis will be analysed in section 4.3. Finally, real practical scenario such as mounting on the different dielectric constant platform, the size of the dielectric platform and comparison of other authors with the same quasi-isotropic radiation RFID tags will be discussed in section 4.4.

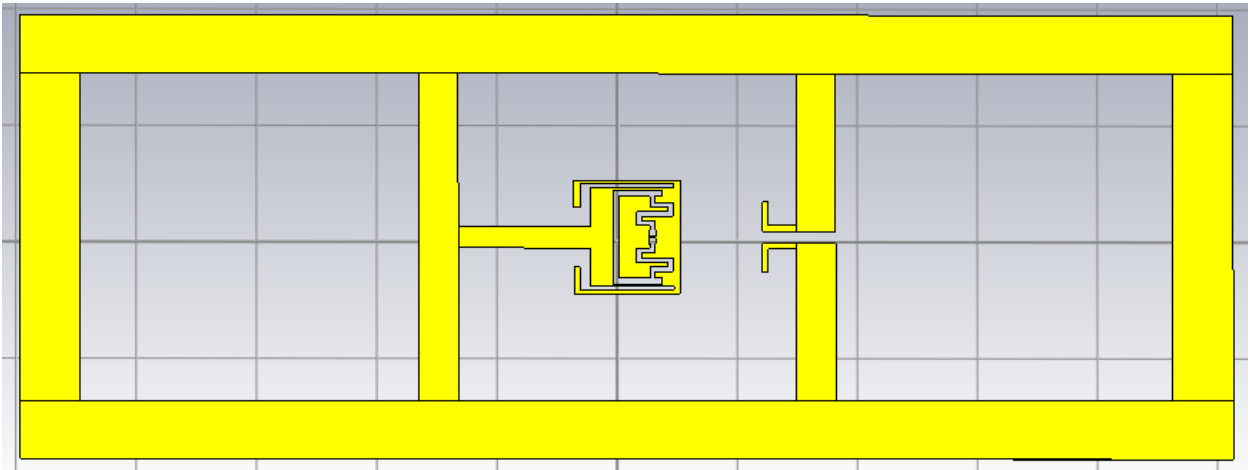
4.2 Proposed Passive UHF RFID Tag Antenna Configuration and Radiation Field Working Principle

From *Figure 4.1* below, the configuration of the proposed passive UHF RFID tag antenna configuration is shown. The material used is a bendable PET (polyethylene terephthalate) substrate with a thickness of 0.05 mm and double sided layer coppers with a thickness of 0.009 mm coated on it. As seen from the naked inlay from *Figure 4.1 (b)* below, The SRR with extended strip-line radiating patch is done by etching unwanted thin copper surface as well as the T-match meandered loop is done by etching it the same way as well. At one side of the end consist of a shorting stub to short both the ground and the patch with a pair of notches for fine resonant frequency tuning. The microchip Monza 5 (IPJ-W1600, 2016) is used for the proposed tag and is bonded across the narrow gap of the meandered T-match loop. When operating at a frequency of 915 MHz, the microchip exhibits the impedance characteristic of $14.56 - j161.25 \Omega$ with a write and read sensitivities of -16 dBm and -20 dBm. Matching between the impedance of antenna structure and the chip is done by applying the meandered T-match loop structure. The top view and the side view of the proposed tag is shown in *Figure 4.2* below. The naked inlay is wrapped symmetrically around the substrate by using adhesive to form a complete tag with a microchip. The substrate used is Duroid[®] 6010 laminates (RT/duroid[®] 6010, 2017) and it is manufactured from ROGERS COOPERATION. The substrate has a thickness of 3.175 mm and the electrical properties of relative

permittivity of $\epsilon_r = 10.2$, and dissipation factor of $\tan \delta = 0.0023$. The substrate has a size of $28 \times 28 \times 3.175$ (all in mm).



(a)



(b)

Figure 4.1: (a) The overall configuration of the optimized proposed tag antenna with parameters $L_1 = 28$, $L_2 = 28$, $w = 1.9$, $L_3 = 11$, $L_7 = 1.7$, $L_4 = 1.4$, $L_6 = 0.9$, $j = 0.3$, $L_5 = 1.6$, $L_{12} = 1.8$, $L_a = 8.8$, $L_8 = 6.9$, $L_9 = 0.3$, $i = 0.2$, $a = 0.5$, $L_{11} = 3.6$, $L_{10} = 7$, $L_{13} = 2.6$, $L_{14} = 0.6$, $e_2 = 0.53$, $g = 1.9$, $L_c = 0.6$, $f = 3$, $e = 0.4$, $b = 0.6$, $c = 0.5$, $e_1 = 0.4$, $L_b = 9.7$, $d_1 = 0.5$, $d_2 = 2.8$, $d_3 = 2$, $d_4 = 3.293$ and $d = 1$ (all in mm). (b) Naked inlay of the fabricated proposed tag before wrapped.

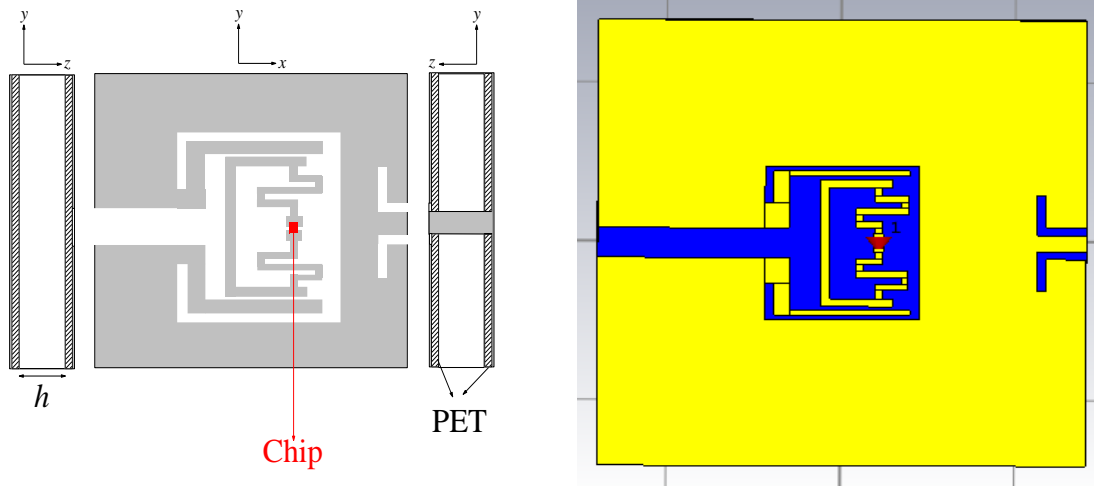


Figure 4.2: The top-down and side view of the completed fabricated tag.

The proposed passive UHF RFID tag is mounted on a substrate material with dielectric constant of 5. The dimension of the dielectric platform is in the size of $24 \text{ cm} \times 12 \text{ cm}$. The entire simulation using CST MWS is done by putting the tag in the middle of the dielectric platform. The proposed passive UHF RFID tag is able to generate quasi-isotropic radiation pattern when it is mounted on the dielectric platform. This is because the proposed tag is excited with an SRR radiated patch. A SRR can be modelled as an electric dipole perpendicular with a magnetic dipole so that the null points of the sole electric dipole are compensated by the magnetic dipole and vice versa for magnetic dipole according to the principle of (Hu et al., 2019). The theory of electric dipole and magnetic dipole aligned in perpendicular is proven in (Luk and Wu, 2012; Long S., 1975) as shown in *Figure 4.3* below. From this *Figure 4.3* as understood in antenna theory, the radiation field pattern of an electric dipole contains a figure-8 in shape in the E-plane E^e and figure-O in shape in the H-plane H^e , whereas for magnetic dipole radiation field pattern contains a figure-O in shape in the E-plane E^m and figure-8 in shape in the H-plane H^m . As these two superimposed, the resultant null points will be added up and give rise to quasi-isotropic radiation pattern. From *Figure 4.4* below, electric dipole's generated surface current superimposed with the surface current of magnetic dipole gives rise to the equivalent surface current which has very high magnitude in the part near the notches of the patch's radiator when the directions of which both having the same direction as seen clearly in *Figure 4.5* in simulation from CST MWS for the proposed tag.

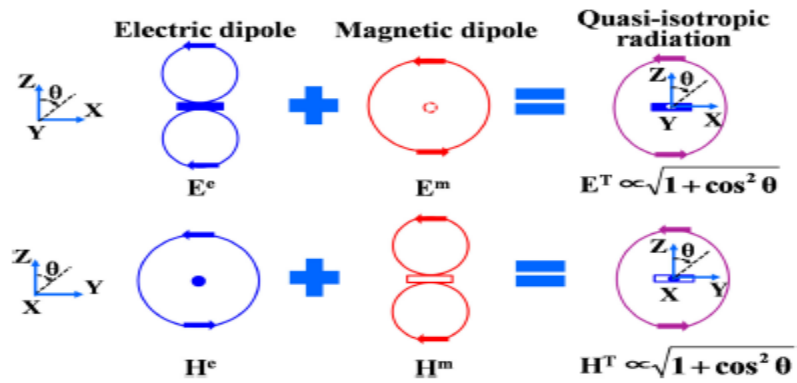


Figure 4.3: The working principle of electric dipole in perpendicular with magnetic dipole (Wang et al., 2019).

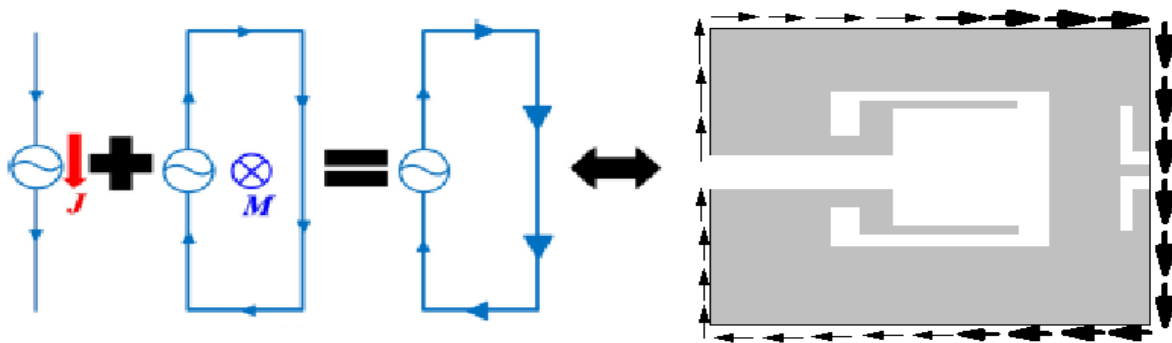


Figure 4.4: The equivalent surface current contributed by the magnetic and electric dipole.

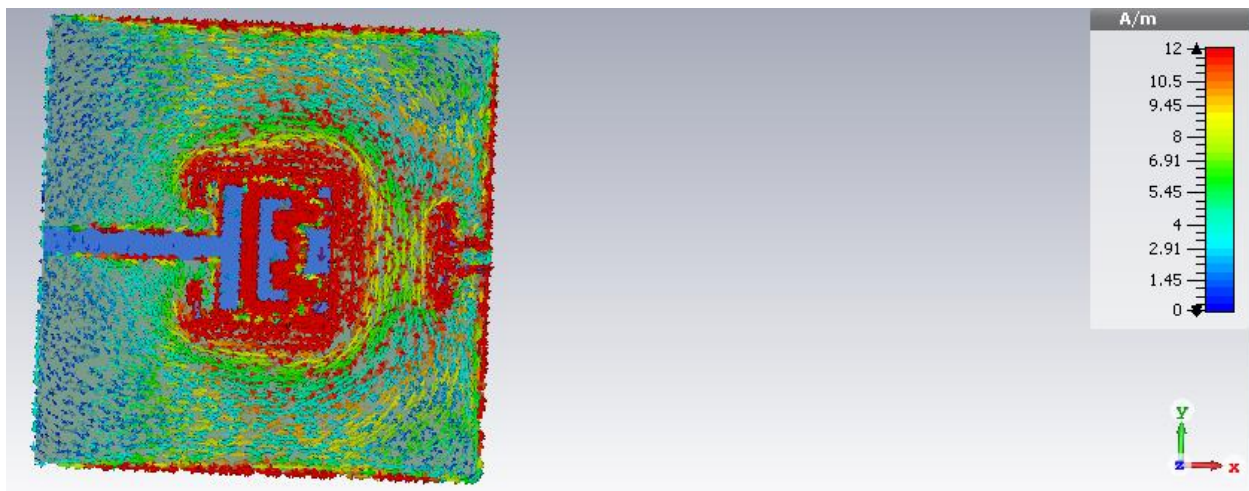


Figure 4.5: The proposed RFID tag surface current simulated using CST MWS.

As depicted from *Figure 4.5*, the simulated surface current distribution of the radiating patch which is an SRR structure exhibits is similar to the theoretical as shown in *Figure 4.4* above. From *Figure 4.5*, very high surface current flow along the meandered T-match loop as depicted to be a good impedance matching as it is a very narrow inductive narrow line to introduce a more inductive property to the tag to cancel out the imaginary part of the chip. The extended strip-line from the SRR shows to have very high surface current flowing through it as well, this indicated this extended strip-line can achieve the good capacitive coupling effect. As a result, L_8 , L_9 , a , and L_{11} are important control parameters to achieve the optimum capacitive coupling effect to excite the radiating patch. Last but not least, the notches shown to have a high magnitude of accumulated surfaces current flowing through it as well as indicated for good fine frequency tuning for impedance matching. Therefore, overall optimized design of the proposed tag shown to have the radiating patch well excited in clockwise manner as predicted, to comply with the theory achieved in *Figure 4.4*. Because of all these properties, the proposed RFID tag is able to give rise to quasi-isotropic radiation pattern and it is very versatile for many applications.

4.3 Parametric Analysis and Radiation Field Pattern Results and Discussion

In this section, parametric analysis will first be discussed as some of the key parameters can help to achieve optimum performance for the proposed tag as it will be crucial to affect the tag's impedance which will directly affect the maximum signal transfer factor also known as the power transmission coefficient. After that, the radiation field pattern of the proposed tag will be discussed in the later section. At first, the effect of the thickness of the T-match loop without the meandering section a is investigated. The thickness varies from 0.5 mm which is the most optimized to 1.5 mm is simulated as shown in *Figure 4.6* and *Figure 4.7* below. In *Figure 4.6*, the input impedance changes are investigated. From there, as the thickness increases, the real part and the reactive part of the impedance is very stable and shifted slightly to the higher frequency range. As for the power transmission coefficient as shown in *Figure 4.7* below, the resonant frequency is also shifted slightly to the higher frequency as the magnitude is dropped as it shifted to the higher frequency. The sensitivity of shifting will be summarised in *Table 4.1*. This is because as the thickness getting thicker, the T-match loop is getting less inductive as it is not able to cancel the imaginary part of the microchip. The most optimized when $a = 0.5$ mm is 90%, but when $a = 1.3$ mm the power

transmission coefficient is only achievable at 75%. Therefore, it is not advisable to increase the thickness of the T-match loop.

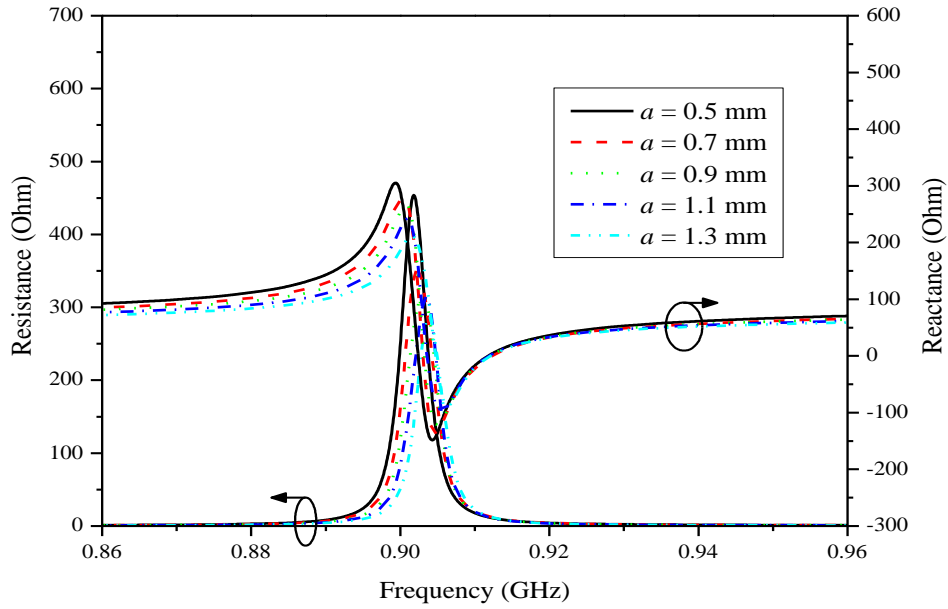


Figure 4.6: The changes of input impedance when the T-match loop thickness a is varied.

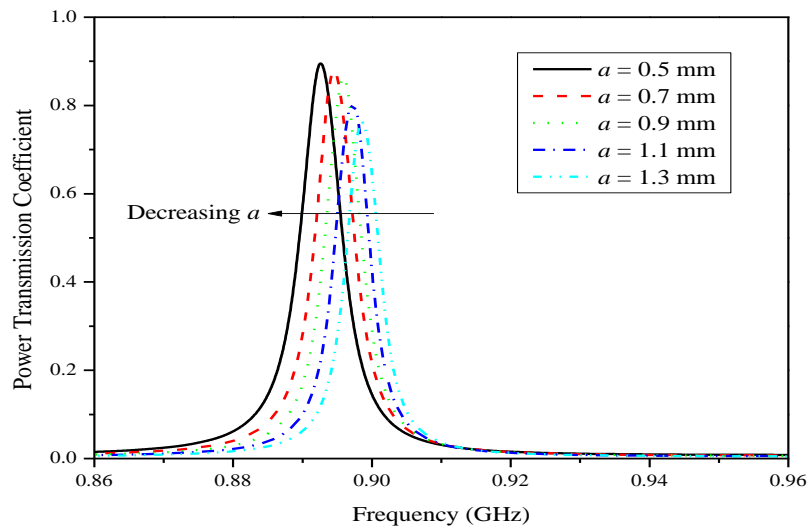


Figure 4.7: The changes of power transmission coefficient when the T-match loop thickness a is varied.

Next, the effect of the length of the pair of notches d_3 will be investigated. The length of the notches is most optimized at $d_3 = 2$ mm and its effect of varying until $d_3 = 6$ mm is investigated for its input impedance changes as shown in *Figure 4.8* below and its power transmission coefficient as shown in *Figure 4.9* below. As observed in the tag's antenna structure input impedance, as the length of the pair of notches increases, the input impedance shifted to the lower frequency as similar trend is observed for its power transmission coefficient as well. From both of the graphs shown, varying the length of the pair of the notches can be used for fine frequency tuning to tune the resonant frequency to the desired resonated UHF range as the sensitivity of the length changes with respect to its frequency is shown to be good for fine frequency tuning as the sensitivity will be listed in *Table 4.1* below. The magnitude of the power transmission coefficient is maintained in 0.9 as it shifted to the lower frequency as this is proven that the length of the pair of the notches is used for fine frequency tuning as it does not influence on the impedance matching.

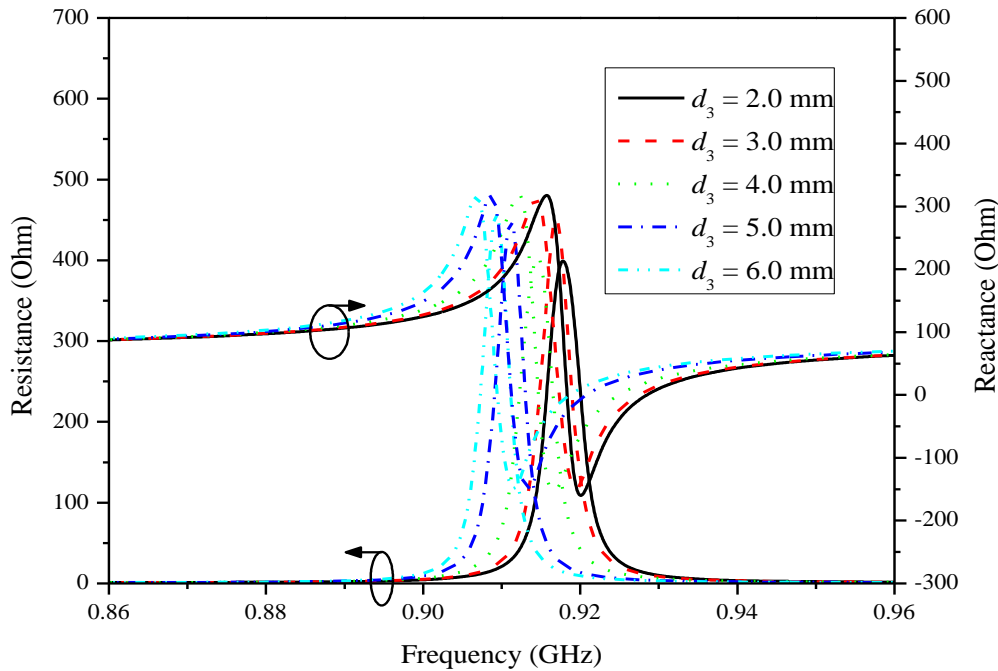


Figure 4.8: The changes of input impedance when the length of the pair of the notches d_3 is varied.

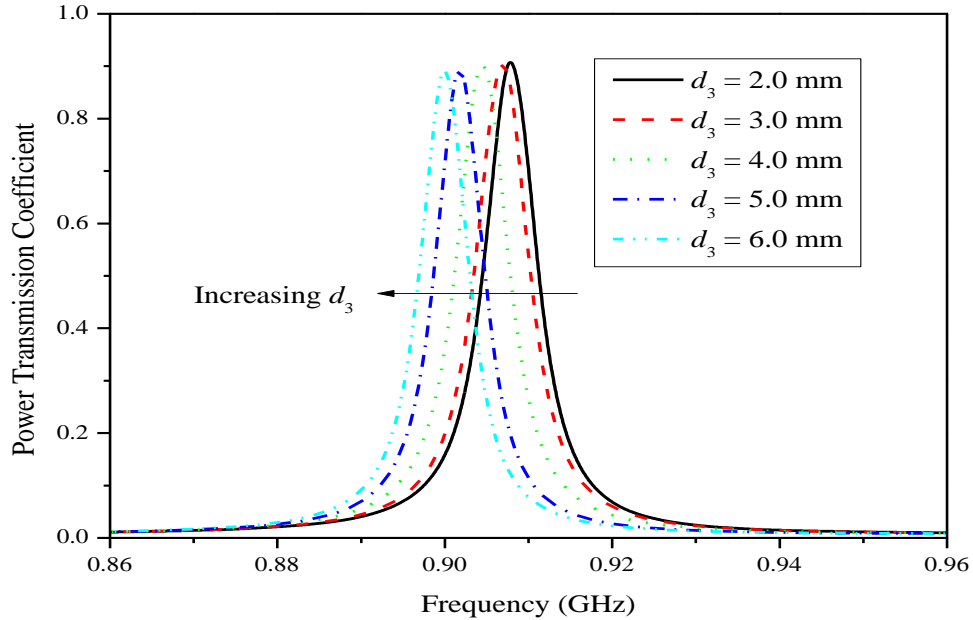


Figure 4.9: The changes of power transmission coefficient when the length of the pair of the notches d_3 is varied.

After that, the length of the extended strip-line L_8 , which is extended from the SRR radiated patch is parametrically analysed. As usual, the most optimized length is when $L_8 = 6.9$ mm as the parametric analysis will analyse the length decreases until $L_8 = 4.9$ mm. The input impedance of the tag's antenna structure composed of resistance and reactance changes is investigated as shown in *Figure 4.10* below. As for the power transmission coefficient changes, it was shown in *Figure 4.11* below. From the input impedance changes, as the length of L_8 decreases, the resistance and reactance of the tag's antenna input impedance is shifted to the lower frequency as expected. The power transmission coefficient with magnitude maintain near to 0.83 and shifted to the lower frequency as well. As a result, the variation of L_8 does not influence on the impedance matching same as d_3 . The length of L_8 as mentioned in section 4.2 is an important parameter to achieve good capacitive coupling between the meandered T-match loop and the radiating patch. Therefore, the sensitivity of frequency shifting will be minimized as summarised in *Table 4.1*. Whereas for the power transmission coefficient analysis, the magnitude near to 0.83 as it shifted slightly to the lower frequency. Therefore, this parameter will affect the radiation efficiency the most of the tag

antenna because of the coupling effect. Additionally, it is worth to mention that it is able to provide fine resonant frequency tuning as well because of the same sensitivity with d_3 .

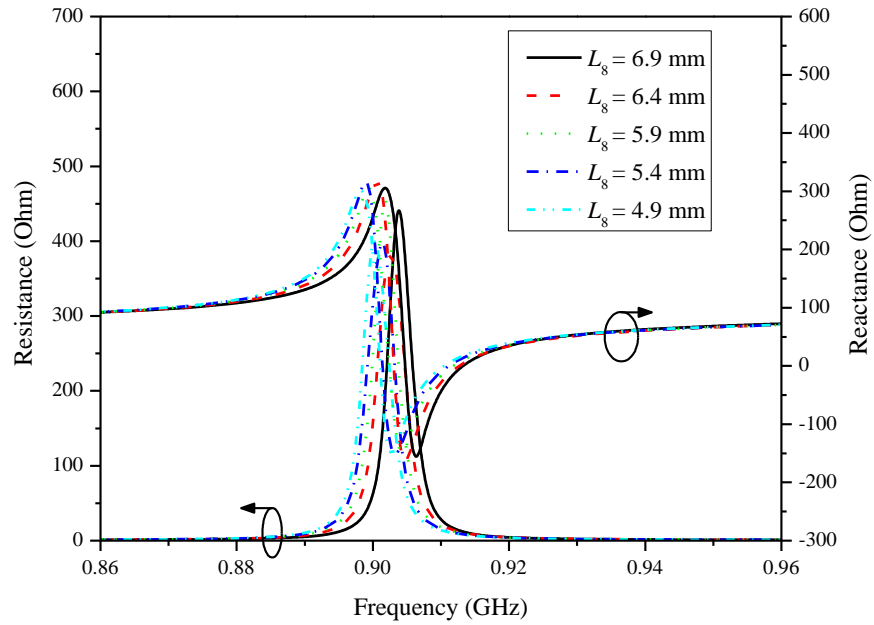


Figure 4.10: The changes of input impedance when the length of the extended strip-line L_8 is varied.

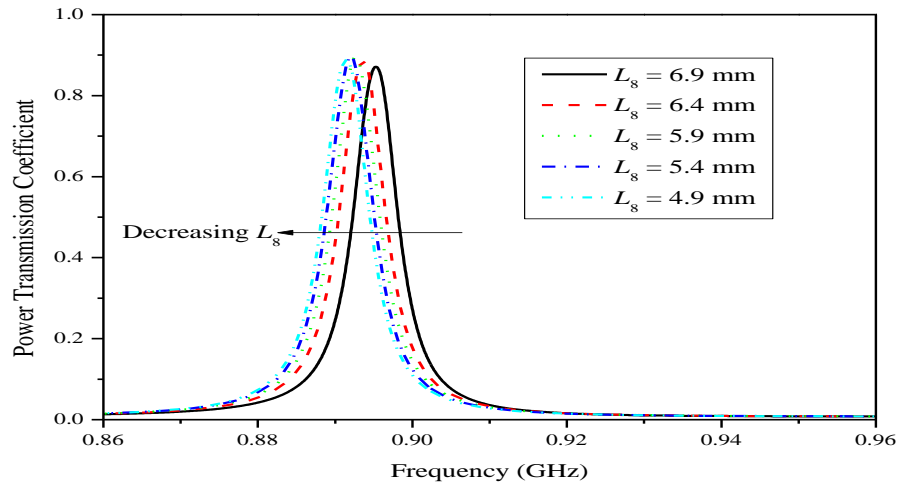


Figure 4.11: The changes of power transmission coefficient when the length of the extended strip-line L_8 is varied.

Finally, power transmission coefficient, which is dependent on the impedance matching are analysed by seeing its changes due to the changes to the length of the narrow L_c gap between the extended strip-line to the right side of the radiating patch is varied as well as the changes of antenna impedance are noticed. The most optimized length is when $L_c = 0.6$ mm and is varied until $L_c = 1.4$ mm and observed the changes of tag's antenna impedance together with the power transmission coefficient simulated by CST MWS. From *Figure 4.12*, the input impedance of the tag's antenna shifted to the lower frequency range together with the power transmission coefficient in *Figure 4.13*. The magnitude of the power transmission coefficient varies in the range from 0.85 to 0.83 as it shifted from the higher frequency to the lower frequency. The sensitivity of shifting is the highest among the four parameters which have been parametrically analysed. This is because the inner width of the SRR loop is getting thinner and the overall tag's antenna radiator is getting narrower as it affected the tag's antenna getting more inductive. As a result, the sensitivity of shifting to the lower frequency is the highest as shown in *Table 4.1*. It is a good tuning of resonant frequency parameter if the tag is resonated out of the UHF spectrum, which is located in the higher frequency range. It is well to mention that slight impedance matching is able to achieve as the power transmission coefficient is varied slightly as it shifted.

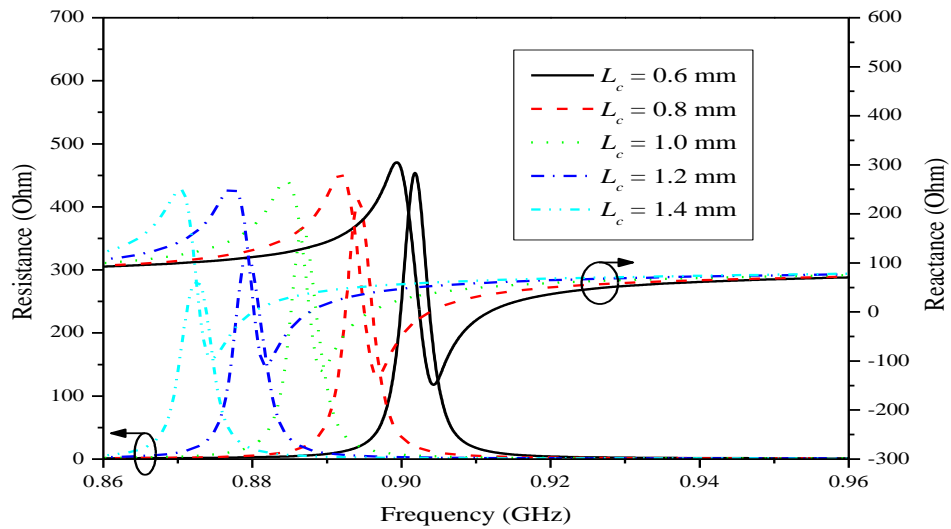


Figure 4.12: The changes of input impedance when the narrow gap length L_c is varied.

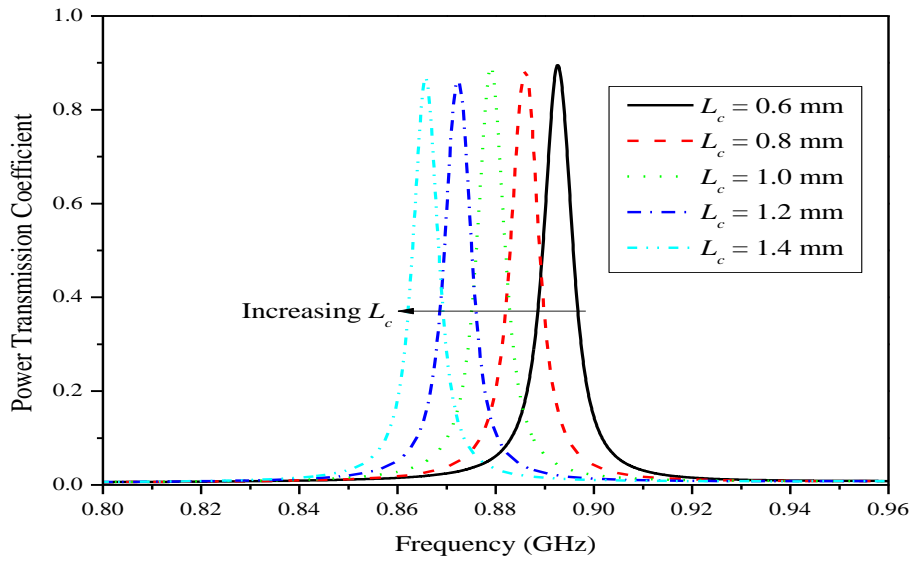


Figure 4.13: The changes of power transmission coefficient when the narrow gap length L_c is varied.

Table 4.1: The key parameters to affect the changes of tuning sensitivity.

Key parameters	Sensitivity of frequency with respect to changes of its length (MHz/mm)
a	9.5
d_3	3.8
L_8	3.8
L_c	28.5

Next, the measurement setup will be discussed. The measurement setup used is a Voyantic Tagformance measurement system (Tagformance, 2012). The fabricated proposed tag will put in the middle of a substrate platform with dielectric constant 5.8 which is made up of wood fiber and phenolic polymers also known as KITE – phenolic papers with dimension of 24 cm × 12 cm × 1 cm. The tag placed together with the substrate platform is placed on a Styrofoam with dielectric constant near to free space. The entire setup is placed inside the anechoic chamber for measurement as shown in *Figure 4.14* below. Some important RFID tag parameters are to be measured by the

measurement setup such as G_r , read distance between the tag and the reader as well as the tag sensitivity. An EIRP of 4 W linearly polarized electromagnetic waves with 8dBi gain is emitted to the RFID tag is generated by the reader part of the system.

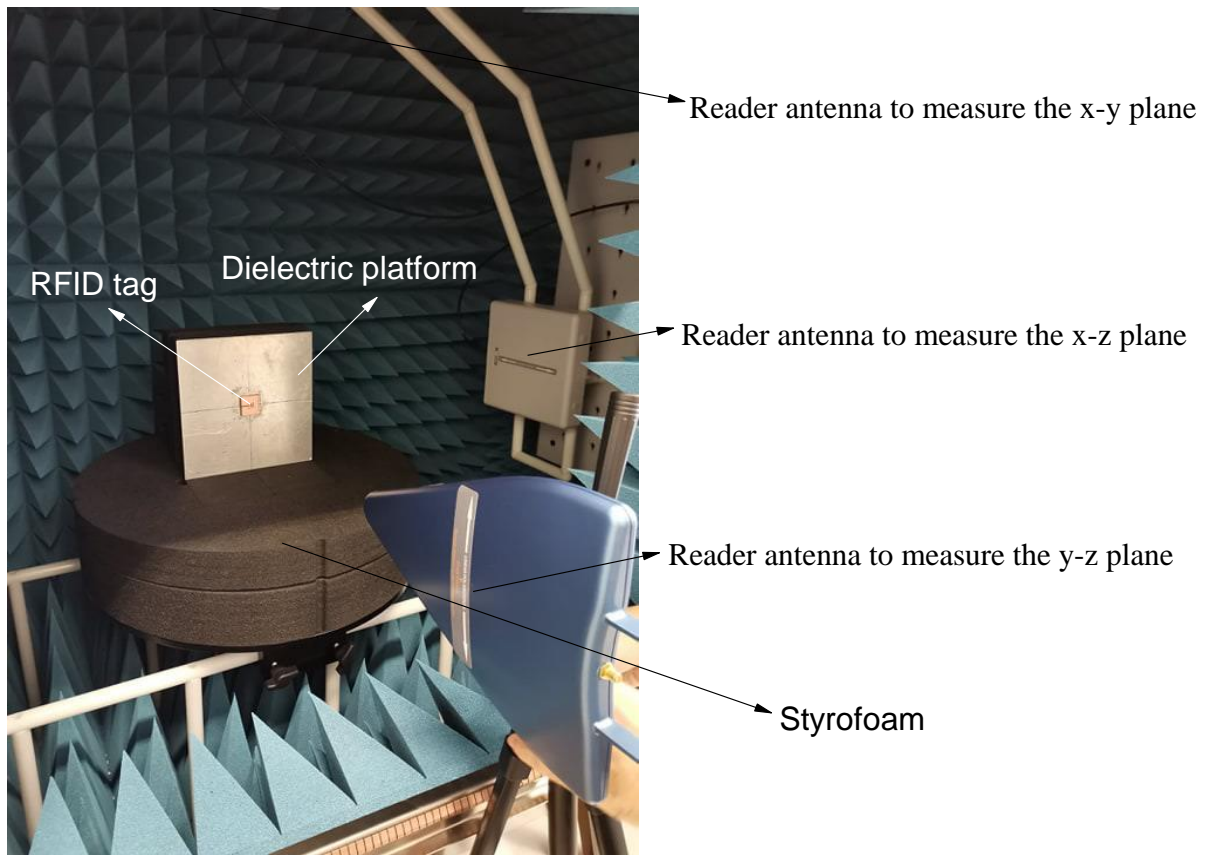


Figure 4.14: Measurement setup in the anechoic chamber.

The most important parameter to determine the performance of a particular passive UHF RFID tag is the realized gain G_r . This is because G_r is a dependant variable that affects the read distance of the tag. Therefore, read distance d is directly proportional to G_r where both of them must be high to give rise to far range detection. The realized gain G_r is dependent on microchip sensitivity, $P_{c,on}$, the minimum transmitted power which the tag is activated which is defined as P_{th} and L_{fwd} constitute by the signal where it reaches to the surface of the tag antenna which constitutes from the reader output port can be formulated as $G_r = [P_{c,on} / (P_{th} * L_{fwd})]$. Hence, the simulated realized gain using CST MWS with respect to the frequency is plotted in *Figure 4.15* below. The

measured realized gain and measured sensitivity is not able to obtain as the movement control order is implemented just after when I was about to measure in the research measurement lab.

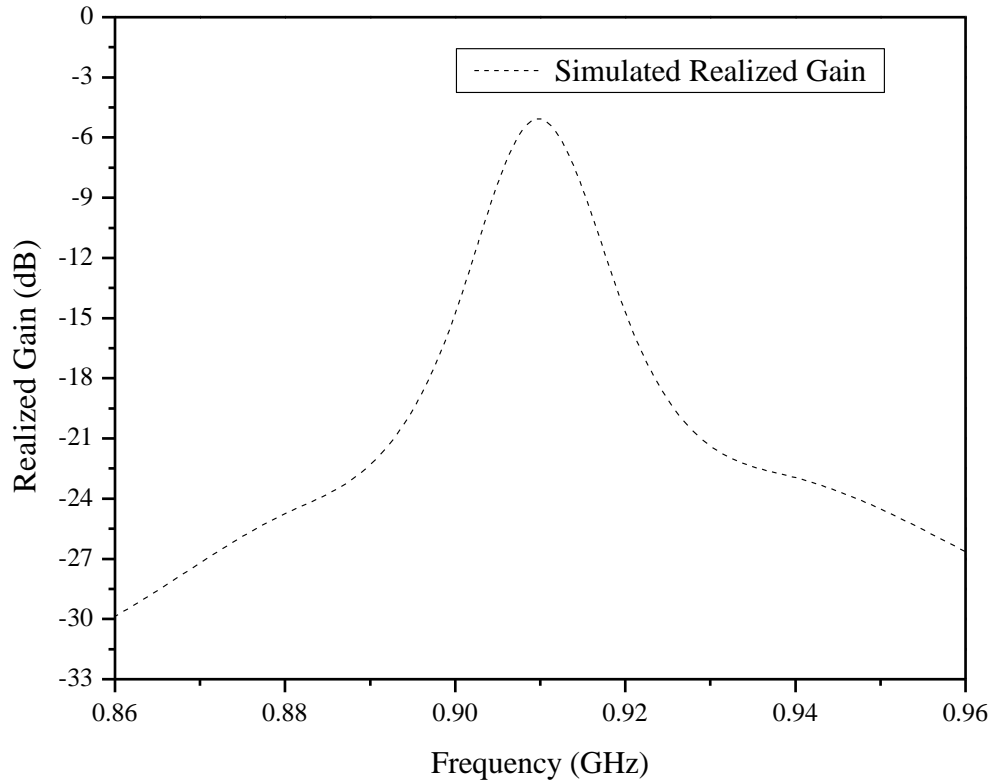


Figure 4.15: Simulated realized gain when the tag is attached in the middle of the 24×12 (all in cm) dielectric constant of 5.8 dielectric back object.

Figure 4.16 below shows the surface current distribution of the meandered T-match loop and the shorting stub that provides a shortening path between the radiating patch and the ground. A 24×12 (all in cm) dielectric constant of 5.8 dielectric back object is being mounted by the tag and placed it in the middle, which the information on surface current can be extracted from the simulation software of CST MWS at the resonating 915 MHz frequency. From the *Figure 4.16* shows, the meandered T-match loop shows to have very high in surface current through it as this proven the meandering of T-match loop is to provide longer current patch to achieve more inductive reactance as well as the thickness of the loop a is a key parameter to control the inductive characteristics of the tag's antenna. This shows that this meandered T-match loop is able to provide

highly inductive to make the tag antenna to be more inductive to cancel out the imaginary capacitive component of the chip. As for the shorting stub, high surface distribution is distributed along the stub as well as proven the stub is made for adjusting the frequency where the tag resonated.

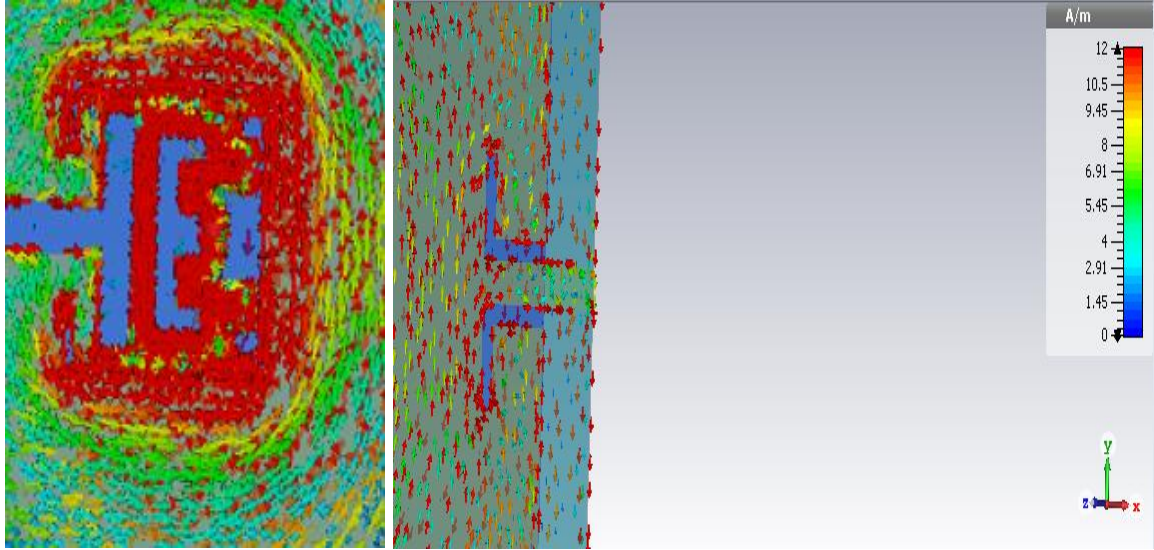
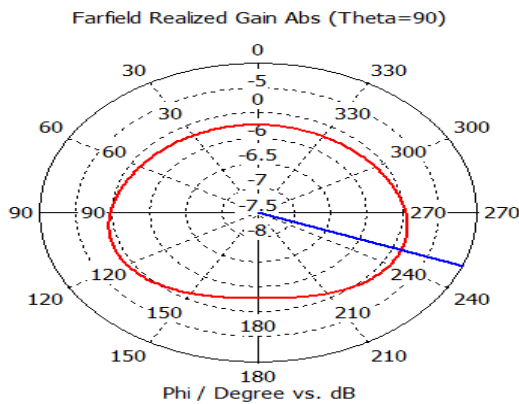


Figure 4.16: The surface current distribution on the tag's antenna when it resonates at 910 MHz by using CST MWS simulation.

Figure 4.17 shows the realized gain pattern simulated using CST MWS generated by the proposed tag design when it is mounted in the middle of the 24 cm \times 12 cm dielectric constant of 5.8 dielectric back object resonates at 910 MHz. *Figure 4.17 (a)* shows the radiation pattern at the x-y plane cut, which is the H-plane ($\theta = 90^\circ$ cut) and it shows a quasi-isotropic radiation pattern with the variation of realized gain varies from -6.28 dB to -5.90 dB. Therefore, it has a consistent radiation field at the H-plane as in two dimensional cut looking at the H-plane is very near to a figure-O in shape. *Figure 4.17 (b)* shows the radiation field pattern on the x-z plane cut, which is the E-plane ($\varphi = 0^\circ$ & $\varphi = 180^\circ$ cut) the obtained realized gain is near to a figure-8 like in shape but slightly tilted to the clockwise direction. A near null-point lobe is located at $\theta = 25^\circ$ ($\varphi = 180^\circ$ cut) is observed with a realized gain of -22.4 dB and its exact opposite direction and $\theta = 155^\circ$ ($\varphi = 0^\circ$ cut) -14.5 dB is the same, whereas the main lobe direction is located at $\theta = 123^\circ$ ($\varphi = 180^\circ$ cut) and $\theta = 57^\circ$ ($\varphi = 0^\circ$ cut) with the realized gain near to magnitude of -5dB. As the cut in the y-z plane, which is also the E plane ($\varphi = 90^\circ$ & $\varphi = 270^\circ$ cut). Two near null points are observed at $\theta = 0^\circ$ and $\theta = 180^\circ$ with a realized gain of -12.18 dB and -10.28 dB and the main lobes located at θ

= 90° with a realized gain of -6 dB as shown in *Figure 4.17 (c)* is near to a figure-8 like shape as well because it is an E-plane cut. As a result, near quasi-isotropic radiation pattern is obtained, but not perfect as the SRR dipoles are not design in half-wavelength electrical length because it will make the tag dimension to be very large in size as it is not desired in UHF RFID tag design. Therefore, near quasi-isotropic radiation is obtained can be good and versatile for many applications. By using equation (3.18), the read distance by considering the main lobe magnitude of the 3-dimensional realized gain, which is -5.06 dB is calculated to be 9.22 m and the near null point of -22.4 dB is calculated to be 1.25 m. Hence, by theoretically the read distance varies from 1.25 m to 9.22 m depending on the tag position varies with respect to the reader antenna. The measurement was not able to carry out to measure the read distance due to movement control order.

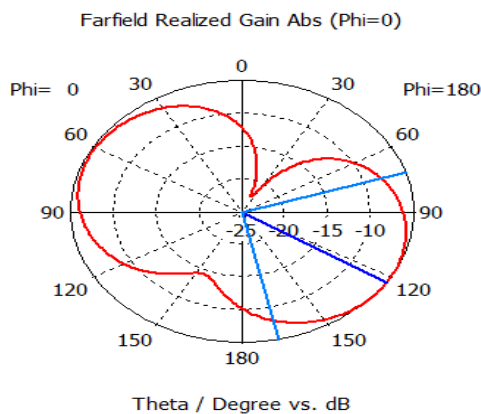


Frequency = 0.9094

Main lobe magnitude = -5.9 dB

Main lobe direction = 249.0 deg.

(a)



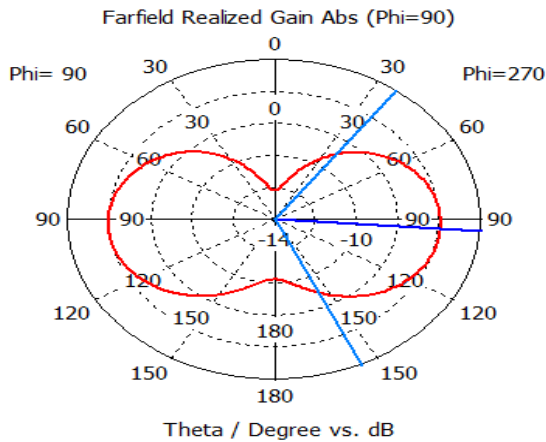
Frequency = 0.9094

Main lobe magnitude = -5.06 dB

Main lobe direction = 123.0 deg.

Angular width (3 dB) = 95.2 deg.

(b)



Frequency = 0.9094
 Main lobe magnitude = -5.97 dB
 Main lobe direction = 94.0 deg.
 Angular width (3 dB) = 119.0 deg.

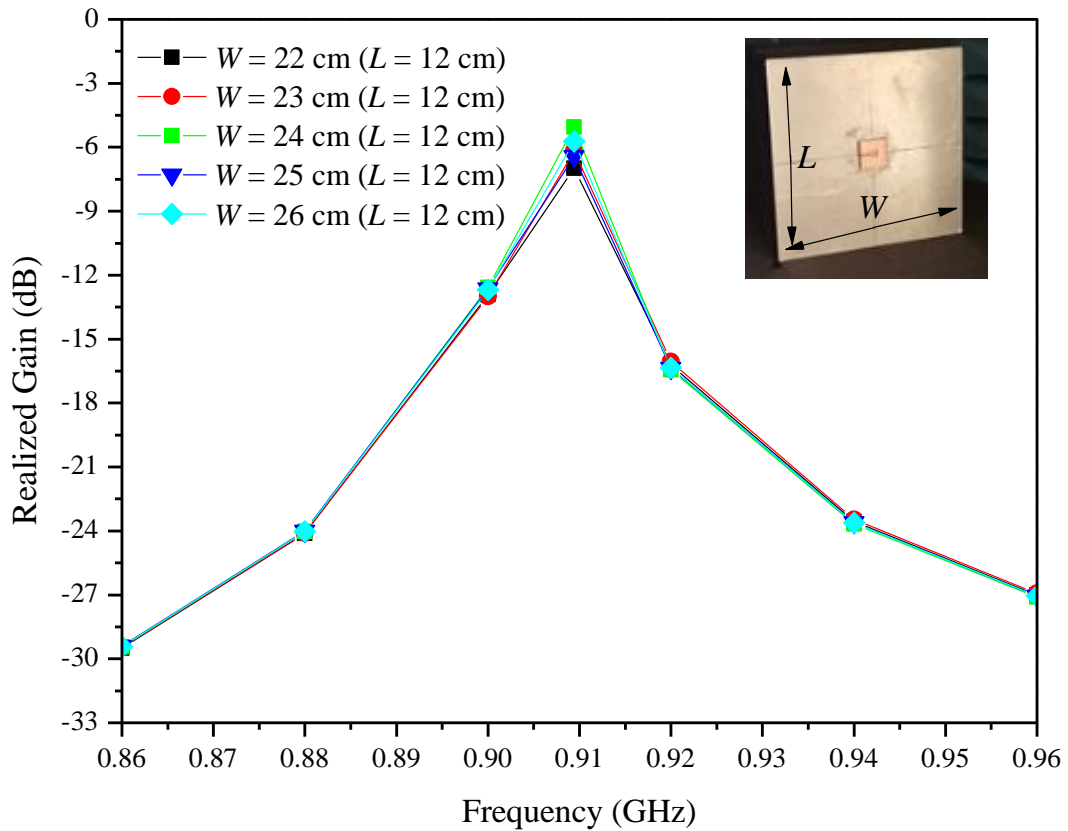
(c)

Figure 4.17: Simulated realized gain at the (a) H-plane ($\theta = 90^\circ$ cut) and (b & c) E-planes ($\varphi = 0^\circ$ & $\varphi = 180^\circ$ cut and $\varphi = 90^\circ$ & $\varphi = 270^\circ$ cut).

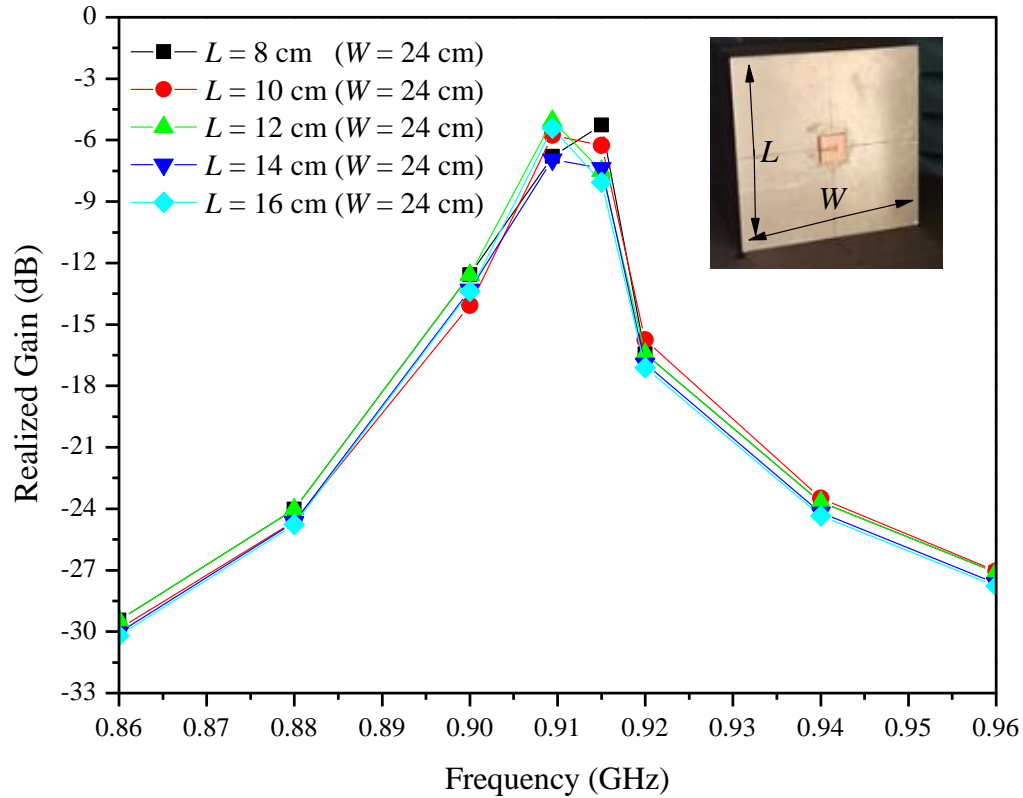
4.4 Real Practical Scenario Simulation Results and Comparison with other Researched Quasi-Isotropic Radiation Pattern UHF RFID Tag

Real practical scenario realized gain simulation results is carried out by using CST MWS to test the proposed tag's performance when it is mounted on different dimensions by varying the dielectric constant 5.8 dielectric back object width and length in the symbol of W and L . As usual, the proposed tag's is placed in the middle of the dielectric platform symmetrically to carry out the test. The purpose of this testing is to test how does different dimension of the dielectric back object will affect the performance of the tag as in the real life practical scenario, the dielectric back object which the tag is mounted on is not fixed as different applications will have different dimension of the dielectric back object. The test will carry out as shown in *Figure 4.18* (a) below to simulate the realized gain with respect to frequency by keeping the $L = 12$ cm constant while varying the W from 22 cm to 26 cm, $W = 24$ cm is the most optimized of the dielectric constant 5.8 dielectric back object. The realized gain is -7 dB at $W = 22$ cm which is the worst result obtained. However, -7 dB is good enough to provide long read range distance as the simulation results shown varies between -5 dB to -7 dB as proven to be not affected much on the performance of the proposed tag as W varies while keeping L as constant. The simulation result of changing L , while keeping W to be fixed as constant is shown in *Figure 4.18* (b) below. The resonant realized gain varies from -8

dB to -5dB as the as L varies while keeping W to be fixed as a constant. From both of the results shown, the proposed tag is insensitive to dimension of the substrate back object mounted on. It is also worth to mention the tag resonant frequency is very stable at 910 MHz, the only shifting of the tag resonant frequency is when $L = 8$ cm and $W = 24$ cm to 915 MHz and it is acceptable for typical scenarios. Therefore, it is one of the figures of merit for the proposed tag antenna to be not sensitive to the dimension of the back substrate object and is useful for many applications. The results obtained are using CST MWS as no actual measurement is measured due to movement control order.



(a)

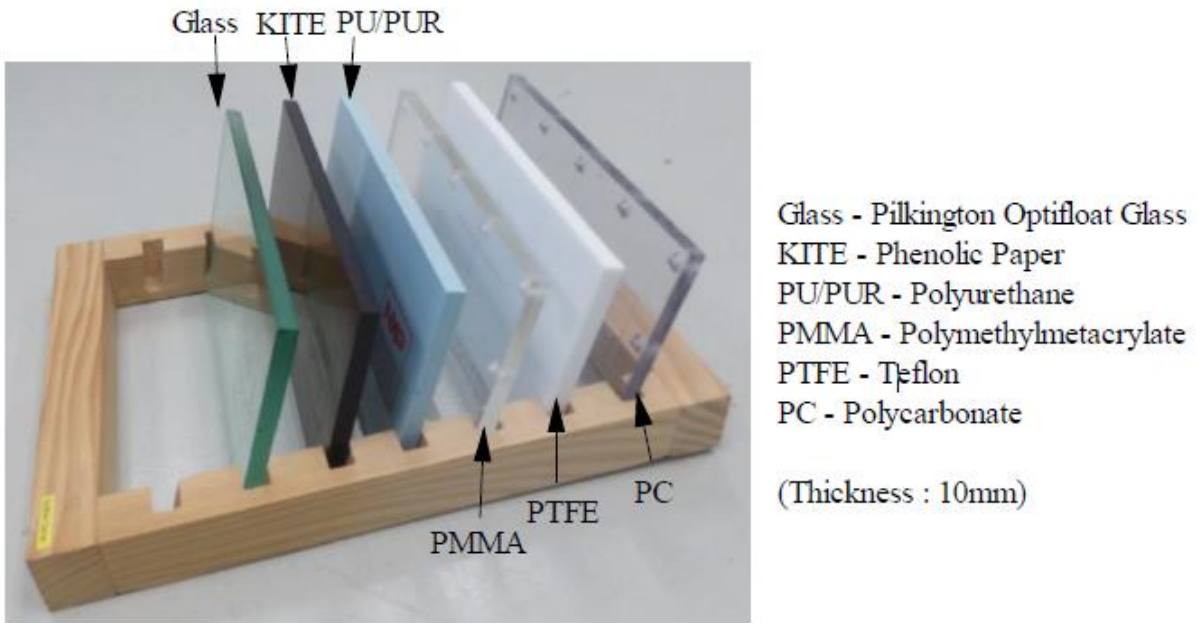


(b)

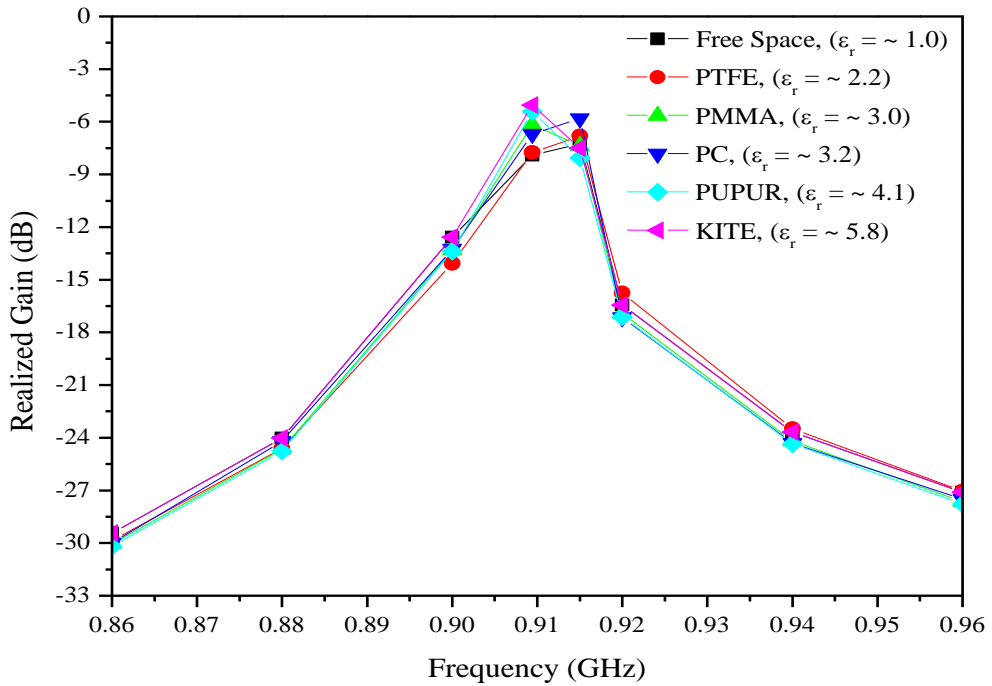
Figure 4.18: Simulated realized gain with respect to the frequency to the case of (a) W changes while L kept constant and (b) L changes while W kept constant.

Lastly, another real life practical scenario as the dielectric constant of the dielectric back object is not fixed and will be randomly mounted on depending on the applications. Hence, the simulated realized gain response with respect to frequency is shown in *Figure 4.19* (b) below. The different dielectric constant dielectric back objects used in practical measurement are manufactured from NXP uses the given reference materials (AN1629, 2008) as shown in *Figure 4.19* (a) below. Slight resonant frequency shifting is observed when it is mounted on free space, PTFE and PC. However, this shifting is not significant as at the frequency of 910 MHz, the realized gain is still above -8 dB for all different dielectric constant back dielectric objects. Hence, a conclusion can be made, which the design of the proposed tag is not affected to the different dielectric constant back objects. It is worth to mention the results obtained are using CST MWS to

analogy the actual measurement as no practical measurement is measured due to movement control order.



(a) (AN1629, 2008)



(b)

Figure 4.19: (a) The dielectric back objects used are manufactured by NXP and (b) the realized gain response as simulated by CST MWS.

Last but not least, is it worth to test out the proposed RFID tag mounted on metal material back object with dimension of $20 \times 20 \times 1$ (all in cm) although the proposed RFID tag is not designed for metal-mountable. *Figure 4.20* shows the realized gain response when the proposed tag is mounted on a metal. It was clearly seen that resonant frequency has shifted to 924 MHz, which has been deviated from the 910 MHz and the magnitude of the G_r is deteriorated to -9.6 dB as well. As for realized gain 3-dimensional radiation pattern shown in *Figure 4.21* below, the radiation pattern changed from quasi-isotropic to bore-sight as the SRR structure mounted on the metal is jeopardized by the cancellation of image current (Dobkin and Weigand, 2005) because the SRR structure is made up of electric and magnetic dipole aligned perpendicular to each other as the dipole structure radiation characteristics is deteriorated by any metal in the vicinity of it. Therefore, the proposed RFID tag has a disadvantage of unable to mount on metal material and future improvement has to be done.

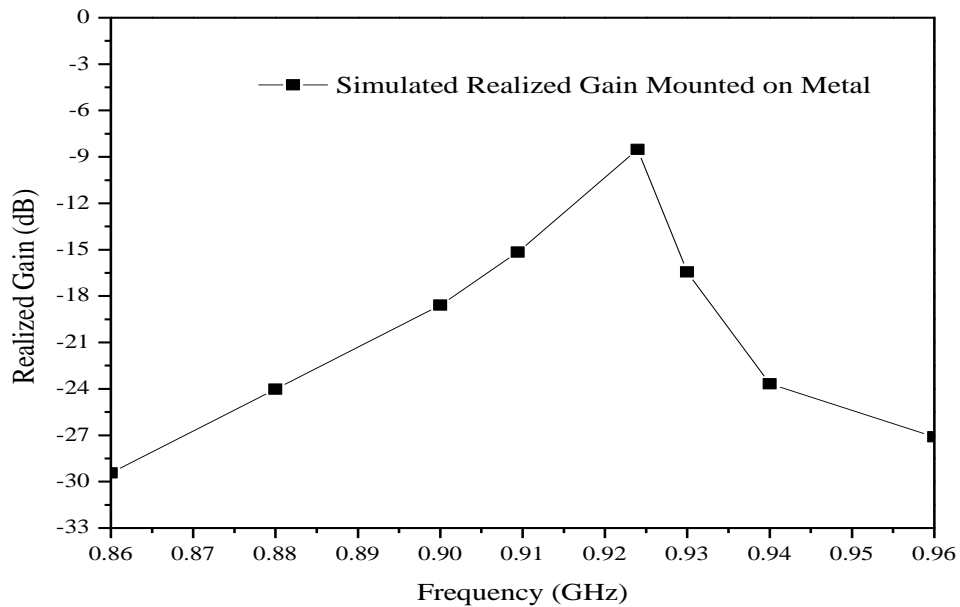


Figure 4.20: The simulated realized gain response mounted on metal.

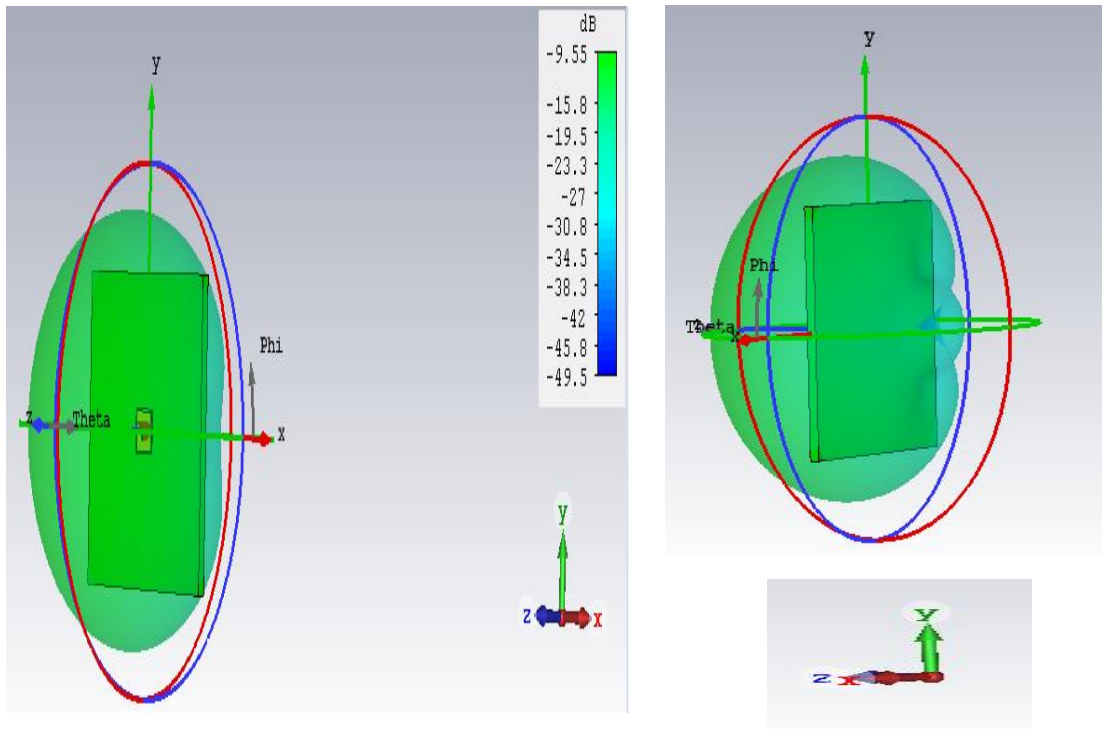


Figure 4.21: The simulated 3-dimensional realized gain response mounted on metal.

Finally, *Table 4.2* below shows the comparison with some other published authors which their passive UHF RFID tags are able to provide quasi-isotropic radiation pattern. In the reference of (Yang and Son, 2016), the author proposed a tag that is able to provide quasi-isotropic radiation pattern even though it is mounted on metal and 10.2 m furthest read range distance is achieved. However, the authors tag's size is very huge in $64 \times 64 \times 2$ (all in mm & with a 2 mm substrate) which is about 3 times larger than the volume of our proposed tag. Additionally, the author also makes use of additional lumped capacitors and vias techniques to achieve impedance matching and resonant frequency tuning, which is not feasible in large scale production as the fabrication technique will be more complicated and additional materials which lead to more cost is incurred. As for the reference of (Lin et al., 2011) the author's proposed tag is mountable on a glass which is a substrate object to provide quasi-isotropic radiation pattern. The footprint of the tag antenna is very large in 91×91 (all in mm & without any substrate) as it is not so convenient for many

applications that required compact tag's size although it is able to achieved the maximum read distance of 9 m. Moreover, a microchip with two ports supported feature has to be implemented to excite both of the dipoles aligned orthogonally as such microchip will be more expensive than the conventional single port chip. After that, the designed tag in (Cho et al., 2005) is able to provide quasi-isotropic radiation pattern as well by making use of two bends dipole incorporated together when it is mounted on the substrate, but again, the tag's dimension is also very huge in 79.2×53.1 (all in mm & without any substrate) as is compactness it not versatile for many applications as well. Although the tag's bandwidth is very wide in the range of 848 to 926 MH, however, the maximum read distance is only 2.4 m which is very low in typical RFID design. Hence, the tag is very limited in applications where it only requires short range distance and the tag's size is not a major issue. Finally, the journal of (Bong et al., 2018) is compared as the journal is able to produce quasi-isotropic radiation pattern mounted on a metal as well. The footprint of the journal is $30 \times 30 \times 1.6$ (all in mm & with a 1.6 mm substrate) which is compact and able to provide a maximum read distance of 3.5 m which is acceptable for many typical applications. However, the only down side of this journal is as well using the two port excitation method to excite the two pairs of dipolar patches as this method requires high cost of the microchip. In my proposed tag, it is very compact with dimension of $28 \times 28 \times 3.293$ (all in mm) and with maximum realized gain of -5.06 dB (9.22 m by using calculation) as well as able to provide quasi-isotropic radiation pattern when mounted on the substrate back object. Additionally, conventional microchips single port is used which is cost saving and the breakthrough of SRR structure itself is simple which is easy to fabricate and model as it already had the features of magnetic and electric dipole orthogonally with each other. However, the only downside of the proposed tag is the tag is not usable for metal-mountable as the resonant frequency is shifted and quasi-isotropic radiation pattern is no longer can be achieved.

Table 4.2: The comparison of the performance of the UHF RFID with quasi-isotropic radiation pattern.

	Power (W)	Quasi-isotropic radiation pattern	Size of the tag (mm), (Substrate)	Metal-mountable or substrate-mountable	Maximum read distance (m)
Proposed tag	4 (EIRP)	Yes	28 × 28 × 3.293, (Duroid® 6010 $\epsilon_r = 10.2$)	Substrate-mountable	9.2 by calculation
(Yang and Son, 2016)	4 (EIRP)	Yes	64 × 64 × 2, (FR4, $\epsilon_r = 4.4$)	Metal-mountable	10.2 by measurement
(Lin et al., 2011)	4 (EIRP)	Yes	91 × 91, (None)	Substrate-mountable	9 by measurement
(Cho et al., 2005)	N/A	Yes	79.2 × 53.1, (None)	Substrate-mountable	2.4 by measurement
(Bong et al., 2018)	4 (EIRP)	Yes	30 × 30 × 1.6, (Softlon, $\epsilon_r = 1.06$)	Metal-mountable	3.5 by measurement

4.5 Summary of Results and Discussion

As a summary, the introduction of an electrical small planar folded patch composes of a rectangle Split-Ring Resonator (SRR) which is excited and fed by a meandered T-match for designing a passive UHF RFID tag is briefly discussed for substrate-mountable. The meandered T-match has shown to be able to provide excellent matching for the impedance for both the chip and the antenna structure in the tag at resonant frequency, whereas the inductive stub provide a shortening patch between the radiating patch and the ground plane provides more inductance to the tag's antenna structure and high dielectric constant to scale down the tag's size as well as the pair of the notches is used adjusting resonant frequency in a very low sensitivity of frequency shifting and ~90%

coefficient of power transmission is achieved. The working principle of quasi-isotropic radiation pattern is discussed and agreement with theory and simulation is achieved. Parametric analysis for some key parameters are simulated to test for how well the tag's resonant frequency shifting with respect to the length changes of the key parameters. Lastly, measurement setup is discussed where the simulated realized gain across the H-plane and E-planes where maximum realized gain of the proposed tag is achievable at -5.06 dB, which is directly proportional influenced to the detection distance of the tag. Last but not least, several real life practical scenarios such as the dimension of substrate back object which the tag mounted on, different dielectric constant of the substrate back objects and metal-mountable realized gain response are simulated to test the tag's performance on these scenarios and comparison with other literatures which all of these tags are able to produce quasi-isotropic radiation pattern is analysed and discussed as well. It is worth to mention all the results obtained are generated by CST MWS and the read distance of the proposed tag is obtained by using equation (3.18) where actual measurement of the read distance is not able to obtain due to the movement control order implemented by the Malaysia government, therefore the student is not able to enter to the university facilities to conduct the measurement.

CHAPTER 5

CONCLUSIONS AND RECOMMENDATION

5.1 Conclusions of the Proposed Passive UHF RFID Tag design.

As a final conclusion, the objectives which had been defined earlier have been accomplished after achieving the targets by writing this final year project thesis. Throughout the project, the SRR structure had been analysed and discovered how it was useful for antenna design, particularly targeted by passive UHF RFID tag application because it is able to provide quasi-isotropic radiation pattern for substrate-mountable. Several techniques of impedance matching and resonant frequency tuning had been explored as well, including the meandered T-match loop, shorting stub and the pair of notches. After that, various type of miniaturization techniques of the tag by other literatures have been well equipped for the proposed tags, including the high dielectric constant technique, which the proposed tag is equipped with $\epsilon_r = 10.2$ Duroid[®] 6010 as well as the shortening stub which shorten the path between the radiating patch and the ground plane to make the antenna structure to be more inductive to tune down the resonant frequency as we know the tag's size when it is small tend to resonate at much higher range of frequency above the UHF spectrum. The overall fabrication process is very simple and cheap because it is just a simple double-sided layer of copper with thickness of 9 μm deposited on the flexible PET substrate with a thickness of 50 μm . Therefore, the desired tag's structure is done by etching unwanted copper part and the overall tag's structure is just this piece of etched PET substrate wrapped symmetrically over the Duroid[®] 6010 substrate with Monza 5 microchip is embedded over the small narrow space along the meandered T-match loop. The overall proposed tag is able to provide quasi-isotropic radiation pattern when it is mounted on a substrate and a maximum realized gain of -5.06 dB is achieved (9.2 m read distance by using equation (3.18)) and the resonant frequency and realized gain is very stable with minimum variation is observed when different dimension and dielectric constant of the back dielectric object where the tag is mounted on are simulated, which is very versatile for many typical practical applications. The simulated radiation pattern and surface current flow comply with the theoretical principle as well. Last but not least, as compared with

other literatures with quasi-isotropic radiation pattern, the proposed tag is among the most compact with tag's antenna structure is simple and yet can provide long read range distance about 9.2 m, which is only lower than the literature of (Yang and Son, 2016).

5.2 Disadvantages and Advices for Future Work

The material used for the conductive part is copper. The production price still considerably high for large volume manufacturing because of the good electrical properties portray by the copper material. Hence, it is much advisable to use aluminium instead of copper without jeopardising much on the tag's antenna radiation efficiency because aluminium is much cheaper and it is being adopted in broader level at the level of commercialisation in the community of RFID. On top of that, the substrate used is high in dielectric constant for the purpose of scaling down the tag's size. The high dielectric constant substrate will introduce high dielectric losses to the tag's antenna performance, which will jeopardise the radiation efficiency as well ultimately lead to lower read range and high dielectric constant will be much more expensive than low dielectric constant substrate. Hence, if the proposed tag is using low dielectric constant substrate will have higher read range, but with the trade-off of the tag's size no longer compact (Rao et al., 2005). One of the major disadvantages of the proposed tag is not able to mount on metal back object, although it is designed for substrate-mountable. In the real life practical scenario, the tag may be used to be mounted on any possible materials. The realized gain is deteriorated as shown in *Figure 4.20* above with resonant frequency shifted to 924 MHz and the radiation pattern is no longer in quasi-isotropic radiation because the image current is being cancelled due to the SRR dipole structure when a metal is acting as a medium which the tag is mounted on. As a result, it is much desirable where the tag at least is able to maintain at the resonant frequency of 910 MHz even though the quasi-isotropic radiation pattern is no longer achievable.

The advices for future work would be using aluminium conductor instead of copper conductor due to lost cost and RF performance is able to maintain. A low dielectric constant substrate has to be used to mitigate high dielectric losses and cost saving and yet still able to maintain the compactness has to be explored. Last but not least, a new tag's antenna structure or modification of the SRR structure that is mounted on both metal and substrate is able to provide

quasi-isotropic radiation pattern and maintain or slight shifting of resonant frequency as long as the resonant frequency at 910 MHz is still able to produce adequate read distance is needed for research. Therefore, ideally the most optimum passive UHF RFID tag is compact and able to produce quasi-isotropic radiation pattern when mounted on both substrate and metal as well as the read distance is sufficiently long enough is needed to be done in the future work as far as the technology advancement is concerned.

REFERENCES

- AN1629 UHF RFID Label Antenna Design. [Online]. Available: http://www.nxp.com/documents/application_note/AN162910.pdf.
- Ali Babar, A. et al., 2012. Small and flexible metal mountable passive UHF RFID tag on high-dielectric polymer-ceramic composite substrate. *IEEE Antennas and Wireless Propagation Letters*, Volume 11, pp. 1319-1322.
- Balanis, C., 2005. *Antenna Theory: Analysis and Design*, John Wiley: New York.
- Björninen, T., Virkki, J., Virtanen, J., Sydänheimo, L. and Ukkonen, L., 2013. Inkjet-printing and Performance Evaluation of UHF RFID Tag Antennas on Renewable Materials with Porous Surfaces. *2013 IEEE European Conference on Antennas and Propagation (EuCAP)*, pp. 1721-1725.
- Bong, F. L., Lim, E. H. & Lo, F. L., 2017. Miniaturized dipolar patch antenna with narrow meandered slotline for UHF tag. *IEEE Transactions on Antennas and Propagation*, 65(9), pp. 4435-4442.
- Bong, F. L., Lim, E. H. & Lo, F. L., 2018. Compact orientation insensitive dipolar patch for metal-mountable UHF RFID tag design. *IEEE Transactions on Antennas and Propagation*, 66(4), pp. 1788-1795.
- Chen, S. L. & Lin, K. H., 2008. A slim RFID tag antenna design for metallic object applications. *IEEE Antennas and Wireless Propagation Letters*, Volume 7, pp. 729-732.
- Chen, H., Tsao, Y., 2010. Low-profile PIFA array antennas for UHF band RFID tags mountable on metallic objects. *IEEE Transactions on Antennas and Propagation*, 58(4), 1087–1092.
- China's RFID standards are coming soon, 2018. [Online]. Available: <http://www.szcanbo.com/en/article-76629-104746.html>
- Cho, C., Choo, H. and Park, I., 2005. Broadband RFID tag antenna with quasi-isotropic radiation pattern. *Electronics Letters*, 41(20), pp. 1091-1092.
- Cho, C., Choo, H. and Park, I., 2008. Design of planar RFID tag antenna for metallic objects. *Electronics Letters*, 44(3), pp. 175–177.
- Collela, R., Catarinucci, L., Coppola, P. and Tarricone, L., 2016. Measurement platform for electromagnetic characterization and performance evaluation of UHF RFID tags. *IEEE Transactions on Instrumentation and Measurement*, 65(4), pp. 905-914.

Deng, C., Li, Y., Zhang, Z. & Feng, Z., 2014. A wideband isotropic radiated planar antenna using sequential rotated L-shaped monopoles. *IEEE Transactions on Antennas and Propagation*, 62(3), pp. 1461-1464.

Dobkin, D.M. and Weigand, S. M., 2005. Environmental effects on RFID tag antennas,” *IEEE MIT-S International Microwave Symposium Digest*, pp. 135-138.

Hu, P. F., Pan, Y. M., Zhang, X. Y., and Hu, B. J., 2019. A compact quasi-isotropic dielectric resonator antenna with filtering response, *IEEE Transactions on Antennas and Propagation*, 67(2), pp. 1294–1299.

IPJ-W1600 Monza 5 Tag Chip Datasheet, 2016. [Online]. Available: <https://support.impinj.com/hc/en-us/articles/202756948-Monza-5-Tag-Chip-Datasheet>.

Kanan, R., Azizi, A., 2009. UHF RFID transponders antenna design for metal and wood surfaces, *2009 IEEE International Conference on RFID*, pp. 270–277.

Kholodnyak, D. V., Turalchuk, P. A., Mikhailov, A. B., Dudnikov, S. Y. and Vendik, I. B., 2006. 3D antenna for UHF RFID tags with eliminated read-orientation sensitivity. *2006 IEEE European Microwave Conference (EuMA)*, pp. 583-586.

Khosravi, M. et al., 2017. An adoption of halal food recognition system using mobile Radio Frequency Identification (RFID) and Near Field Communication (NFC). S.I., *Institute of Electrical and Electronics Engineers Inc.*, pp. 70-75.

Kynix S., 2018. RFID Technology: System, Principle, Classification and Application [Online]. Available: <http://www.apogeeweb.net/article/136.html>.

Lin, Y.F., Yeh, S.A., Chen, H.M. and Chang, S.W., 2011. Design of an omnidirectional polarized RFID tag antenna for safety glass applications. *IEEE Transactions on Antennas and Propagation*, 60(10), pp. 4530-4537.

Long, S., 1975. A combination of linear and slot antenna for quasi-isotropic coverage. *IEEE Transactions on Antennas and Propagation*, 23(4), pp. 572-576.

Luk, K. M. & Wu, B., 2012. The magnetoelectric dipole wideband antenna for base stations in mobile communications. *Proceedings of the IEEE*, 100(7), pp. 2297-2307.

Mark R., 2005. The history of RFID. [Online]. Available: <https://www.rfidjournal.com/articles/view?1338>.

Marrocco, G., 2003. “Gain-optimized self-resonant meander line antennas for RFID applications,” *IEEE Antennas and Wireless Propagation Letters*, 2, pp. 302-305.

Marrocco, G., 2008. The art of UHF RFID antenna design: impedance matching and size-reduction techniques. *IEEE Antennas Propagation Magazine*, 50(1), pp. 66-79.

Mathis, H., 1951. A short proof that an isotropic antenna is impossible. *Proceedings of the IEEE (Correspondence)*, volume 39, pp. 970.

Moh, C. W., Lim, E. H., Bong, F. L. & Chung, B. K., 2018. Miniature Coplanar-Fed Folded Patch for Metal Mountable UHF RFID Tag. *IEEE Transactions on Antennas and Propagation*, 66(5), pp. 2245-2253.

Ott, H., 2009. *Electromagnetic Compatibility Engineering*. John Wiley and Sons.

Pan, G., Li, Y., Zhang, Z. & Feng, Z., 2012. Isotropic radiation from a compact planar antenna using two crossed dipoles. *IEEE Antennas and Wireless Propagation Letters*, volume 11, pp. 1338-1341.

Pan, Y. M., Leung, K. W. & Lu, K., 2014. Compact quasi-isotropic dielectric resonator antenna with small ground plane. *IEEE Transactions on Antennas and Propagation*, 62(2), pp. 577-585.

Rao, K.V.S., Nikitin, P.V. and Lam, S.F., 2005. Antenna design for UHF RFID tags: A review and a practical application. *IEEE Transactions on Antennas and Propagation*, 53(12), 3870–3876.

RT/duroid® 6006 and 6010.2LM Laminates Datasheet, 2017 [Online]. Available: <https://rogerscorp.com/advanced-connectivity-solutions/rt-duroid-laminates/rt-duroid-6006-and-6010-2lm-laminates>.

Ryu, H.K., Jung, G., Ju, D.K., Lim, S. and Woo, J.M., 2010. An electrically small spherical UHF RFID tag antenna with quasi-isotropic patterns for wireless sensor networks. *IEEE Antennas and Wireless Propagation Letters*, 9, pp. 60-62.

Suzanne S., 2014. UHF RFID Frequency Regulations. [Online]. Available: <https://blog.atlasrfidstore.com/uhf-rfid-frequency-regulations>.

Suzanne S., 2017. 7 Things You Can Track in Hospitals Using RFID. [Online]. Available: <https://blog.atlasrfidstore.com/7-things-can-track-hospitals-using-rfid>.

Tran, H.H., Ta, S.X. and Park, I., 2015. A compact circularly polarized crossed-dipole antenna for an RFID tag. *IEEE Antennas and Wireless Propagation Letters*, 14, pp. 674-677.

Virtanen, J., Virkki, J., Sydänheimo, L., Tentzeris, M. and Ukkonen, L., 2013. Automated identification of plywood using embedded inkjet-printed passive UHF RFID tags. *IEEE Transactions on Automation Science Engineering*, 10(3), pp. 796-806.

Voyantic Ltd. Voyantic Tagformance Lite. [Online]. Available: <http://www.voyantic.com/>.

Xi, J. and Ye, T.T., 2011. Wideband and Material-Insensitive RFID Tag Antenna Design Utilizing Double-Tuning Technique. *IEEE Antennas and Propagation Society International Symposium (APSURSI)*, pp. 545-548.

Wang, Y. et al., 2019. Design of Low-Cost, Flexible, Uniplanar, Electrically Small, Quasi-Isotropic Antenna. *IEEE Antennas and Wireless Propagation Letters*, 12 7, 18(8), pp. 1646-1650.

Yang, E.S. and Son, H.W., 2016. Dual-polarised metal-mountable UHF RFID tag antenna for polarization diversity,” *Electronics. Letters*, 52(7), pp. 496-498.

Yang, P. H., Li, Y., Jiang, L., Chew, W.C. and Ye ,T.T., 2011. Compact metallic RFID tag antennas with a loop-fed method. *IEEE Transactions on Antennas and Propagation*, 59(12), pp. 4454-4462.

APPENDIX

Appendix A: The investigation of the error in the first proposed tag design to the finalised design.

Figure A.1 shows the first design of the proposed passive UHF RFID tag, which the T-match loop without meandering with thickness of 0.2 mm. The main problem of this narrow thickness, although is able to provide very inductive tag's antenna characteristics which will help the impedance matching however, the tolerance of the fabrication is simply too high which jeopardise the tag antenna resonant frequency to be shifted to above 1 GHz as shown in *Figure A.3 below*, which is simply not acceptable for UHF tag design. Hence, the finalised design is modified by meandering the T-match loop while increases its thickness of 0.5 mm to reduce the fabrication tolerance as shown in *Figure A.2* below. It may be wondered increasing the thickness will made the tag's antenna to be less inductive and impedance matching will be deteriorated, however the purpose of meandering is to improve the inductance characteristics introduce to the tag's antenna to compensate the increasing thickness inductance because meandering the T-match loop will make the surface current patch to be much longer and hence increasing its inductance.

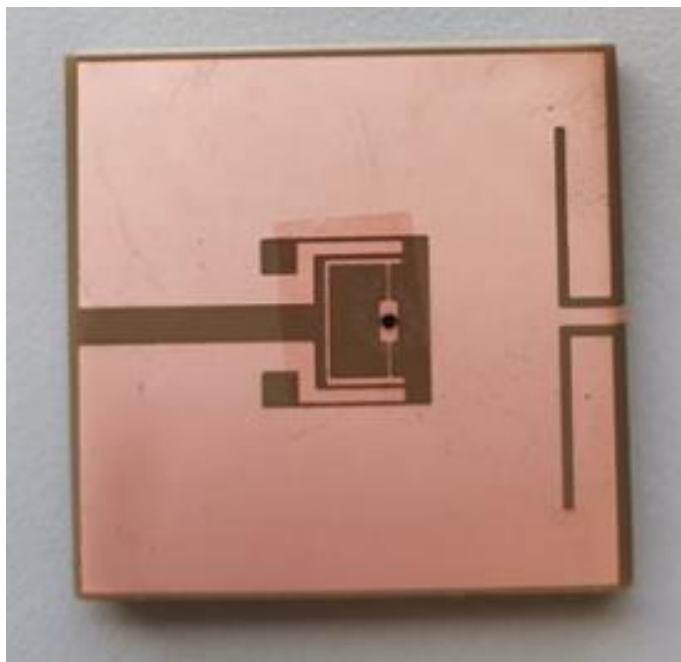


Figure A.1: The first design of the passive UHF RFID tag.

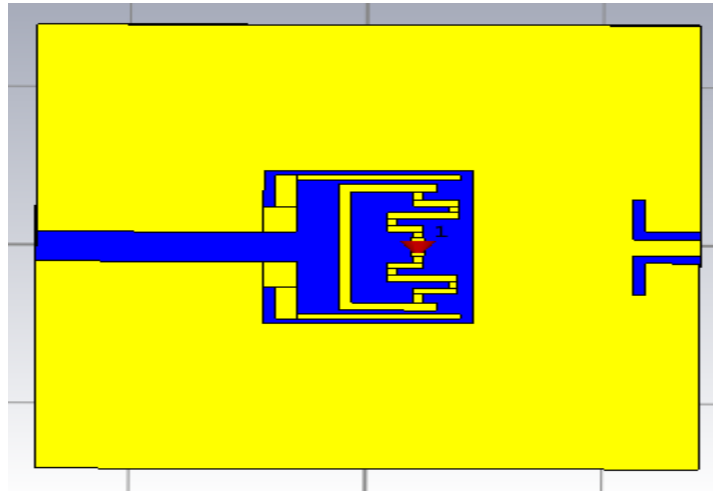


Figure A.2: The finalised design of the passive UHF RFID tag.

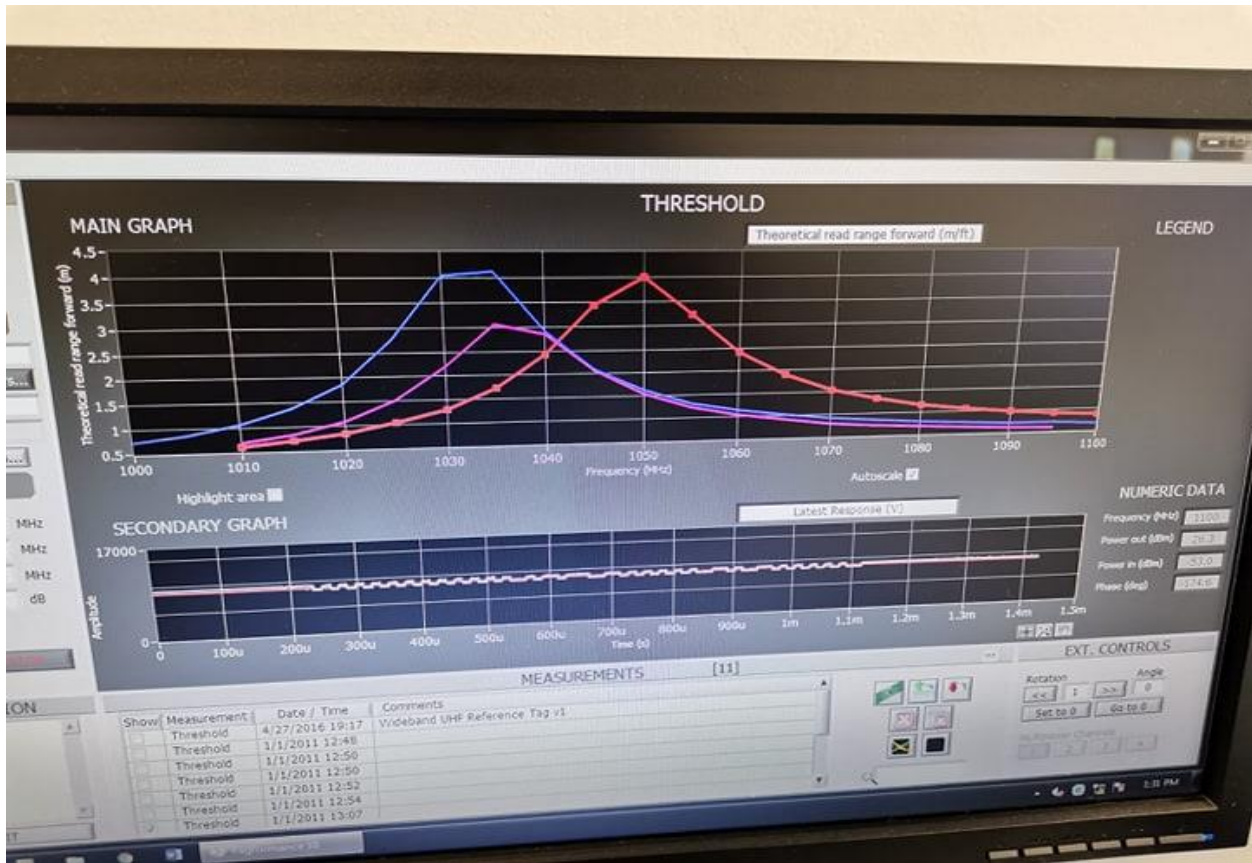


Figure A.3: The measured read distance shown for the first tag design as shown in *Figure A.1* above shows the read distance measured has shifted to above 1 GHz.